MEAN CIRCULATION OF THE INDONESIAN THROUGHFLOW AND A MECHANISM OF ITS PARTITIONING BETWEEN OUTFLOW PASSAGES: A REGIONAL MODEL STUDY

by

Ana Paula Berger, B.A. B.Sc.

Submitted in fulfilment of the requirements
for the Degree of Doctor of Philosophy

Department of Institute for Marine and Antartic Studies (IMAS)
University of Tasmania

August, 2019

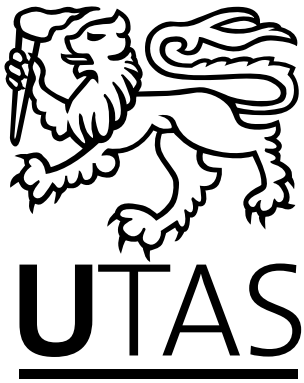

I declare that this thesis contains no material which has been accepted for a degree or diploma by the University or any other institution, except by way of background information and duly acknowledged in the thesis, and that, to the best of my knowledge and belief, this thesis contains no material previously published or written by another person, except where due acknowledgement is made in the text of the thesis.

Signed: _____
Ana Paula Berger

Date: 20/04/2020

Signed: _____
Ana Paula Berger

Date: 20/04/2020

ABSTRACT

The Indonesian Throughflow (ITF) is the only low latitude connection of the global circulation and is an essential pathway for mass, heat and salt exchange between the Pacific and Indian Oceans. The ITF is a boundary current constrained by topography and is characterised by two source pathways, a western and an eastern. At the exit to the Indian Ocean, observations show the ITF partitions amongst the three major outflow straits. The westernmost, Lombok Strait, has the lowest transport even though it is expected to carry most of the flow given that the ITF is a boundary current and this strait is a direct continuation of the western pathway. Heat and saltwater transports are different in each outflow strait and thus exchanged properties depend on the partitioning, consequently affecting the contribution to the Indian Ocean. In this study, we explore the ITF circulation and local dynamics that control the ITF partitioning.

To explore what controls ITF partitioning in the context of western boundary current theories, we simulate a steady ITF in a high-resolution (4-km) regional model. The forcing consists of time-averaged velocity, temperature and salinity fields from the global model Ocean Forecasting Australia Model v3 (OFAM3). We investigate what sets the amount of western pathway water that exits via Lombok Strait in the regional model. Our reference simulation confirms the two ITF pathways and gives a mean ITF of 14.1 Sv and an outflow partitioning of 0.2:0.4:0.4 (Lombok:Ombai:Timor), consistent with observations. Focusing on the western pathway, comprising 70% of the total ITF, we investigate the routes this water follows to the Indian Ocean. Here we consider partitioning as the ratio between transport in Lombok and Makassar Straits. Relative to only Makassar Strait transport, Lombok Strait still has the lowest transport portion of the three outflows (27%). Idealised perturbation experiments help us to investigate boundary current dynamics; combinations of slip/non-slip boundary conditions and linear/non-linear advection in the momentum equations illustrate the effects of current width (CW) on partitioning. Our key finding from this analysis is that the CW in the Makassar Strait controls the Lombok Strait transport; a narrower boundary

current can fit more flow through a narrow strait. To understand what sets the CW, we perform a vorticity budget. The reference simulation reveals that the leading order term that balances change in planetary vorticity is advection of vorticity. The vorticity term diagnostics for the perturbation experiments suggest non-linearity is the main term controlling the ITF current width.

We test how CW influences partitioning in more realistic conditions and evaluate how low-frequency variability affects partitioning, analysing 18-yr of a global fully-realistic model OFAM3. Consistent with our perturbation experiments, we find CW in Makassar Strait controls transport in Lombok Strait. Further, we find that, on the inter-annual scale, the Makassar Strait CW is approximately constant. This suggests that Makassar Strait may be saturated and similar dynamics could also take place upstream in the ITF western pathway. Specifically, we find that the width of Makassar Strait constrains the CW, independent of variations in CW at the upstream inflow ITF at Mindanao boundary current. As a consequence, during years when Mindanao current is wide at the Indonesian Seas entrance, the flow does not entirely fit in Makassar Strait. This flow that did not fit in Makassar Strait joins the eastern pathway. The increase of inflow in the eastern pathway produces a change in transport at Timor Passage, providing a link between variability at Timor Passage and that of the Mindanao.

Our results suggest that, given the ITF complexity, the simple concept of partitioning cannot be easily used as a proxy for ITF transports and predictions cannot be made based on single strait measurements. The ITF western pathway provides a more direct connection to the Indian Ocean compared to the eastern pathway. The changes eastern pathway waters undergo while circulating in the Indonesian Seas are crucial for understanding heat and tracers exchange between the two oceans. Finally, understanding what controls the ITF circulation and its variability is critical to better predicting how the ITF responds to climate change.

ACKNOWLEDGEMENTS

Not just a science degree, this PhD was an amazing experience in learning about life and myself, for which I will be forever thankful. I want to highlight here how immeasurably grateful I am to my parents who are the most supportive and beautiful people.

Thank you to my supervisors Dr Bernadette Sloyan, Dr Maxim Nikurashin, Dr Beatriz Peña-Molino and to Dr Susan Wijffels who also participated in the early stage of my PhD. This PhD was a great opportunity that I always dreamed of, and I am truly grateful for their patience with my learning process, the discussions, suggestions, and support.

Some awesome people who helped me with such great company, advice and friendship: Leo, Makrina, Sam, Matt, Habacuc, Hugo, Gabi, Eva, Wilma, Sibele, Natalia, Elisa, Cailin; I love you all! And lastly but not least, my beloved cats Gatinho and Oshee, you were essential.

I also would like to mention here what a great time I had in Tasmania, this lovely island, full of beautiful music, interesting people, and nature.

This PhD would not have been possible without the funding from the Brazilian Agency 'Coordenação de Aperfeiçoamento de Pessoal de Nível Superior' (CAPES). So I would like to say a big thank you for the support of the Brazilian Government.

TABLE OF CONTENTS

LIST OF TABLES

LIST OF FIGURES

LIST OF ABBREVIATIONS AND ACRONYMS

ADCP	Acoustic Doppler Current Profiler
ADV	Advection Term in the Vorticity Equation
β**V**	Planetary Vorticity
CARS	CSIRO Atlas of Regional Seas
CCMP	Cross-Calibrated Multi-Platform
COSIMA	Consortium for Ocean-Sea Ice Modelling in Australia
CTD	Conductivity, Temperature, Depth
CW	Current Width
EKE	Eddy Kinetic Energy
ENSO	El Niño - Southern Oscillation
FRI	Friction Term in the Vorticity Equation
HE	Halmahera Eddy
HYCOM	Hybrid Coordinate Ocean Model
INSTANT	International Nusantara Stratification and Transport
IMOS	Integrated Marine Observing System
IOD	Indian Ocean Dipole
ITF	Indonesian Throughflow
KPP	K-Profile Parameterization
ME	Mindanao Eddy
MOC	Meridional Overturning Circulation
MWIR	Microwave and Infrared
NEC	North Equatorial Current
NECC	North Equatorial Countercurrent
NEMO	Nucleus for European Modelling of the Ocean
NGCC	New Guinea Coastal Current
NGCUC	New Guinea Coastal Under Current
NGDC	National Geophysical Data Center
OFAM3	Ocean Forecasting Australian Model version 3
SEC	South Equatorial Current
SECC	South Equatorial Countercurrent
SODA	Simple Ocean Data Assimilation
SOI	Southern Oscillation Index
SSH	Sea Surface Height
SSS	Sea Surface Salinity
SST	Sea Surface Temperature
Sv	Sverdrup (10^6 m^3/s)
TWT	Transport Weighted Temperature
WBC	Western Boundary Current
XBT	Expendable Bathythermograph

Chapter 1

The Indonesian Throughflow

The Indonesian Throughflow (ITF) is a unique cross-equatorial current providing the inter-oceanic connection between the Pacific and Indian Oceans (Figure 1.1). As part of the global circulation, the ITF provides an important pathway for the exchange of mass, heat and salt, and biogeochemical tracers between the two oceans. On the global scale, compared to other boundary currents, the ITF is a flow comprised of many different currents through various straits and has a total transport of 15 Sv (1 Sv $\equiv 10^6$ m^3/s; Sprintall et al., 2009). Although it plays a critical role in global thermohaline patterns and circulation (Hirst and Godfrey, 1993). The current flows through the complex topography region of the Indonesian Seas. The presence of several islands, shallow and deep pathways and narrow straits bounds the ITF to follow a complex and dynamically poorly understood pathway within the Indonesian Seas. For that reason, the ITF consists of a number of jets (Sprintall et al., 2009; Schiller et al., 2010; Sprintall and Revelard, 2014) that together form a boundary current constrained by topography.

The ITF has two distinct pathways with different inflow sources. The western pathway provides shallow, low salinity and relatively warm North Pacific water to the ITF (Gordon,

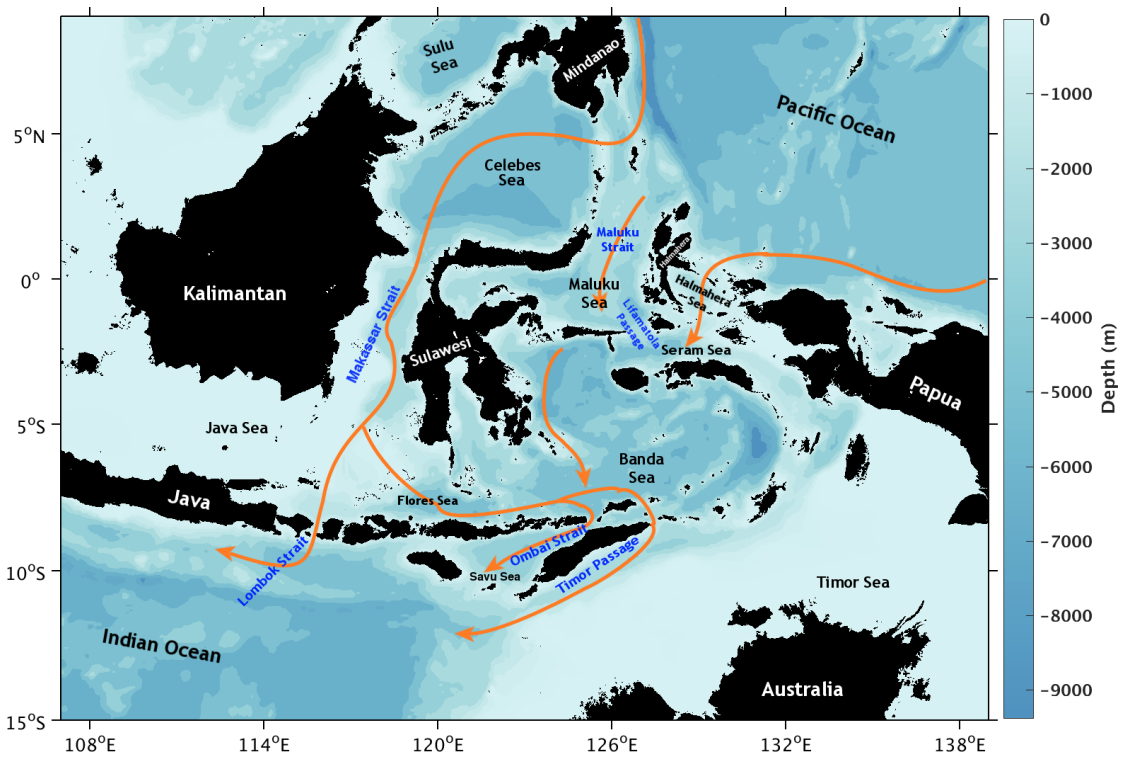

Figure 1.1: Indonesian Seas and the Indonesian Throughflow (ITF) pathway (arrows) with the names of the main islands, seas and straits in the region. Names of land places in white, seas in black and major passages in blue.

2005; Koch-Larrouy et al., 2008), with the Makassar Strait as the main channel (Wajsowicz, 1996; Sprintall et al., 2014) and circulates mostly thermocline water (Gordon et al., 2008, 2010b). The eastern pathway brings colder and saltier South Pacific water to the Banda Sea and is characterised by deep flows and strong mixing (van Aken et al., 2009; Koch-Larrouy et al., 2015). At the entrance to the Indian Ocean, observations show the ITF outflow partitions amongst the three major outflow straits, Lombok Strait, Ombai Strait and Timor Passage. Heat and saltwater transports are different in each outflow strait and thus exchanged properties depend on the partitioning, consequently affecting the contribution to the Indian Ocean. In this study, we explore the ITF circulation and local dynamics that determine the partitioning of the ITF.

Here we provide a brief introduction to the ITF. We present the ITF important role in the global circulation and climate (Section 1.1), the geography of the Indonesian Seas and

the ITF general circulation as it is currently known (Section 1.2) followed by a discussion on the ITF variability (Section 1.3). We introduce a theory for the ITF circulation (Section 1.4), and lastly, we summarise our goals for this Thesis, considering the gaps in the knowledge about ITF pathways and partitioning (Section 1.5).

1.1 ITF's role in the global ocean circulation and climate

The ITF has an essential role in the global ocean circulation, it impacts both the local and remote climate (Schneider, 1998; Schiller et al., 2010; Sprintall and Revelard, 2014) and affects the ecosystem of the surrounding seas (Talley, 2005; Castruccio et al., 2013; Ayers et al., 2014). The inter-basin exchange of heat and freshwater by the ITF impacts the Indian Ocean, which gets warmer and fresher at the expenses of the Pacific Ocean (Vranes et al., 2002). The exchanged waters are subject to local processes while in transit through the Indonesian Seas, such as mixing by internal tides, wind-induced mixing and transformation via atmospheric exchange. These processes are responsible for the modification of water masses (Ffield and Gordon, 1992, 1996; Sprintall et al., 2014). Changes in physical properties such as temperature and salinity have an effect on the thermohaline circulation (Wijffels et al., 1992; Gordon et al., 2010a; Sprintall et al., 2014) producing changes on the strength of the currents and sea surface temperature (SST) distribution (Kida and Wijffels, 2012). Highlighting the role of the ITF on regulating climate, the comparison of a normal ITF model simulation and a simulation with a complete blockage of the ITF passage, showed that the Indian Ocean is warmer and the Pacific Ocean is cooler due to the presence of the ITF (Hirst and Godfrey, 1993). Once in the Indian Ocean, the ITF waters influence the equatorial currents and the Leeuwin Current that flows southward along the west coast of Australia and brings tropical waters towards the pole (Domingues et al., 2007). ITF waters can reach as far as the eastern coast of Africa flowing across the Indian Ocean, as Song et al. (2002) showed with particles tracking in an ocean general circulation model (OGCM) study.

The ITF transports climate signals and their anomalies to the tropical oceans (Sprintall et al., 2014), as the ITF contributes to the surface branch of the Meridional Overturning Circulation (MOC; Shriver and Hurlburt, 1997). The ITF also affects atmosphere-ocean coupling and has a major influence on the Indian Ocean climate (Godfrey, 1996; Sprintall et al., 2003; Gordon et al., 2012). This in turn modulates the air-sea interaction, deep atmospheric convection and the monsoonal response. Locally, the monsoon regimes (Schott and McCreary, 2001; Wiggert et al., 2006) influence precipitation patterns that can be affected by the strength of the ITF (Fieux et al., 1994; Sprintall et al., 2014).

In terms of the ecosystems, the ITF is vital for larval dispersion and coral reefs biodiversity. They are influenced not only by the ITF transport but also by the ITF water properties and nutrient fluxes (Edinger et al., 2000; Ayers et al., 2014). Additionally, upwelling in the ITF region plays a role in the biodiversity and ecology of localised species, especially in coastal fisheries (Susanto et al., 2001), which are highly significant for the local economy.

1.2 Geography and circulation of the ITF region

The Indonesian archipelago (Figure 1.1) has a large number of landmasses that divide the region into passages and seas of varying depth. The main islands in the area which interact with the ITF pathway from the Pacific towards the Indian Ocean are Irian Jaya/Papua New Guinea, Mindanao and Halmahera at the entry from the Pacific Ocean. Sulawesi and Kalimantan define the main inflow passage for the ITF, the Makassar Strait. At the western exit to the Indian Ocean, the islands of Bali, Lombok, Nusa Tenggara and Timor Leste define the exit passages and small straits. The seas involved in the ITF pathway are, from the Pacific towards the Indian Ocean, the Halmahera Sea, Maluku Sea, Seram Sea, Celebes Sea, Java Sea, Flores Sea, Banda Sea, Savu Sea, and finally the Timor Sea. The straits that connect these seas are crucial for the ITF volume and properties transport; these are the

Lifamatola Strait, Makassar Strait, Maluku Strait, Lombok Strait, Ombai Strait and Timor Passage.

At the Indonesian Seas entrance, around 5°N 126°E, the circulation is complex (Figure 1.2). As part of this circulation, the South Equatorial Current (SEC) flows westward and meets the Australasia landmass where it bifurcates and forms the low latitude boundary currents. These currents flow towards the equator some which return eastward to the Pacific and the remainder enter the Indonesian Seas. In the North Pacific, the Mindanao Current flows southward as a reflection of the North Equatorial Current (NEC). The eastward North Equatorial Counter-Current (NECC) generates an eddy, the Mindanao Eddy (ME; Godfrey, 1996), which returns much of the water to the Pacific but some water enters the Indonesian Seas (Meyers et al., 1995). Studies of the ITF origin reveal that most of the contribution comes from the North Pacific (Godfrey et al., 1993; Koch-Larrouy et al., 2008) with a small flow from the South Pacific (Gordon, 2005). As a result, the Western Pacific is a leaky boundary (Fieux et al., 1994) and together, these two water sources (North and South Pacific) provide a connection between the western tropical Pacific and the Indian Ocean (Mayer et al., 2010).

1.2.1 ITF pathways

The main force driving the ITF is the difference in sea level between the Pacific and Indian Oceans (Wyrtki, 1987). Higher sea level at the Pacific side is a result of the westward trade winds, which pile up water in the western tropical Pacific (Sprintall and Revelard, 2014). This pressure gradient drives the flow through the complex topography of the Indonesian region. Besides that, given the topography constraint the ITF is also a meandering boundary current.

The Mindanao Current flows into the Celebes Sea first and then through the Makassar Strait. This strait is the primary inflow passage known as the western pathway. Downstream

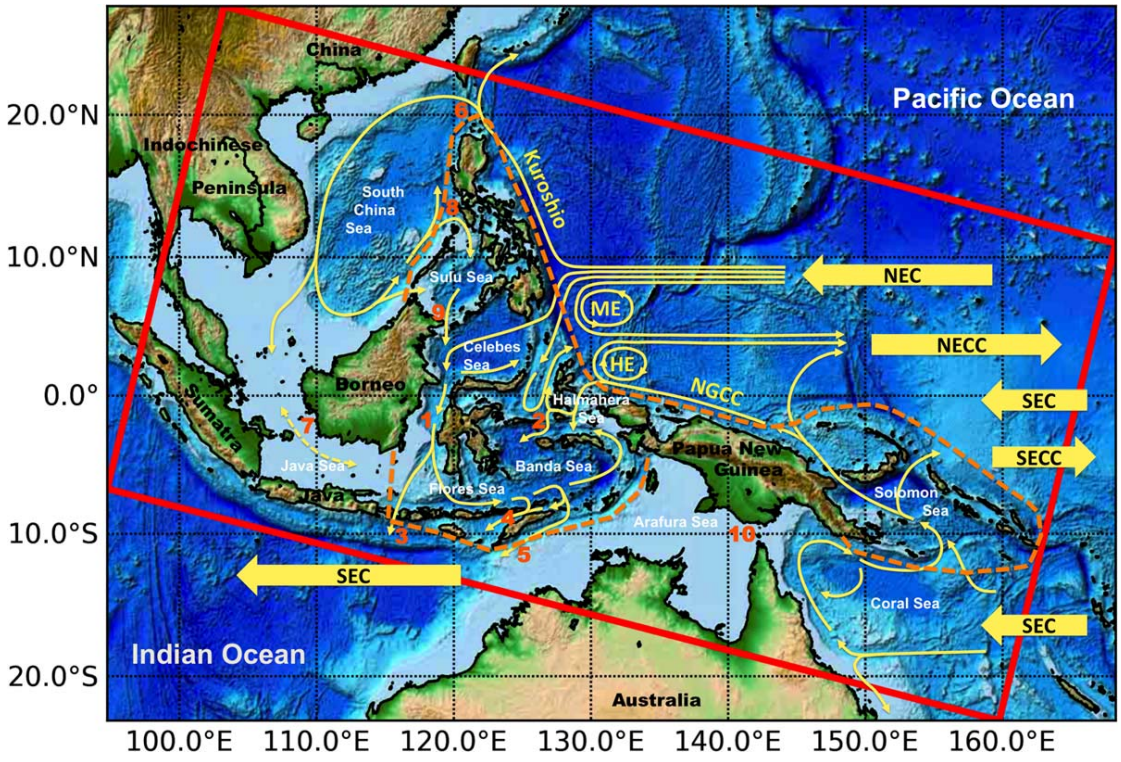

Figure 1.2: Circulation in the ITF area. Caption as in the original source (Castruccio et al., 2013) describing the Coral Triangle region: the dashed orange line delineates the Coral Triangle following Veron et al. (2009). Numbered passages are: (1) Makassar Strait, (2) Lifamatola Strait, (3) Lombok Strait, (4) Ombai Strait, (5) Timor Passage, (6) Luzon Strait, (7) Karimata Strait, (8) Mindoro Strait, (9) Sibutu Strait, and (10) Torres Strait. Abbreviations are: NEC, North Equatorial Current; NECC, North Equatorial Countercurrent; SEC, South Equatorial Current; SECC, South Equatorial Countercurrent; ME/HE, Mindanao/Halmahera Eddy; and NGCC, New Guinea Coastal Current. Figure from Castruccio et al. (2013).

of Makassar Strait, the flow encounters its first entrance to the Indian Ocean, the Lombok Strait, where a portion of the ITF exits. The remaining water flows eastward in the Flores Sea to the Banda Sea, eventually exiting to the Indian Ocean through the Ombai Strait and finally the Timor Passage (Sprintall and Revelard, 2014). The second inflow pathway of the ITF is the eastern pathway. Here, water from the New Guinea Coastal Current (NGCC) flows into the Indonesian Seas through Halmahera Sea, Maluku Strait and Lifamatola Passage. Water from the eastern pathway can only get to the Indian Ocean by Ombai Strait and Timor Passage (Figure 1.2).

The Makassar Strait is the main and westernmost passage for the inflow ITF. It carries

surface and upper thermocline waters from the North Pacific (Sprintall et al., 2003; Mayer et al., 2010). The secondary inflow channels, Lifamatola Strait in Maluku Sea and Halmahera and Seram Seas, are responsible for transporting the lower thermocline and deeper water masses from the South Pacific.

1.2.2 The ITF outflow passages partitioning

The INSTANT Program (International Nusantara Stratification and Transport) is the most reliable dataset that provided a consistent and simultaneous time series of transport estimates (Sprintall et al., 2003; Gordon et al., 2008; Sprintall et al., 2009; van Aken et al., 2009; Gordon et al., 2010b). It spans a period from January 2004 to December 2006 of full depth, *in situ* velocity, temperature and salinity profiles that correspond to a reasonable steady ITF as the sampling period is considered neutral in terms of climate modes of variability. This dataset provides the mean transports at the ITF outflow straits and is our reference for partitioning.

Makassar Strait carries between 5 - 15 Sv (around 80% of the total ITF, Gordon et al., 2008; Gordon, 2005). The mean flow in Makassar Strait, measured in the INSTANT Program, for the period between years 2004 to 2006, is 11.66 $\pm$ 3.3 Sv (Gordon et al., 2008). The upstream sill depth is 1300 m, and the sill depth in Makassar Strait is 680 m, which limits the depth of the western pathway ITF that consists of thermocline water (upper 1000 m).

The eastern ITF pathway, consisting of Maluku Strait, Lifamatola Passage and the Halmahera Sea, is not very well observed nor understood. It carries the remaining 20% of the ITF. The mean volume transport measured in INSTANT at Lifamatola Passage is 2.7 $\pm$ 1.3 Sv (van Aken et al., 2009). As the sill depth in Lifamatola Passage is 2000 m, this pathway contains the intermediate and deeper ITF (Gordon et al., 2008).

The total mean ITF inflow from INSTANT as the sum of the transports in both Makassar Strait and Lifamatola Passage is 14.3 Sv, and the sum of the outflows through the exit passages into the Indian Ocean measured by INSTANT was 15 Sv (Sprintall et al., 2009). The difference between the sum of the inflow and outflow (0.7 Sv) is because Lifamatola Passage is not the only inflow strait of the eastern pathway, and the two others, Maluku Strait and the Halmahera Sea, were not measured. The 15 Sv partition between the three main outflow straits as follows: Lombok Strait has a mean volume transport of 2.6 Sv, Ombai Strait has 4.9 Sv and Timor Passage has the largest amount of 7.5 Sv (Sprintall et al., 2009). This gives an approximate partitioning of 17%:33%:50% of ITF through the outflow straits.

Lombok Strait is at the end of a deep (1000 - 1200m) bathymetric trench in the Flores Sea. Lombok Strait provides continuity along the western boundary to the Makassar Strait flow, over the Dewakang sill south of Makassar Strait with a depth of 650 m, and is a direct link between the North Pacific Ocean water and the Indian Ocean. Lombok Strait is a 35 km wide channel and between 800 - 1000 m deep, but at the south end a small island, Nusa Penida, is connected to Lombok Island by a shallow 300 m depth and 20 km wide sill. This sill is crucial for the circulation in Lombok Strait as it constrains the flow. The vertical structure of the velocity in Lombok shows a western intensification of the current (Sprintall et al., 2009). Between the three outflows, Lombok Strait has the lowest percentage (17%) of the ITF entering the Indian Ocean.

To the east of Lombok Strait along the Nusa Tenggara island chain is Ombai Strait. It has a width of 37 km and depth of approximately 3250 m and is the second outflow for the ITF from Makassar Strait. Ombai Strait is located between the two islands Alor and Timor and is one of the deepest exit passages to the Indian Ocean (Molcard et al., 2001). Downstream of Ombai Strait two other passages Sumba and Savu/Dao Straits with depths of 900 m and 1150 m respectively, constrain the outflow from Ombai Strait to the Indian Ocean. In the INSTANT measurements, Sprintall et al. (2009) found that the velocity profile reaches 1200 m depth and shows two main features in the jet (Sprintall et al., 2009).

Timor Passage is the widest ITF exit strait and is the furthest east. It is 160 km wide, with depths ranging from 1250 to 1890 m and its location is to the south of Banda Sea. The vertical velocity profile for Timor Passage (Sprintall et al., 2009) shows a surface core in the upper 200 m depth. Different from Ombai Strait, INSTANT data shows a deeper secondary core around 1200 m. Between 1100 and 1400 m there is also a deep maximum (Molcard et al., 1996, 2001). Sprintall et al. (2009) also observed a much deeper flow at 1600 m in the opposite direction with high variability. At the three outflow straits, reversals of the flow have been previously observed and are related with variability.

There are a number of small passages between Lombok and Ombai Straits (e.g. Alas Strait, Flores Strait and Alor Strait), all believed to have small transports and generally neglected in observations. Therefore, their contribution to the ITF is considered to be small but remains uncertain. Koch-Larrouy et al. (2008) provided estimations for poorly observed narrow straits, for example, the Java route (0.8 Sv) and the Sulu route (0.4 Sv).

1.2.3 Forcing, tides and mixing in the ITF pathway

The Indonesian archipelago is also a region where Kelvin and Rossby waves reflect from the boundaries and contribute to biased estimates in ITF transport, even contributing to previously observed reversals (Schiller et al., 2010) and likely influencing mixing. In addition to that and the complex topography in the ITF region, intense tidal mixing and surface forcing enhance the ITF complexity. Along both western and eastern pathways, these processes influence the ITF by changing water mass properties such as temperature and salinity. Strong internal tides contribute to water mass modification (Ffield and Gordon, 1996), and they are more significant in the shallow areas of the Indonesian Seas than in other ocean regions (Koch-Larrouy et al., 2009). Whether these processes are more relevant in either the western or eastern pathway and what effect tides may produce in the outflow ITF affecting partitioning remain poorly understood (Sprintall et al., 2019).

The active air-sea fluxes and monsoonal wind-induced upwelling significantly contribute to mixing within the ITF region (Sprintall et al., 2014). The upwelling along the Java-Sumatra Indian Ocean coasts is a consequence of regional winds and the monsoon system. For example, during the southeast monsoon (June to August), when the winds are from the southeast (from Australia), upwelling takes place on the Indian side of the Java-Sumatra (Susanto et al., 2001). The opposite happens at the northwest monsoon when northwest wind results in upwelling close to Makassar Strait (Kida and Wijffels, 2012), on the northern side of the Java-Sumatra. The equatorial downwelling Kelvin waves, generated by the westerlies in the Indian Ocean during the monsoon transition periods, also influence upwelling processes in the region (Schiller et al., 2010).

The tidal driven mixing vigorously modifies the water properties of North and South Pacific water as it transits the Indonesian Seas (Sprintall et al., 2003; Koch-Larrouy et al., 2009; Sprintall et al., 2014). Most of the mixing occurs before the waters enter the Banda Sea with an eroded salinity structure observed already in Maluku, Seram and Flores Sea (Sprintall et al., 2014). Mixing modification mostly influences the properties of water that exit through the Ombai Strait and Timor Passage. This results in temperature and salinity characteristics of the water in Lombok Strait being significantly different from Ombai Strait and Timor Passage waters (Sprintall et al., 2003).

1.3 ITF Variability

The interaction between the Pacific and Indian Ocean basins and their modes of variability (e.g. El Niño and IOD) happens both through atmospheric teleconnections and the ocean link via the ITF. This atmospheric and ocean Indo-Pacific link has been studied in great detail (Wijffels and Meyers, 2004; Sprintall et al., 2009; Metzger et al., 2010; Sprintall and Revelard, 2014). The large number of modes of variability makes understanding of the ITF dynamics

puzzling as they can overlap each other, amplifying their effects or act in opposing ways and modulate or cancelling each other (Sprintall et al., 2009; Schiller et al., 2010; Sprintall and Revelard, 2014).

The ITF responds to remote wind forcing from the Pacific and Indian Oceans and local winds (Schiller et al., 2010). El Niño – Southern Oscillation (ENSO), Indian Ocean Dipole (IOD), Madden-Julian Oscillation (MJO) and Pacific Decadal Oscillation (PDO), acting remotely along with the reversal of the local winds following the monsoon, influence the strength and dynamics of the ITF (Schiller et al., 2010). Wind anomalies in the Indian Ocean associated with the IOD, for example, influence the ITF volume transport in the outflow straits. The mechanism by which the IOD controls the outflow transport is due to wind anomalies that excite Kelvin waves. These waves reach the west coast of Sumatra and propagate along the south coast of Java, continuing along the southern side of the Nusa Tenggara island chain (Wijffels and Meyers, 2004). Lombok and Ombai Straits show reversals in the flow as a consequence of these Kelvin waves (Sprintall et al., 2009; Schiller et al., 2010).

The reversing wind of the Asian-Australian monsoon drives seasonal variability (Sprintall and Revelard, 2014). The monsoonal system affects ITF transports; larger ITF transport is observed during the southeast monsoon (June to August) as the wind drives substantial Ekman divergence from the internal seas (Sprintall et al., 2009), and the opposite happens during the northwest monsoon (December to February). The seasonal variability affects each strait differently and can also be modulated by the intra-seasonal MJO. The Kelvin waves from the Indian Ocean and Rossby waves from the Pacific propagating along the equator to the Indonesian Seas can contribute to variability in the intra-seasonal band too. At all levels, Makassar and Timor throughflow are relatively steady, in comparison to Lombok and Ombai, which are rich in intra-seasonal oscillations (Gordon et al., 2010b).

1.4 Theory of the ITF circulation

Although a significant amount of studies have already been done on the variability of the ITF (Sprintall et al., 2003, 2009; Sprintall and Revelard, 2014; Sprintall et al., 2014), there are still remaining questions. Considerable challenges remain to tease out the individual effect of each climate mode on the ITF variability (Sprintall and Revelard, 2014) but even understanding the steady-state is not clear yet. Limited studies have been done to understand the mean circulation and dynamics of the steady ITF.

The western boundary current theory (WBC) explains the western intensification of the return currents on the boundary. The circulation in the North and South Pacific Ocean, as in other ocean basins is primarily driven by the wind and is dominated by two large gyres. The return flow is a strong current in the western side of the basin, which colorred represents the western intensified boundary current, explained by the simplistic approach in the Sverdrup relation (Sverdrup, 1947). The ITF is a boundary current that is part of this return flow in the Pacific Ocean gyre, as an extension of Mindanao Current (Figure 1.2). Therefore, it is expected that all or most of the flow should exit through Lombok Strait. However, the presence of an island changes the behaviour of a WBC as noted by Godfrey (1989). The Island Rule was one of the first approaches to estimate the ITF transport based on the WBC theory. An early analytic model study of the ITF applied this rule, estimating an ITF of 16 $\pm$ 4 Sv (Godfrey, 1989).

The eastward flow direction in the Flores and Banda Seas, after a portion of the western pathway ITF exits at Lombok Strait, shows there are unexplained dynamics at the outflow ITF. Lombok Strait is the continuation of the western pathway and directly connected to Makassar Strait. From the INSTANT partitioning, we see that only a small portion flows through Lombok Strait. The remaining, which is most of the outflow transport, exits to the Indian Ocean by the eastern passages, Ombai Strait and Timor Passage. The reason why

the mean transports in Lombok Strait, Ombai Strait and Timor Passages are 2.6 Sv, 4.9 Sv and 7.5 Sv respectively, with a mean partitioning of 17%:33%:50% has not been explored and remains an open question. Considering that, for this study, we simplify the system by removing the ITF variability to look at the steady-state, focusing on understanding the mechanism that results in the partitioning of the ITF at its exit passages.

1.4.1 Previous modelling efforts on the ITF circulation

A variety of modelling studies have been conducted to understand the ITF. From simple models of an electrical circuit analogy (Wajsowicz, 1996), idealised simulations of gaps in a wall to reproduce chocked flows (Nof, 1995; Wang and Yuan, 2012, 2014) and global models (Schneider, 1998; Potemra et al., 2003; Metzger et al., 2010; van Sebille et al., 2014; Nagai and Hibiya, 2015). These modeling studies employ varying resolutions and range from idealised to realistic to explore the impacts of the ITF on the global and regional circulation. The present study considers an idealised steady ITF for understanding its partitioning and behaviour as a boundary current. Here we give a brief description of some important modelling studies that motivate our study.

Nof (1995) used an idealised model to simulate the flow between two oceanic basins with a meridional wall with a gap to represent the choked connection, similar to the Indonesian islands and the ITF. He suggests the widths of the Indonesian straits are too large to allow the hydraulic control but also too narrow to allow free flow through them. The flow is choked and only a fraction of a typical western boundary current transport enters the passages. As a comparison to electrical circuits, Wajsowicz (1996) demonstrate that the westernmost strait carries the ITF transport up to a friction-determined limit and so on eastward until it finds a large passage that provides no resistance. Wang and Yuan (2012, 2014) also did an idealised study focusing on the complex topography (Gordon et al., 2003) at the entrance of the Indonesian Seas. Due to the presence of the large landmass (Australasia), it interrupts

the circulation and creates a condition for the collision of two western boundary currents at a gap, forming the ITF. They show that the WBC may extend into a gap and the proportion of each current depends on the strength of the boundary current.

Those previous modelling studies did not focus on the steady ITF. Many aspects regarding the fundamental and local dynamics still need to be explored in terms of modelling this region of the world.

1.5 This PhD project goals and outline

How the ITF waters partition between the different routes and straits is critical to the net heat and freshwater contribution to the Indian Ocean. Different mixing processes along the circulation pathway through the Indonesian Seas and the multiple choice of straits the flow exits to the Indian Ocean, affect the water properties. The outflow straits, in turn, can have different heat and freshwater content. The heat exchange between ocean basins is crucial for understanding climate change and variability. Given that ITF partitioning is poorly explained, the main goal of this Thesis is to understand what controls partitioning.

The ITF is a boundary current and the western pathway directly connects to the westernmost ITF outflow, Lombok Strait. However, this strait has the lowest outflow transport even though it is expected to carry most of the flow as the western boundary current theory predicts. No previous study investigated the partitioning dynamics. To be able to explore the controlling dynamics in the exit passages, we exclude the complexity of variability and initially focus on the balance of a steady ITF and its relation to the various pathways and the complex topography. We develop a high-resolution regional model that can resolve the partitioning between the passages to simulate the steady current. Modelling also allows simulations in which components of the dynamics can be considered separately to simplify

the system. Our primary concern is to represent the passages with realistic topography, as it may be essential for resolving partitioning. The INSTANT data is our reference for the simulation of a steady ITF, given that it sampled the ITF during a relatively neutral period. We will also explore the circulation of the ITF in the mean state. Lastly, we revisit inter-annual variability based on what we learned from the simpler steady-state theory for the partitioning.

This Thesis is structured as follows:

- Chapter 2 introduces the tool we use for this study, the high-resolution regional model for the steady ITF using MITgcm (Table 2.2), along with the configuration of our perturbation experiments (Table 2.3).
- Chapter 3 presents a description of the control run for the steady ITF, introduced in Chapter 2. We discuss the western and eastern pathways of the ITF, and present a refined view of the system through vertical pathways, with an upper layer and a deep layer circulation.
- Chapter 4 explores what controls the partitioning, defined here as the fraction of Makassar Strait water that flows through Lombok Strait. Using a reduced gravity 1.5 layer model and perturbation experiments, we show that current width controls partitioning. Furthermore, we explain the changes in current width with a vorticity budget for the ITF western pathway. According to this budget, current width is set by non-linearity, as the leading order balance is between advection of vorticity (non-linear terms) and the change in planetary vorticity.
- Chapter 5 tests our theory linking current width and partitioning in a global model with full-variability forcing. We focus on the ITF inter-annual variability and explore how the concept of partitioning applies to other choke points along the ITF pathway. Overall we also discuss implications for the circulation in the internal seas.
- Chapter 6 provides a conclusion and presents suggested future work.

Chapter 2

The Indonesian Throughflow Regional Model

To investigate the mean Indonesian Throughflow (ITF) we develop a high-resolution regional model for the Indonesian Seas using a hydrostatic configuration of the MITgcm (Marshall et al., 1997a,b). The model domain that represents the Indonesian Seas is bounded by 107°to 139°W and 15°S to 9°N (Figure 1.1). Given our interest on exploring possible interactions with the complex topography of the area and the local dynamics controlling the ITF transports, we aimed for a good representation of the straits and chose a 4-km resolution in order to accurately reproduce the regional processes influenced by topography.

We simulate a steady state ITF and as a first approach we develop a reference setup we call the control run. Our control run of the ITF considers an idealised current (without variability in the forcing) in a non-linear configuration with non-slip condition at the boundaries. In this Chapter we provide a detailed description of the control run and later, in Chapter 4, we present sensitivity experiments.

2.1 Model Setup

The near-global eddy resolving model Ocean Forecasting Australian Model v3 (OFAM3), has an Indonesian Seas circulation consistent with observations (Oke et al., 2013). The 18-year averaged ITF volume transport in OFAM3 are -1.9, -3.4 and -7.6 Sv in Lombok Strait, Ombai Strait and Timor Passage, respectively. The partitioning between these exit passages is 15%:26%:59% (Lombok:Ombai:Timor), calculated from the volume transports. This relation agrees well with the observed partitioning of 17%:33%:50% from the INSTANT 3-year average (Sprintall et al., 2009). Time series of velocity compare well with the observations, including the observed reversals at the exit passages from INSTANT data (not shown). For those reasons, we use OFAM3 outputs as boundary conditions for our regional ITF model.

The OFAM3 is run at 10-km resolution, a good choice for a global model for studying large scale ocean circulation. However, in order to resolve important details in the bathymetry and study regional processes and local dynamics, we run our regional model with 4-km resolution. This allows improved resolution of the narrow channels and straits along the ITF pathway. For example, Lombok Strait is 35 km wide, which means at 10-km resolution the strait is represented by just three grid points. In our regional ITF 4-km model, Lombok Strait is represented by nine grid points (Table 2.1), better resolving the boundaries that interact with the jet and thus the dynamics that control the flow, since higher resolution impacts the structure of western boundary currents (Kiss et al., 2019).

Passage	**Width (km)**	**OFAM3 10km**	**ITF model 4km**
Lombok	35	3	9
Ombai	37	4	10
Timor	160	16	40

Table 2.1: Total number of grid points covering the channels in the 10-km OFAM3 global model and in the 4-km resolution ITF regional model.

Setup details of our model can be found in Table 2.2 and are as follows: the model horizontal resolution is 1/25° (4-km) and the vertical resolution follows an exponential function with 2 m resolution at the surface increasing to 260 m at depth (4.5 km). We use OFAM3 to provide the forcing at the open boundaries, where the boundary conditions are velocity, temperature and salinity fields averaged over three years from 2004 to 2006 and interpolated into our regional model grid. As our goal is to investigate a steady ITF, we simulate the current using constant forcing in time which is the three years average for all variables, including wind. The selected years have observational data available for the ITF outflows from the INSTANT Program, hence they can be used for comparison.

Control Run Model Setup	
Topography	ETOPO2 v2 - 2' gridded
Model grid horizontal resolution	4-km
Model grid vertical resolution	2 m at surface to 260 m at depth
Initial/Boundary conditions	Ocean Forecasting Australian Model v3 (OFAM3) 1/10°
Relaxation time	3 days
Vertical mixing	10^{-5} m^2/s
Vertical viscosity coefficient	10^{-3} m^2/s
Mixing parameterization	KPP
Boundary conditions	non-slip
Viscosity parameterization	A_H (lateral eddy viscosity) and Smagorinsky scheme
Advection of momentum	non-linear
Wind stress	Cross-Calibrated Multi-Platform (CCMP)

Table 2.2: (top) Common features of the regional model setup and parameters for the control run and for the sensitivity experiments. (bottom) Characteristics of the control run.

The regional model topography is from the high-resolution data ETOPO2v2 from the National Geophysical Data Center (National Geophysical Data Center, 2006), presented in Figure 1.1 in Chapter 1. The model timestep is 90 seconds. The initial conditions are also derived from OFAM3 by spatially averaging temperature and salinity vertical profiles within the regional domain, to avoid the initial transient adjustment of OFAM3 field to new bathymetry. At the surface, SST and SSS are restored to OFAM3 time means fields. Given that the uppermost grid cell is 2 m resolution at the surface, the restoring time scale is three days (Haney, 1971). The wind stress is derived from a higher resolution data source,

the Cross-Calibrated Multi-Platform (CCMP) gridded surface vector winds from satellite, moored buoy, and model wind data (Wentz et al., 2015), instead of the OFAM3 averages (in OFAM3 the momentum fluxes are derived from ERA-Interim; Dee and Uppala, 2009). CCMP wind product has high spatial (0.25°) and temporal (6-hourly) resolutions, which is spatially more appropriate forcing field for our high-resolution regional model. We use sponges of 2°extension at the boundaries. In the sponges, model fields are restored to open boundary values on a time scale changing from ten days in the interior to one day at the boundary.

For the model parameterization we have a constant vertical mixing coefficient of 10^{-5} m^2/s, for uniform background mixing. The mixing in the Indonesian Seas varies for different areas with stronger mixing coefficients between 5×10^{-4} and 5×10^{-1} m^2/s (Koch-Larrouy et al., 2015). In the center of Banda Sea values are similar to open ocean mixing (10^{-6} m^2/s). In the regional high-resolution model we use a constant value since water masses and mixing processes are not the focus of this work. To represent the upper ocean mixed layer we use K-Profile Parameterization (KPP) mixing schemes (Large et al., 1994). The regional model also has a Smagorinsky horizontal viscosity scheme (Smagorinsky, 1963), which is resolution dependant, reducing viscosity as resolution gets higher (Griffies and Hallberg, 2000). The vertical viscosity is 10^{-3} m^2/s (Table 2.3).

For completeness, we present here the specific setups for the perturbation runs in Chapter 4 (Table 2.3). The perturbation experiments include changes in lateral boundary conditions, non-linearity, local wind and lateral friction to evaluate their effects on the ITF partitioning. The linear experiments showed in Table 2.3 as 'non-linearity off' mean those runs do not include non-linear terms (advection of momentum) in the model solution. To change friction, we superimposed a constant lateral eddy viscosity $A_H = 1000$ m^2/s on the top of the Smagorinsky scheme viscosity, in order to have increased friction.

The model is run for eight years (Figure 2.1). The velocity field rapidly adjusts to the

Experiment	**slip boundary**	**constant lateral eddy viscosity A_H (m^2/s)**	**non-linearity**	**wind stress**
non-linear slip	on	0	on	CCMP
linear non-slip	off	0	off	CCMP
linear slip	on	0	off	CCMP
>friction non-slip	off	1000	on	CCMP
>friction slip	on	1000	on	CCMP
2xWind	off	0	on	CCMPx2

Table 2.3: Sensitivity experiments model setup. Experiments with lateral eddy viscosity A_H=1000 m^2/s means we superimposed a constant lateral eddy viscosity on the top of the viscosity from Smagorinsky scheme.

new topography and the forcing (one year). For the thermodynamics the equilibrium time is much longer as it depends on slower diffusive processes. Kinetic energy (KE) for the monthly averaged fields show the initial adjustment of 12 months for the upper ocean (0 - 1000 m) and around two years for the deeper ocean (Figure 2.2.a). The upper ocean kinetic energy also shows the model intrinsic variability. The model heat content reaches equilibrium after approximately 18 months (Figure 2.2.b). The minor drift in the deeper ocean is acceptable, given that the initial condition for temperature is the mean vertical profile. This is not significant for this study as the ITF is a surface intensified current and from the point of view of the circulation this small drift at depth has a likely negligible effect.

For the perturbation experiments to adjust, we allow them to run for extra six months, after year five (Figure 2.1). The perturbation runs start at the end of year five of the control run. The next six months (second semester of year 6) composes our analysis period. We use daily average outputs in this study.

Although the model has reached equilibrium, it still contains intrinsic variability. We check the eddy kinetic energy (EKE) for the averaged period between years five and six of the spin-up (indicated as 'intrinsic variability check' in Figure 2.1). The EKE is calculated from velocity anomalies, calculated with respect to the mean of the last three years of the spin up run, which represents the long term mean (Equation 2.1). The EKE is dominated

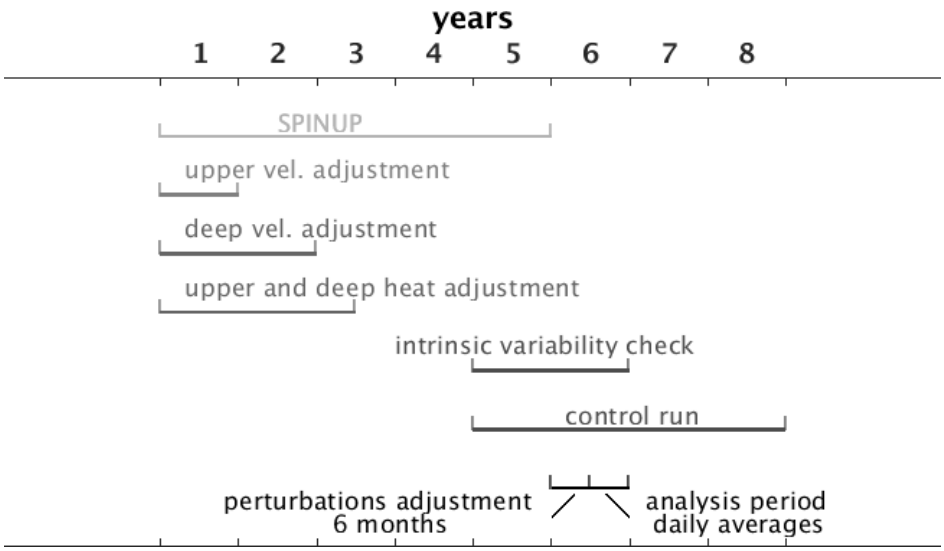

Figure 2.1: Diagram of the model runs periods. The spinup is five years. The intrinsic variability check is for years five and six. The analysis period is the last six months of daily averages, from of year six.

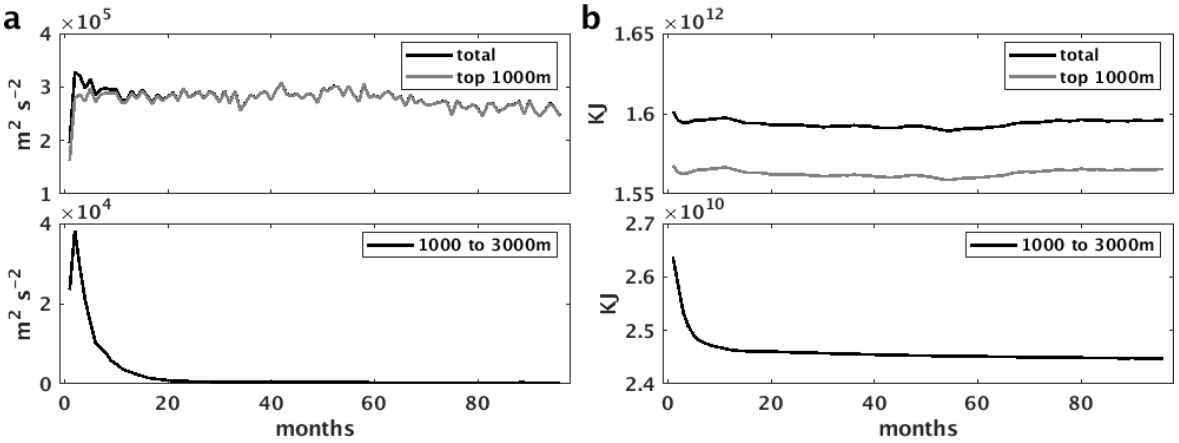

Figure 2.2: Averaged model (a) total kinetic energy and (b) total heat content timeseries in the upper and bottom ocean for eight years of spin-up run.

by the turbulent energy from eddies in the Celebes Sea and Pacific Ocean, generated by the internal variability in the model. The two areas of high EKE, in the Pacific Ocean is where Halmahera and Mindanao Eddies interact and in the Celebes Sea permanent gyres (Figure 2.3). Elsewhere, EKE is low. Based on the distribution of EKE we choose three points along the ITF pathway to further analyse the nature and magnitude of this intrinsic variability in the model.

We extract three points on the ITF pathway to evaluate variability (one in the south of Celebes Sea, one close to the chocking point of Makassar Strait and one in between Ombai and Timor Strait; Figure 2.3). The timeseries of U and V velocity components show the intrinsic variability (Figure 2.4.a). A spectral analysis of the sixth year timeseries of daily averages from the control run showed the six months period captures the intrinsic variability in the model. The spectra of the speed shows the percentage of the variability contained in periods shorter than 60 days is high (Figure 2.4.c). The lowest frequencies with the highest power are between 30 and 60 days (or 0.033 and 0.017 cycles/day). Therefore the six months period is enough to capture the ITF model's intrinsic variability ITF variability.

$$U' = U - \overline{U}_{yr_{5\&6}}; V' = V - \overline{V}_{yr_{5\&6}}$$
$$\overline{EKE}_{yr_{5\&6}} = \frac{\overline{U'^2_{yr_{5\&6}} + V'^2_{yr_{5\&6}}}}{2} \tag{2.1}$$

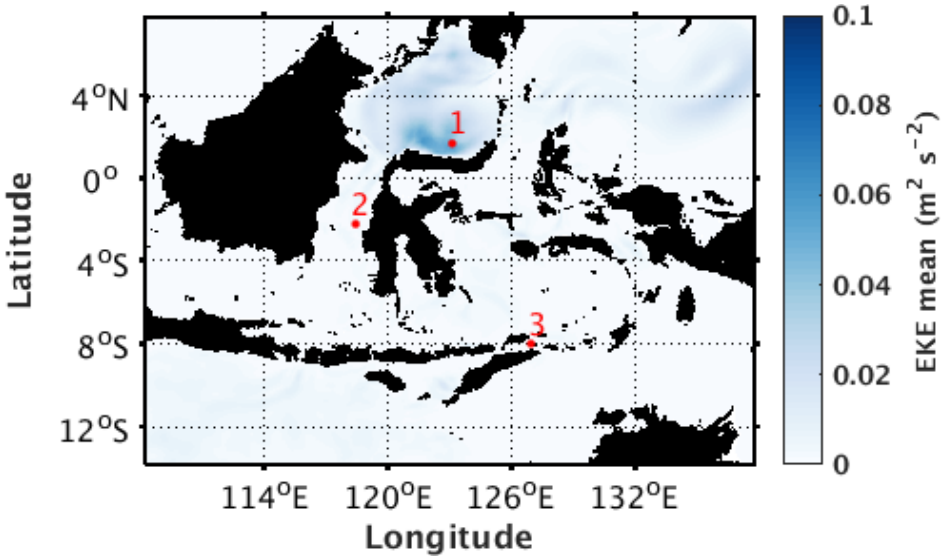

Figure 2.3: Surface mean Eddy Kinetic Energy (EKE) for years 5 and 6 of the spin up run. The three points indicated on the maps are where we do further spectral analysis.

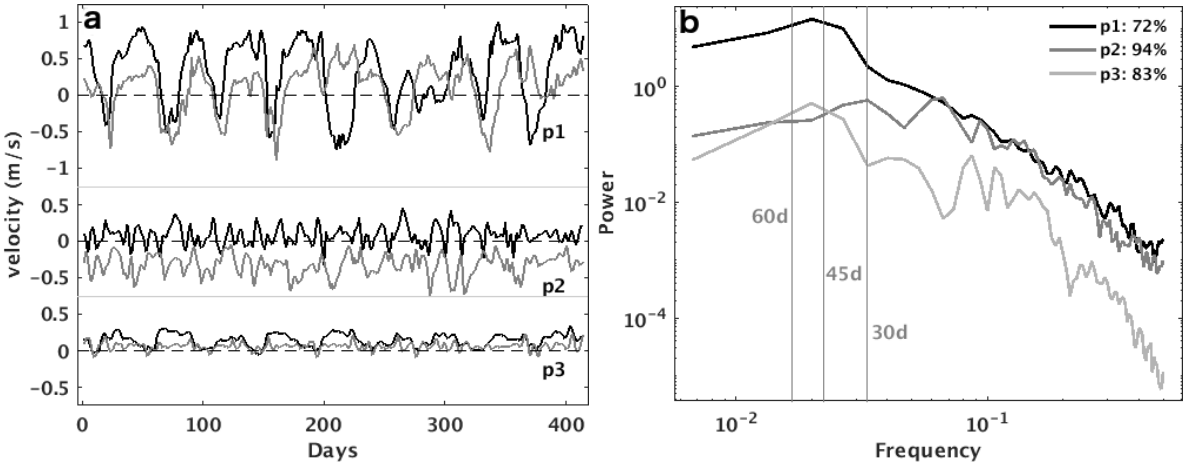

Figure 2.4: (a) Timeseries of U (black line) and V (grey line) for the three points along the ITF pathway indicated in Figure 2.3. p1 is at the southeast of Celebes Sea, p2 is at the choking point in Makassar Strait and p3 is in between of Ombai Strait and Timor Passage. (b) The power spectra for each timeseries. The spectra represents both velocity components U and V for each point. The percentage of the energy contained in periods shorter than 60 days for each point is indicated.

2.2 Model Validation

Here we compare mean fields from the regional ITF model to OFAM3 outputs and to available observations. We expect the regional model to reproduce large scale features similar to OFAM3 while also including the regional intrinsic variability due to local dynamics. Further comparisons with observation allow us to identify possible biases and to understand the model's limitations. We provide comparisons for surface temperature and velocity fields, transports in the main passages and the vertical structure of the flow. The datasets we use are climatology from CSIRO Atlas of Regional Seas with resolution of 1/2°grid (CARS; www.cmar.csiro.au/cars), satellite sea surface temperature from microwave and infrared data with 9 km resolution (MWIR SST; www.remss.com/measurements/sea-surface-temperature/oisst-description) and INSTANT mooring data (Sprintall et al., 2009; Gordon et al., 2010b).

2.2.1 Surface temperature and velocity fields

We use 3-year (from years five to eight) mean fields from the regional ITF model control run to compare with the 3-year mean fields from OFAM3 for the INSTANT period we used to generate the forcing for the regional ITF model (years 2004 to 2006). For temperature we compare to CARS climatology and MWIR SST climatology.

Temperature

Mean temperature from CARS and satellite SST show similar features (Figure 2.5.c and 2.5.d). The warmer region to the northeast of the domain represents the North Pacific warmer waters that enters the Indonesian Seas. Warmer waters are also found near the equator especially in the Gulf of Sulawesi. In the shallow waters around Kalimantan and in Celebes Sea the temperatures are higher than in the south of the domain. The colder spots just south of Nusa Tenggara islands chain and downstream of the outflow passages Lombok and Ombai Straits show the influence of monsoon driven upwelling. In Banda Sea temperatures are lower (but less cold than south of Nusa Tenggara). These colder waters are connected to the Arafura Sea and the Gulf of Carpenteria.

In general, OFAM3 and the regional model mean fields are very similar. This similarities are expected since SST in the regional model is restored to OFAM3. The models' surface temperature pattern (Figure 2.5.a and 2.5.b) are similar to the observations but temperatures are on average higher by approximately one degree (Figure 2.5.c and 2.5.d). In this area, global models generally are warmer due to high-frequency wind variability and unresolved ocean dynamics (Wang et al., 2014; Clement et al., 2005; Nagai and Hibiya, 2015). This can also be explained by the effect of seasonality on regulating the temperature. There is cooling associated with upwelling processes along the north and south of Nusa Tenggara chain (Kida and Wijffels, 2012), which is smoother in the models as it represents the 3-year mean and the

constant forcing. The north inflow just east of Mindanao is characterised by colder waters than the surroundings, a feature not seen in the observations.

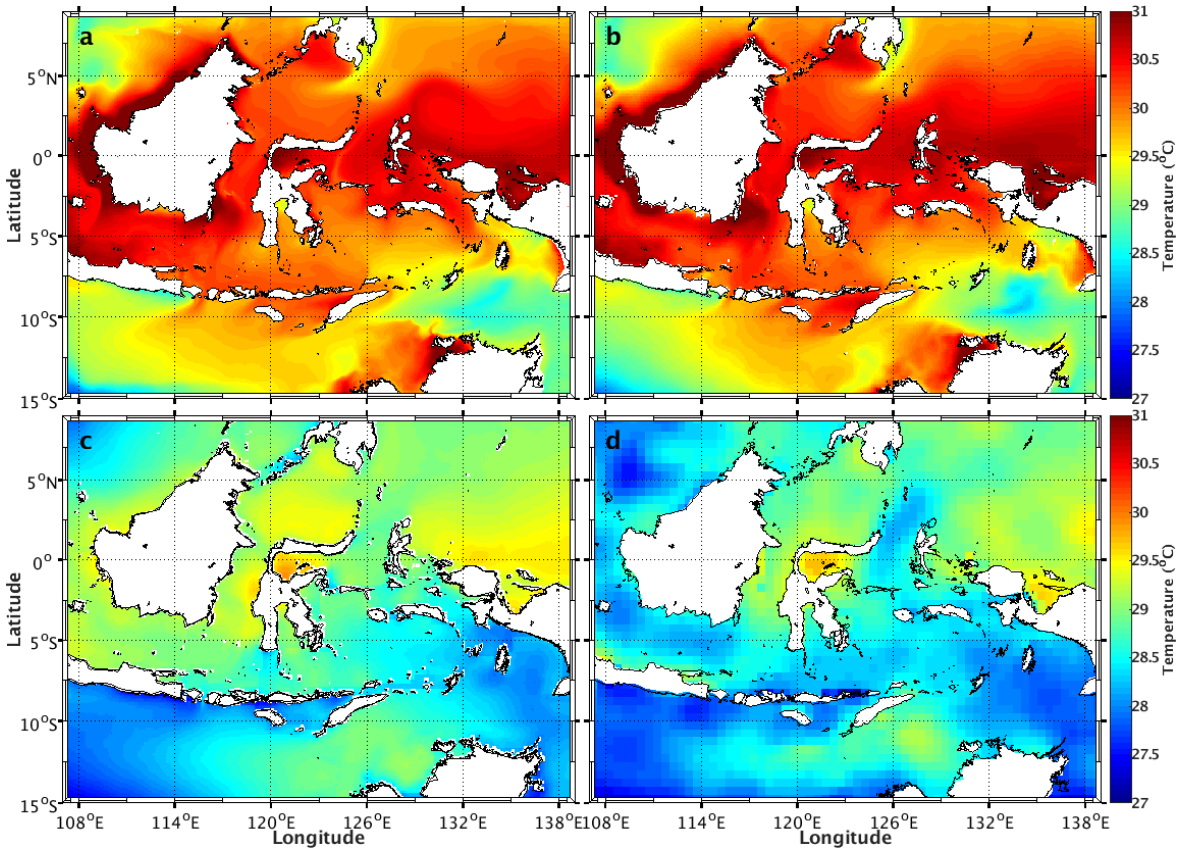

Figure 2.5: Mean surface temperature from 3-year mean from (a) the regional ITF model 4km resolution, (b) OFAM3 mean for INSTANT period, (c) MWIR Climatology and (d) CARS Climatology.

Speed

Altimetry in the ITF area do not provide reliable products due to the high frequency of wind-forcing in shallow seas, that are potentially aliased in the frequency of the satellite timing. Therefore we use only the model speed to compare both models. The regional ITF model and OFAM3 surface speed comparison shows that the currents have more detailed features in the high-resolution model (Figure 2.6). More intense jets are also seen in the regional model. In both models we see the main ITF pathway, starting from meandering flows

in the western Pacific and entering the Indonesian Seas mainly by the north boundary east of Mindanao (around 7°N and 126°E), the eastern flow in Maluku (around 1°N and 126°E) and Lifamatola Straits (around 2°S and 127°E). The eastern ITF pathway has stronger jets in the regional model compared to OFAM3. In Makassar Strait, the jet is stronger in the regional model than in OFAM3, and a continuous jet is found along the boundary (around 1°N and 119°E) in both models. A recirculation feature just north of Ombai Strait in the regional ITF model, absent in OFAM3, show differences between models in Banda Sea (5°S, 126°E). The outflow jets are also stronger in the regional model than in OFAM3, with the exception of the jet in Timor Passage, which is faster in OFAM3.

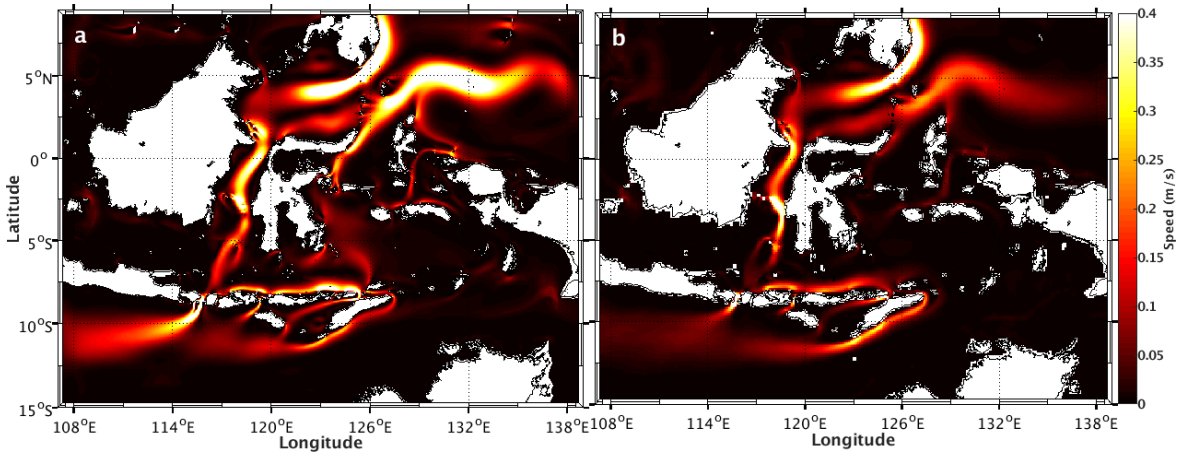

Figure 2.6: Mean speed from the (a) regional ITF model 4km resolution and (b) the INSTANT period in OFAM3.

2.2.2 Transports in the ITF outflow straits

Volume transport timeseries estimated from OFAM3 for the INSTANT period show more variability than the regional model forced with steady fields (Figure 2.7). OFAM3 timeseries has variability at different time scales, especially seasonal and intra-annual. Inter-annual variability is supposed to be reduced during those 3-year, given that the INSTANT years were a relatively neutral period in terms of climate modes of variability. Sources of variability at those time scales are not included in our runs, thus the regional model only represents

the mean state of the ITF. Here we compare the mean transports. The transport in Timor Passage for the regional model is the only one with a large difference to OFAM3 transports. It is the most downstream strait for both western and eastern pathway so it is suggested that Timor Passage accumulates any differences further upstream. Also Timor Passage is the largest strait and because of resolution dependency it is the strait that reflects the differences most.

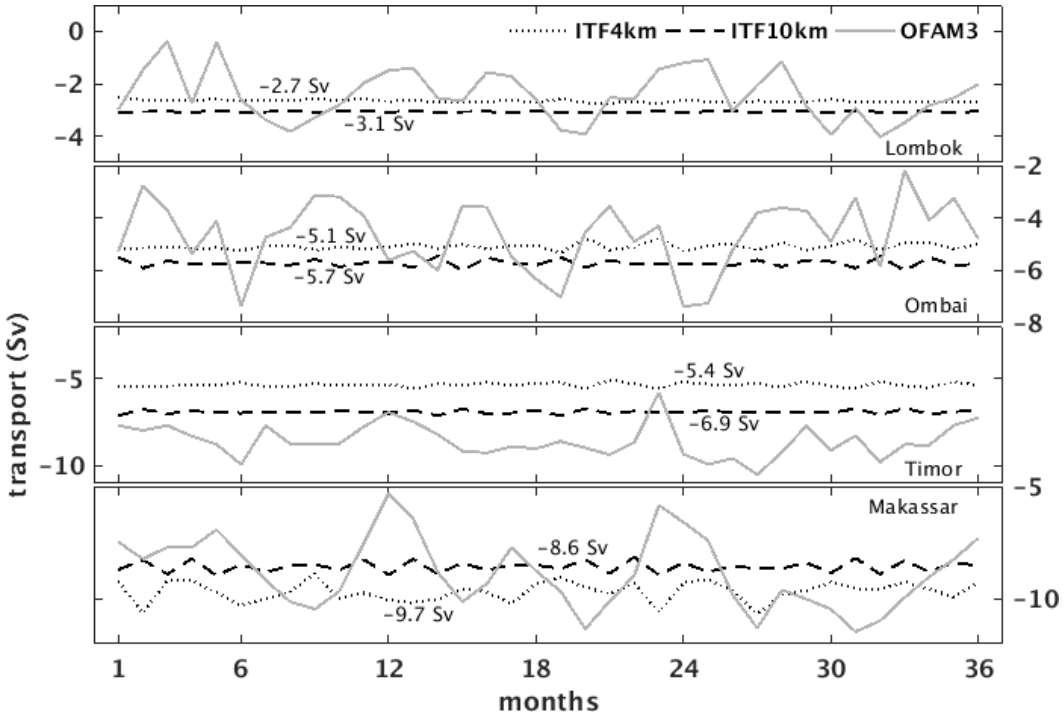

Figure 2.7: Volume transport timeseries in the three ITF exit passages, Lombok Strait, Ombai Strait and Timor Passage, for the 3-year period of INSTANT Program for OFAM3 (solid grey) and for the regional model control run (years five to eight) in two versions, a high-resolution of 4-km and a lower resolution of 10-km, in dotted and dashed black, respectively. The numbers are the transport averages for both resolutions and they are closer to the line of the respective model.

We run a 10-km resolution version of the ITF regional model to observe the effect of resolution on the transports at the straits. The lower resolution version of our ITF model shows similar ITF transport to OFAM3 (15.7 Sv and 15.5 Sv), as well for the inflow passages (8.6 Sv and 8.8 Sv in Makassar Strait). However, the distribution between the outflow straits is different (Table 2.4). We compare the mean transports at the straits between both resolution versions on Figure 2.7. The 10-km resolution version of the ITF model has higher transport in all three outflow straits than the 4-km resolution, and lower only at Makassar

Strait. Here we see that resolving the straits topography indeed influence the transports. We are not able to say which resolution gives more realistic transports, but because topography is important for a boundary current and can affect how the flow interacts with the straits, we decide to use the higher resolution.

The mean ITF volume transport estimated from INSTANT data (15 Sv in Sprintall et al., 2009; Gordon et al., 2008) are compared to the mean transports calculated from OFAM3 (15.5 Sv) and the regional model (13.2 Sv). Transports in the main ITF passages (Table 2.4) show that the regional model agrees reasonably well with INSTANT. Transport in Lombok Strait is similar for both models (-2.4 Sv in OFAM3 and -2.7 Sv in the regional model), also similar to INSTANT data (-2.6 Sv). In Ombai Strait, mean transport is also comparable to the observed transport from INSTANT. The largest differences between models and model and observations are in Timor Passage (the easternmost passage). In OFAM3 the mean transport is -8.5 Sv, 1 Sv higher than the transport estimated in INSTANT (-7.5 Sv). For the regional model the mean volume transport in Timor Passage is -5.4 Sv, 2.1 Sv lower than INSTANT observation. This difference is approximately the same as the difference between the total ITF transport. In Makassar Strait there are also small differences between the regional model and INSTANT (-9.7 Sv versus -11.6 Sv) and OFAM3 (-8.8 Sv). However, the transport distribution at the straits is within the uncertainty in the observations. Both OFAM3 and the regional model (in both resolutions) show the expected pathways for the main ITF and similar partitions between the exit channels (Lombok:Ombai:Timor - 17:33:50 in INSTANT, 15:26:59 in OFAM3 and 20:39:41 in the regional 4km ITF model).

Both observations and the model OFAM3 show similarities and differences to our regional model. The inflow is lower for the regional model and this an issue attributed to the interpolation of the boundary conditions to generate the forcing. We are considering the inflow as the sum of the outflow straits and the 4-km resolution resolves the small straits topography, which may be closed at the 10-km version. Therefore, these transports are included in the three main straits outflow at the 10-km version of the regional model. Lombok

Passage	INSTANT	OFAM3	ITF model 10-km	ITF model 4-km
Makassar	11.6	8.8	8.6	9.7
Lifamatola	2.5	2.8	2.3	2.1
Lombok	-2.6	-2.4	-3.1	-2.7
Ombai	-4.9	-4.6	-5.7	-5.1
Timor	-7.5	-8.5	-6.9	-5.4

Table 2.4: Mean volume transports from INSTANT, OFAM3 and the regional ITF model at the main inflow passages and the three exit passages. All three datasets contain a three year mean corresponding to the INSTANT years. For the regional model the mean here is from years six to eight of the spin-up run. Values are in Sv (10^6 m^3/s). Positive and negative values means ITF inflow and outflow, respectively.

and Ombai Straits reproduce similar transports, the lower transport in Timor Passage may be a reflection of the difference in the inflow. Timor Passage shows the largest differences in transport across the models, giving an indication that it is probably the one that may reflect resolution dependency the most. In Kiss et al. (2019) they mention that because Timor Passage is the last strait of the route, when Lombok Strait transport is large, taking more water from Makassar Strait, the transport in Timor Passage reduces. This is the case for our 10-km regional model, but the same is not observed in the higher resolution of 4-km where both transport are lower. Here as in Kiss et al. (2019) we find that the resolution of straits is critical for the ITF region. The transport in each strait may vary depending on boundary conditions, model bathymetry and resolution, but our results agree with observations given uncertainties.

2.2.3 Vertical distribution of transport

The vertical distribution of transport at the outflow passages differs slightly from the structure observed in INSTANT mooring data (Sprintall et al., 2009). In the regional model, Timor Passage has a surface maximum that is not observed in the INSTANT data, but both have a subsurface maximum around 50 - 60 m in INSTANT (Figure 2.8). Ombai Strait, on the other hand, has a surface maximum in INSTANT data that is not simulated by the model.

The transport maximum at 120 m is located at 180 m in INSTANT data. INSTANT data uses extrapolation to surface to estimate transport from discrete mooring measurements and there are uncertainties in these upper ocean observations. In Lombok Strait, the maximum is at the same depth in the regional model and INSTANT data, but larger in INSTANT. In conclusion, the model represents the overall vertical structure below 100 m for the main passages compared to INSTANT.

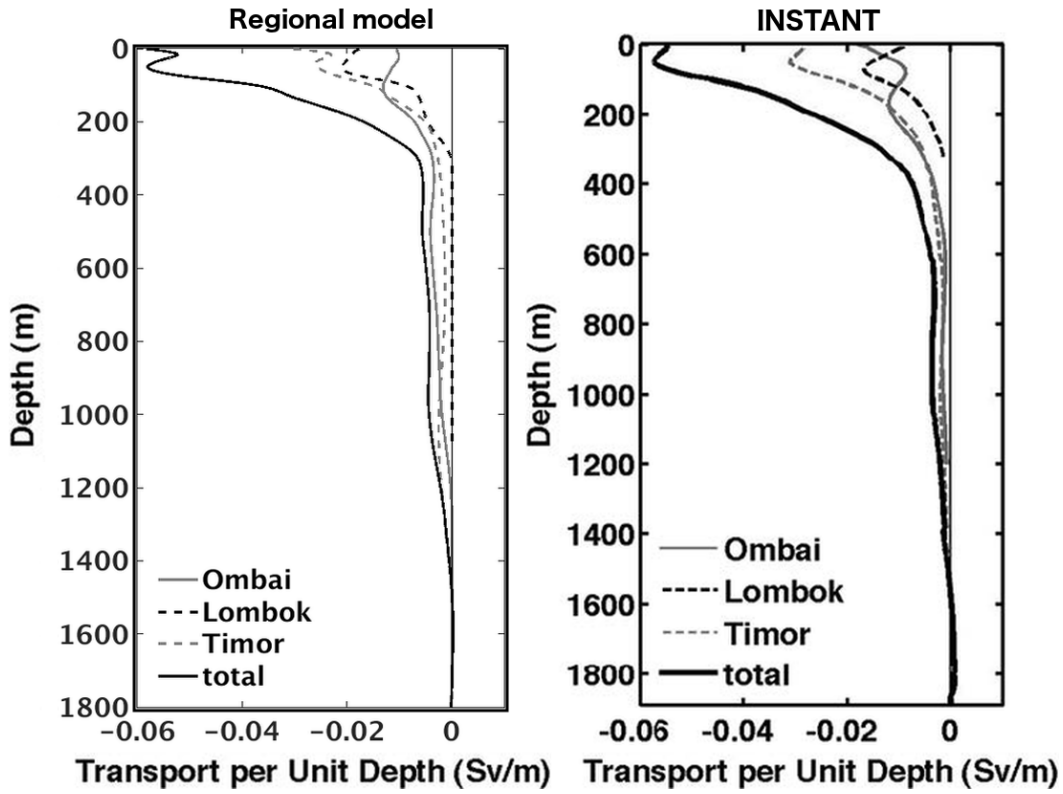

Figure 2.8: Transport per unit depth comparison between (a) the regional model and (b) INSTANT (Figure 7 in Sprintall et al., 2009).

2.3 Summary

We present details of our model runs developed to study the ITF dynamics at the outflow passages which is one of the topics of this Thesis. The main feature of our model is increased resolution compared to most global ocean models that allows us resolve topography of narrow

and shallow straits and focus on regional processes. Our experiments, while idealised, reproduce the main features of a steady ITF (our control run). Later on, we build upon our control run through a series of sensitivity experiments to understand the control of partitioning.

In this Chapter, besides the configuration details, we show comparisons of our control run with available observations for the ITF straits from moorings, satellite and climatology datasets. The main reference is the INSTANT measurements, given that they are the only simultaneous measurements at the outflow and inflow straits. The INSTANT period also provided the basis for our model development, as we use the averages for the same period as forcing to the regional model. We also compare our simulations to the model OFAM3, which provides the forcing for the open boundaries of our regional ITF model, and they show good agreement in terms of surface fields of temperature and speed. Though there are limitations and biases inherited from the forcing, they are not significant for the purpose of this study. Our conclusion is that despite some small differences, the ITF regional model reasonably reproduces the transports at the various straits and the partitioning amongst them, as well as the two main pathways, western and eastern, through the internal seas. More importantly, comparisons with observations (mainly Figure 2.8) are very good and we are confident the model is a good tool to proceed with our analysis.

The analysis of the effect of resolution on the ITF circulation and dynamics is outside the scope of this study. However, our simple comparison show differences in how the flow is partitioned for different resolutions of the ITF model (4-km and 10-km), demonstrating it is important to resolve the straits. Furthermore, based on Kiss et al. (2019) conclusions, the ITF region small straits are important to be resolved. Therefore, we use 4-km grid to improve resolution of narrow channels and straits of the ITF pathway. The next Chapters discuss the results of our model runs in the context of the ITF circulation and the dynamics of ITF partitioning.

Chapter 3

The Mean Circulation in the Indonesian Seas

In this Chapter we characterise the mean circulation in the Indonesian Seas and the pathways of the Indonesian Throughflow (ITF) as represented by the control run of the 4 km resolution ITF regional model. The model resolves the major circulation features of the Indonesian Seas, including the flow at the main inflow and outflow passages (Chapters 1 and 2). The partitioning of the ITF between the three main exit passages as well as the vertical structure of the transports in the passages agree well with previous model and observation-based studies. In addition, the model allows us to explore the dynamically complex circulation pathways between the inflow and outflow passages. The analysis reveals new insights about the routes by which water from the North and South Pacific circulate in the Indonesian Seas and exit to the Indian Ocean. The transport budget we present here as a quantitative analysis of the ITF circulation brings a novel approach for tracing and connecting the inflow and outflow ITF.

3.1 Main circulation pathways

The mean ITF has been previously described in models but not simulated as a steady current with a constant forcing. Observations provide estimates about mean transports but they lack an overview of the mean circulation in the entire Indonesian Seas. The regional high-resolution model is a good tool to explore local features and details of the circulation. In general, the ITF is the current that moves water from the Pacific to the Indian Ocean. The ITF has two main pathways with local recirculations. In this section we present a description of these two pathways by the horizontal analysis of the net transports along key transects. We first discuss the western pathway, followed by the more complex eastern pathway.

3.1.1 ITF western pathway

The circulation of the western North Pacific Ocean is characterised by the strong Mindanao current with a southward flow of 15.3 Sv (Figure 3.1 - transect A). At approximately 5°N this current bifurcates with some water (0.4 Sv) turning eastward into the Pacific forming the Mindanao Eddy. The remaining 14.9 Sv flow westward into the Celebes Sea, a feature previously observed by Kashino et al. (2001). The circulation in the Celebes Sea is dominated by two gyres: a cyclonic gyre circulating approximately 10 Sv in the south and a smaller anti-cyclonic gyre with transport ranging from 2.5 and 5 Sv in the north. The cyclonic gyre recirculates 6.4 Sv back towards the Pacific Ocean, which contributes to the eastward flow of the Mindanao and Halmahera eddies (Figure 3.1). This results in a net inflow into the Indonesian Seas from the Mindanao Current of 8.5 Sv (Figure 3.1 - transect G).

The circulation features produced by the model in the Celebes Sea agree well with observations (Kashino et al., 2001) and modelling studies (Masumoto et al., 2001; Chen et al., 2018). Kashino et al. (2001) completed two cross sections across the Celebes Seas, one

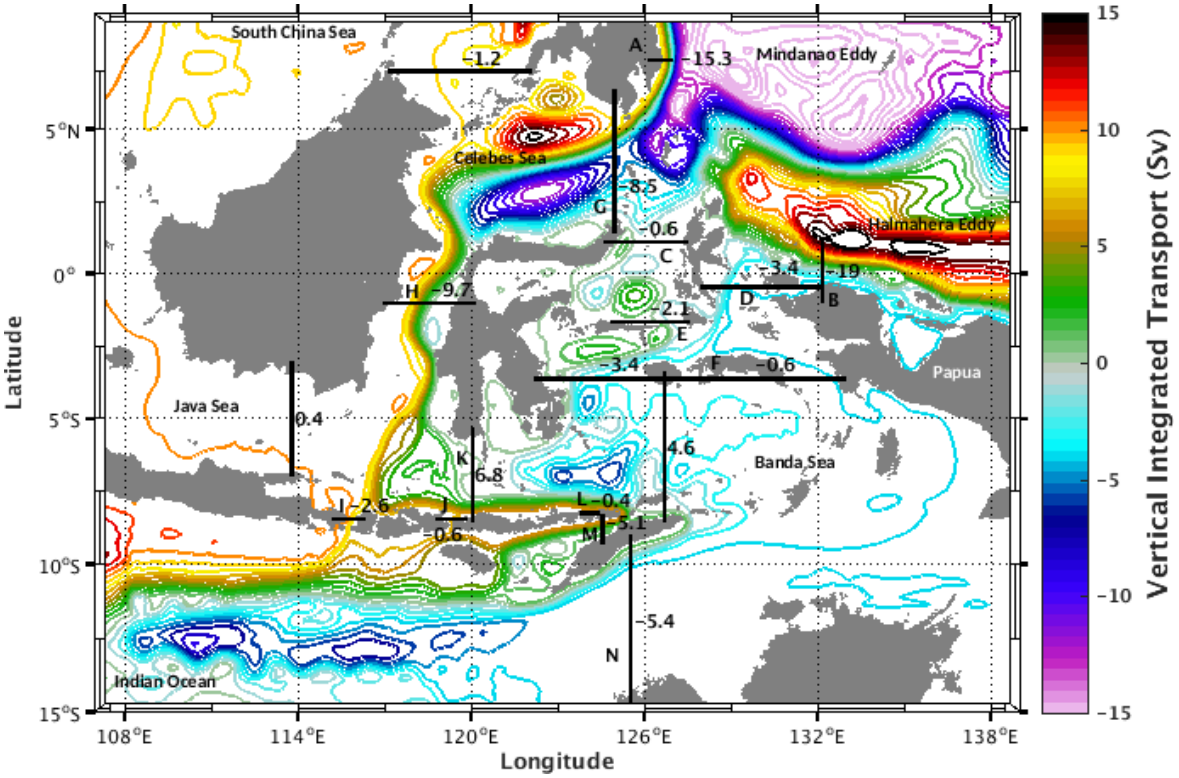

Figure 3.1: Transport streamfunction (in Sv) of the modeled Indonesian Seas. Negative (positive) sign means westward or southward transports (eastward or northward transports). Contour interval is 1 Sv and the colours are the value of the streamfunction. The transport in major passages and interior seas are shown (black lines identified by letters from A to Q).

meridional and one zonal, and collected ADCP data along these sections. They confirmed the presence of the cyclonic gyre in the south, but they did not identify a second anti-cyclonic gyre in the northern part of Celebes Sea, possibly due to the synopcity of the data. That indicates the northern gyre might be not permanent. In agreement with our model results, on the other hand, Masumoto et al. (2001) found in their simulation of the Princeton Ocean General Circulation Model (OGCM), a chain of eddies including a pair of clockwise and anticlockwise gyres in Celebes Sea. More recently Chen et al. (2018) described inter-annual modulations affecting the 50-day oscillations previously observed in Celebes Sea (Kashino et al., 1999).

Further south, along the western pathway, the Celebes Sea water combines with a small contribution from the South China Sea (SCS; 1.2 Sv, Figure 3.1) resulting in a total flow of

9.7 Sv through the Makassar Strait (Figure 3.1 - transect H). Although the contribution of the SCS to the mean circulation is small, 10 - 15%, it is reported to contribute significantly to the variability in Makassar Strait (Gordon et al., 2012). Similar time-averaged transport is found in a seasonal forced HYCOM model (Gordon et al., 2012). They detected a 1.62 Sv flow through Sibutu Passage that brings water from the SCS and Sulu Sea to the Celebes Sea. Along the same transect, using Lagrangian particle tracking in the NEMO OGCM Koch-Larrouy et al. (2008) found a net inflow of 0.4 Sv.

The flow in the Makassar Strait is constrained by topography. The narrowest part of Makassar Strait is the Labani Channel, which has a width of 45 km and maximum sill depth of 680 m (Figure 1.1). The Makassar Strait transport in our model comprises approximately 70% of the total ITF, in agreement with Gordon et al. (2008) and Gordon (2005). From observations, the average transport in Makassar Strait found by Gordon et al. (2008) is 11.6 Sv (9.7 Sv in our model). Upon exiting Makassar Strait, at 5°S, the flow bifurcates around the Dewakang Sill where the bottom rises to approximately 300 m deep (Figure 1.1). Approximately 2.5 Sv flows southeastward toward Nusa Tenggara (located along the latitude of 8°), and the other 7 Sv of the Makassar flow continues south toward Lombok Strait. A small input of 0.4 Sv from Java Sea joins the flow in our model, while in Koch-Larrouy et al. (2008) the Java sea contribution is estimated to be 0.8 Sv. Leakage directly to the Indian Ocean includes 2.6 Sv via Lombok Strait (Figure 3.1 - transect I) and 0.6 Sv in the Flores Strait (Figure 3.1 - transect J). The remaining 6.8 Sv (Figure 3.1 - transect K) forms an eastward jet on the northern side of the Nusa Tenggara chain.

In summary, the western pathway originates in the Mindanao boundary current that enters the Celebes Sea. There, the flow recirculates in a northern and a southern gyre before entering to the main strait of the western pathway, Makassar Strait. This strait is characterised by the constrained shallow Labani Channel, circulating thermocline water. Towards the Nusa Tenggara chain to the south, the direct ITF route to the Indian Ocean is mostly the Lombok Strait, the first and westernmost exit passage. The remaining water

that does not flow through Lombok Strait takes an eastward direction to finally reach the Indian Ocean through the Ombai Strait and Timor Passage, which together comprises more than half of the ITF outflow.

3.1.2 ITF eastern pathway

The eastern pathway is fed both from the North and South Pacific Ocean. Along the northern coast of Papua, 19 Sv (Figure 3.1 - transect B) flow northeastward towards the equator. Most of this transport (15.7 Sv) forms a recirculation cell, the Halmahera retroflection (Kashino et al., 2013) that connects the low latitude western boundary current of the South Pacific to the equatorial circulation. Between 129°- 130°E, in our model, the boundary current supplies 3.4 Sv of water to the Halmahera Sea which flows into the Seram Sea (Figure 3.1 - transect D). At this same location, a mean southward transport of 1.5 Sv was observed between 350 - 700 m from a 1-year mooring located at 0.17°N, 129.26 °E (Cresswell and Luick, 2001), which is less than the half of the transport we found. While the Halmahera Sea has a depth of 2000 m, flow in and out of it is controlled by shallow sills at its inflow (700 m) and outflow (600 m).

West of the Halmahera Sea sill (approximately sill depth of 700 m; Figure 1.1) are the much deeper Maluku Strait (sill depth of 2200 m) and Lifamatola Passage (sill depth of 1940 m). The flow in these deep passages brings the deepest waters into the Indonesian Seas (Luick and Cresswell, 2001; Gordon et al., 2003, 2010b; van Aken et al., 2009). In Maluku Strait, 0.6 Sv flows into Maluku Sea (Figure 3.1 - transect C). The source of this water is from the North Pacific, via the recirculation gyre in Celebes Sea as described previously. We find a clockwise circulation in Maluku Sea which agrees with analysis of 13-month current meter record in the Maluku Sea (Luick and Cresswell, 2001). However, they found a much stronger transport of 7 Sv southward in the deeper layer. In contrast, Yuan et al. (2018) analysed the first observational measurements of the upper layer above 300 m in Maluku

Sea. They reported a northward (out of the internal seas) flow of 1.04 - 1.31 Sv, which is subjected to variability related to the Mindanao western boundary current seasonal shift. None of these observations represent the net flow as they only consider discrete measures of the water column, as opposed to our total vertically integrated transport in the model (Figure 3.1).

The 3.4 Sv from the Pacific and 0.6 Sv from Celebes Sea and Mindanao Eddy combine to contribute 2.1 Sv into Lifamatola Passage (Figure 3.1 - transect E), just downstream of Maluku Passage, and adjacent gaps to both east and west of Lifamatola Passage. The transport through Lifamatola Passage is about 50% of the total 4 Sv that enter Banda Sea (Figure 3.1 - transect F). Collectively, this circulation forms the eastern pathway of the ITF. Along the eastern ITF pathway the flow remains concentrated in the western side of the basin (3.4 Sv) with only 0.6 Sv across the eastern section.

The bathymetry along the eastern pathway is complex, with numerous deep and shallow sills and deep basins. Previous studies have identified the Maluku and Lifamatola Passages as the primary routes that form the eastern pathway (van Aken et al., 2009; Luick and Cresswell, 2001; Potemra et al., 2003; Kashino et al., 2001; Ffield and Gordon, 1992; Gordon and Fine, 1996; Gordon et al., 2003, 2010b; Yuan et al., 2018). In addition, our model shows the inflow at the Halmahera Sea (3.4 Sv) is equally important. This inflow has been noted before with a mean southward transports of 1.5 Sv (from observations in Cresswell and Luick, 2001), 0.8 Sv and 2.2 Sv (from models in Koch-Larrouy et al., 2008; Potemra et al., 2003, respectively). However, observational studies in the eastern pathway are extremely limited and model estimates differ. Our model resolves most of the complex bathymetric features of the eastern pathway and allows us to shed some light into the complex circulation of this area. Compared to other models, the high-resolution of our model shows how important it is to resolve the bathymetry.

Downstream in the eastern pathway, the Banda Sea receives water from both the western

and eastern routes. The eastward flow across Flores Sea towards the Banda Sea is composed of 6.8 Sv from the western pathway (Figure 3.1 - transect K). From the eastern pathway 4 Sv flows southward in Banda Sea (Figure 3.1 - transect F). These, along with a small contribution from Torres Strait (0.2 Sv) leave the Indonesian Seas via Ombai Strait (5.1 Sv, Figure 3.1 - transect M) and Timor Passage (5.4 Sv, Figure 3.1 - transect N) with small leakage at Nusa Tenggara by Alor Strait (0.4 Sv, Figure 3.1 - transect L). A complex weak gyre just north of Ombai Strait recirculates some of this water in the Banda Sea and the contribution of the western pathway to Banda Sea is unclear since we cannot estimate from the streamfunction analysis in the model how much of the western pathway flow effectively penetrates into Banda Sea. Together the water from all the outflow passages supply 14.1 Sv to the Indian Ocean.

Our high-resolution model also provides estimates in the shallow and narrow straits such as the inflows from South China Sea (1.2 Sv) and Java Sea (0.4 Sv) and the outflows of Flores (-0.6 Sv) and Alor Straits (-0.4 Sv) and their contribution to the mean ITF transport (inflow of 1.3 Sv and outflow of -1 Sv; Table 3.1). The contribution of these minor passages makes a small portion of the total flow.

The eastern pathway carries deep and cold waters and the longer resident time compared to the western pathway allows significant mixing and modification of waters. The main entrance to the eastern pathway, observed in mooring data, is through Maluku Strait (Luick and Cresswell, 2001). We highlight in our model the important contribution of South Pacific water via the Halmahera Sea to the eastern pathway. The different routes into the eastern pathway and strong mixing at Banda Sea (Koch-Larrouy et al., 2015, 2008) are critical to determining the properties of the water flowing into the Indian Ocean through the two exit passages of Ombai Strait and Timor Passage.

While the streamfunction in Figure 3.1 provides a detailed description of the pathway and total transport, both observations (Luick and Cresswell, 2001; van Aken et al., 2009; Gordon

et al., 2010b) and models (Metzger et al., 2010; Morey et al., 1999) show that different passages contribute at different depths. To further explore this we look next at the vertical structure of the flow.

3.2 The vertical structure of the ITF

The total vertically integrated view (Figure 3.1) does not tell us where the cores of the jets are or if reversals or recirculation patterns exist in the various passages at different depths. To characterise the vertical structure of the circulation, we show velocity vectors averaged in the upper layer (0 to 300 m; Figure 3.2.a), intermediate layer (300 to 600 m; Figure 3.2.b) and deep layer (600 to 1200 m; Figure 3.2.c).

In the upper layer the western pathway through the Makassar Strait has the strongest velocities (Figure 3.2.a). The main features of this upper circulation are the recirculation gyre in Celebes Sea, the strong southward flow in the Makassar Strait, the outflow through Lombok Strait, the eastward flow along Nusa Tenggara joining the recirculating gyre in the Banda Sea and the other two main outflow passages, Ombai Strait and Timor Passage. The gyre in the south of the Banda Sea just north of Ombai Strait suggests the fraction of water that does get to Banda Sea from the western pathway penetrates only slightly into Banda Sea interior. From the velocity vectors we can see that those waters do not reach the eastern Banda Sea. Although not quite as vigorous as the western pathway the upper layer velocity vectors also show the incoming water in eastern pathway through the Halmahera gap into the Seram Sea, which recirculates out through Lifamatola Passage and Maluku Strait. Hence, most of this South Pacific water does not contribute to the net ITF but returns to the Pacific Ocean via the Halmahera Sea and Seram Sea as previously noted by Koch-Larrouy et al. (2008). Only a small fraction of these waters appear to reach Banda Sea.

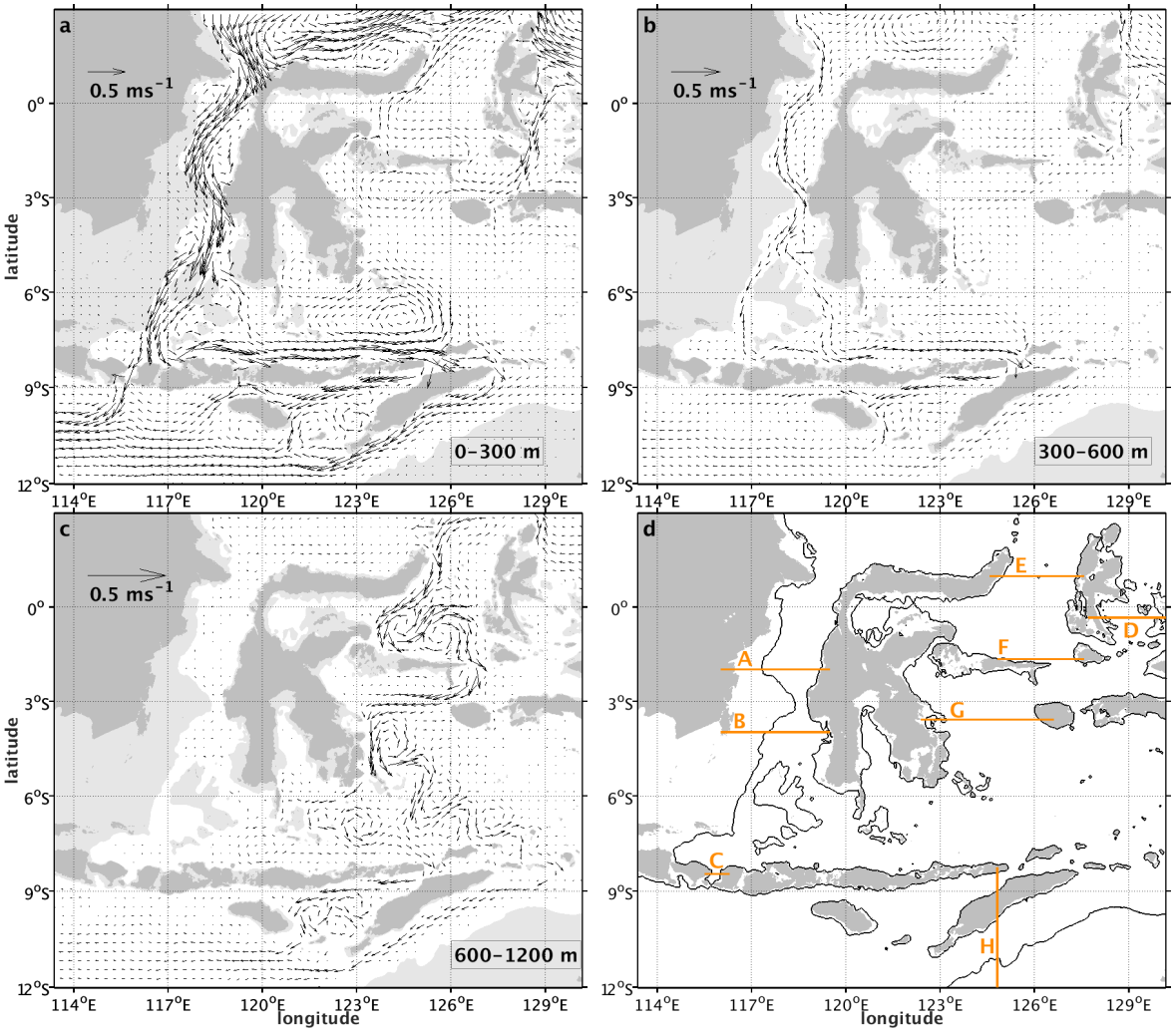

Figure 3.2: (a) Mean velocity vectors averaged in the top 300 m, (b) between 300 and 600 m and (c) between 600 and 1200 m. Vectors in (c) are scaled 1.5x larger than in (a) and (b). The light grey area highlights depths shallower than 300 m. (d) The transects where we proceed with further vertical analysis are shown in orange. Black contour show the 300 isobath.

At the intermediate layer (300 - 600 m), the western pathway is still the most pronounced (Figure 3.2.b). A large gyre is present in Celebes Sea. At this depth range there is no flow in Lombok Strait as it is completely blocked by the sill. The flow splits upstream of Lombok and rejoins in the eastward current along the Nusa Tenggara. Outflow at this depth range is only through Ombai Strait and Timor Passage, albeit weaker velocities than in the upper layer. Along the eastern pathway, we find the strongest velocities entering Halmahera Sea and otherwise weak southward flow across the Banda Sea.

Finally, the deep layer shows there is flow only in the eastern pathway (Figure 3.2.c; note vector scale is different from the upper layers). A meandering current with various small eddies crosses the whole Banda Sea towards the outflow passages. In Maluku Sea two recirculation cells feed Lifamatola Passage. In this passage, we see the surface and deep circulation are not connected: the 0 - 300 m layer has a recirculation towards the South Pacific, while the 600 - 1200 m layer has a southward flow into Banda Sea. Once in Banda Sea, the deep flow is strongest on the western side, but recirculation cells and meanders are also present. The outflow passages Ombai and Timor also have relatively strong deep flows, comparable in magnitude to the intermediate layer flows.

We integrate the transport in each layer across various sections of the ITF (Figure 3.3). The velocity vectors illustrate well the recirculation in Halmahera Sea, however they do not allow a quantitative analysis of transports in each layer (Table 3.1). We investigate the complexity of the recirculation in Halmahera Sea. In the top layer (0 - 300 m, Figure 3.3.a) the western pathway is dominated by southward flow of 8.3 Sv. From the three inflow passages at the eastern pathway, Halmahera Sea is the only one with large net southward transport (2.9 Sv) that mostly leave the Maluku Sea via the Maluku Strait (1.9 Sv; Figure 3.2.a and Figure 3.3.a). Thus, the contribution of Halmahera Sea to the eastern pathway upper layer circulation is 1 Sv. Hence most of the surface flow in Ombai Strait and Timor Passage must come from the western pathway. Ombai and Timor carry 2.7 and 3.4 Sv, respectively within the top 300 m. These transports are more than the double of the deep transport in the same straits (Figure 3.3.c).

In the intermediate layer (300 - 600 m, Figure 3.2.b and 3.3.b) the largest transports are in Makassar and Ombai Straits with net flows of 1.4 and 1.1 Sv, respectively. Timor Passage transport is weaker in this layer with only 0.5 Sv. Similarly, there is only a small contribution from Halmahera Sea of 0.5 Sv southward, of which 0.2 Sv circulates back to Pacific Ocean. Thus, between 300 and 600 m there is a net inflow of the eastern pathway of 0.3 Sv.

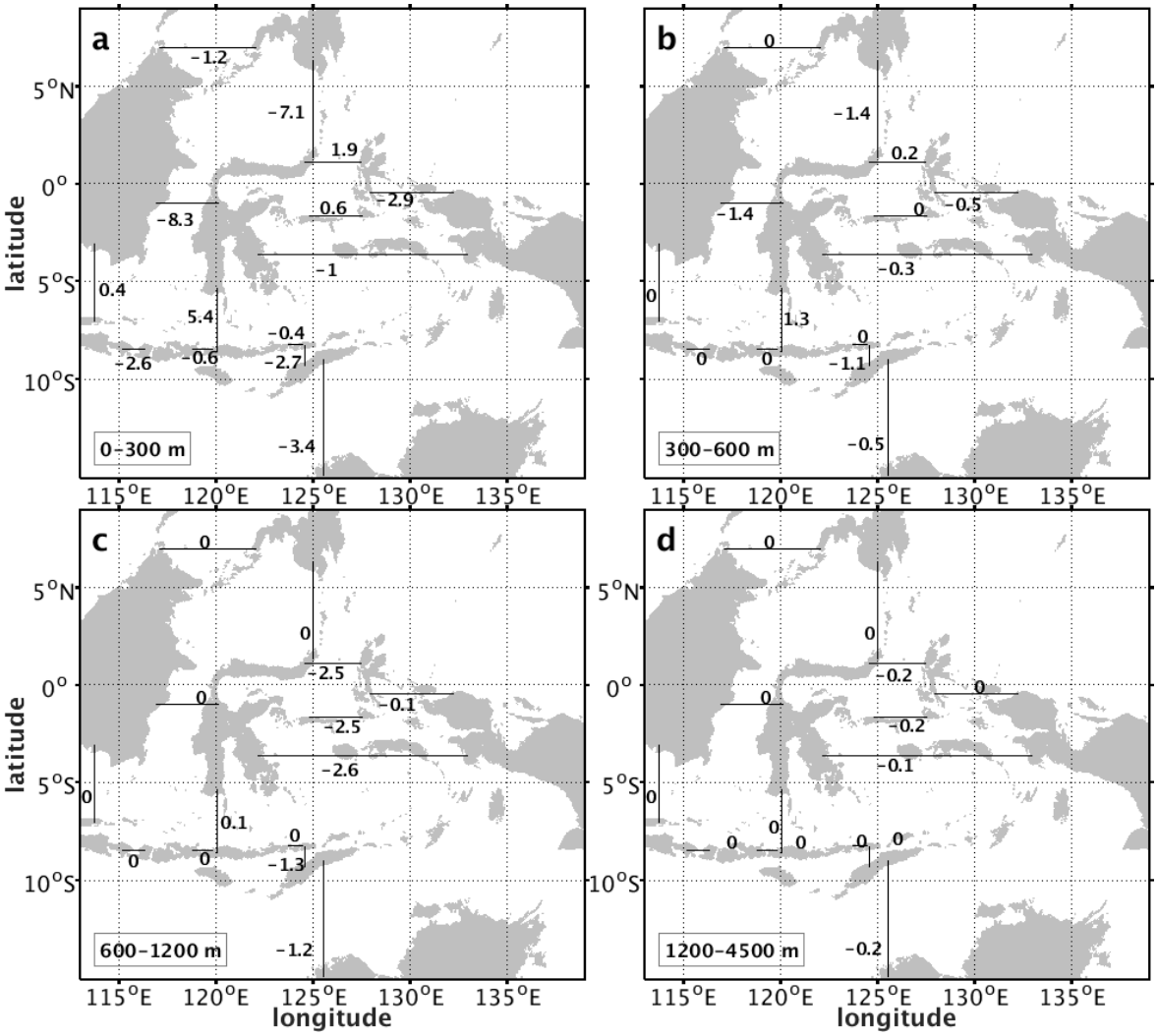

Figure 3.3: (a) Transport integrated along a top layer - surface to 300 m depth -, (b) intermediate - 300 to 600 m -, (c) deep layer - 600 to 1200 m and (d) below 1200 m. Transects show the net transport (numbers in Sv) across each transect in that layer.

In the deep layer (600 - 1200 m), inflow from the Pacific is limited to the eastern pathway. The deeper flows are smaller than to the upper layer in the western pathway. The mean deep layer transport at the Maluku Strait is 2.5 Sv, which results from a balance between 3.1 Sv southward and a small transport of 0.6 Sv northward (not shown but can be seen as side to side flows in the cross-section velocity in Figure 3.5). Luick and Cresswell (2001), from a 13-month mooring array, found the mean flow was directed southward at 740 m, 1250 m and 1750 m in Maluku Strait. The southward transport between 740 m and 1500 m found in Luick and Cresswell (2001) was 7 Sv, which is more than double the transport in our

regional model of the ITF. The difference may be due to the mean forcing applied to the model and annual variability of the observations, along with interpolation and extrapolation of discrete mooring observations that may miss the cross-passage structure. The deep layer inflow results in a deep southward transport of 2.5 Sv at the Lifamatola Passage, which added to a small input (0.1 Sv) from Halmahera Sea makes the 2.6 Sv we find below 600 m in the Banda Sea.

Ombai Strait and Timor Passage deep transports are 1.3 and 1.2 Sv, respectively (Table 3.1). This deep flow is fed solely from the eastern pathway through a convoluted series of currents that carry the water southward (Figure 3.2 and Figure 3.3.c) as we showed before.

Using the same sections from Figure 3.3, excluding Lifamatola Passage, we next calculate a volume budget for various depth layers within four boxes in the Indonesian Seas (Figure 3.4). The residual between the transports across the lateral sides of each box is assumed to be the vertical transport across the top/bottom of the layers. The Banda Sea box containing Ombai Strait and Timor Passage is the only region with significant vertical exchange between the layers. The deep layer defined as 600 to 1200 m has a small divergence of approximately 0.22 Sv of which 0.072 Sv is transferred down to the lowest layer (1200 m to bottom), 0.073 Sv is transferred up to 300 - 600 m layer and 0.072 Sv to the top 0 - 300 m layer. These vertical transports are small compared to the horizontal transport. For all the other boxes the budget is closed within each layer. Therefore, we find there is basically no communication between surface, intermediate and deep layers.

Transports across various passages may be dependant on the position of the jet core in the vertical with respect to sill depth. To investigate how changes in the vertical structure of the jet cores control transport, we next examine the cross-section velocity in the transects from A to H on the map (Figure 3.2.d). A velocity cross-section upstream of the Makassar Labani Channel shows a strong and wide jet extending from the surface to 600 m (Figure 3.5 A). It is surface intensified with the core centered at 15 m, also seen in the profile of

Passage	Sill depth (m)	Maximum depth (m)	Width (Km)	Total net transport (Sv)	Net transport at 0-300m (Sv)	Net transport at 300-600m (Sv)	Net transport at 600-1200m (Sv)
Halmahera gap	700	.	.	3.3	-2.9	-0.5	-0.1
Maluku Strait	2200	.	230	0.6	1.9	0.2	-2.5
Lifamatola Passage	2000	.	36	*2.1*	-	-	-
Banda Sea	-	-	-	4.0	-1	-0.3	-2.6
Makassar Strait	680	.	45	9.7	-8.3	-1.4	0
South China Sea	-	-	-	1.2	-1.2	0	0
Java Sea	-	-	-	0.4	0.4	0	0
Net inflow	-	-	-	**14.1**			
Lombok Strait	300	1100	35	-2.6	-2.6	0	0
Ombai Strait	1450	3250	37	-5.1	-2.7	-1.1	-1.3
Timor Passage	1250	1890	160	-5.4	-3.4	-0.5	-1.2
small straits (Flores/Alor)	-	-	-	-1	-1	0	0
Net outflow	-	-	-	**-14.1**			

Table 3.1: Geometry of the main inflow and outflow ITF passages (sill depth, maximum depth and width), the integrated net transport (in Sv or 10^6 m^3/s) for the whole water column and details of transport in the vertical (the maximum depth of transport). The depth of maximum transport considers just southward (westward in considering Ombai and Timor). This is valid especially for the eastern pathway passages that have strong northward flow at the top layer (Maluku, Lifamatola and Banda sea). Positive and negative values for the total net transport means ITF inflow and outflow, respectively. The net transport per layers in the last three columns although have the signals positive and negative indicating the direction of the flow (positive means southward/westward and negative means northward/eastward).

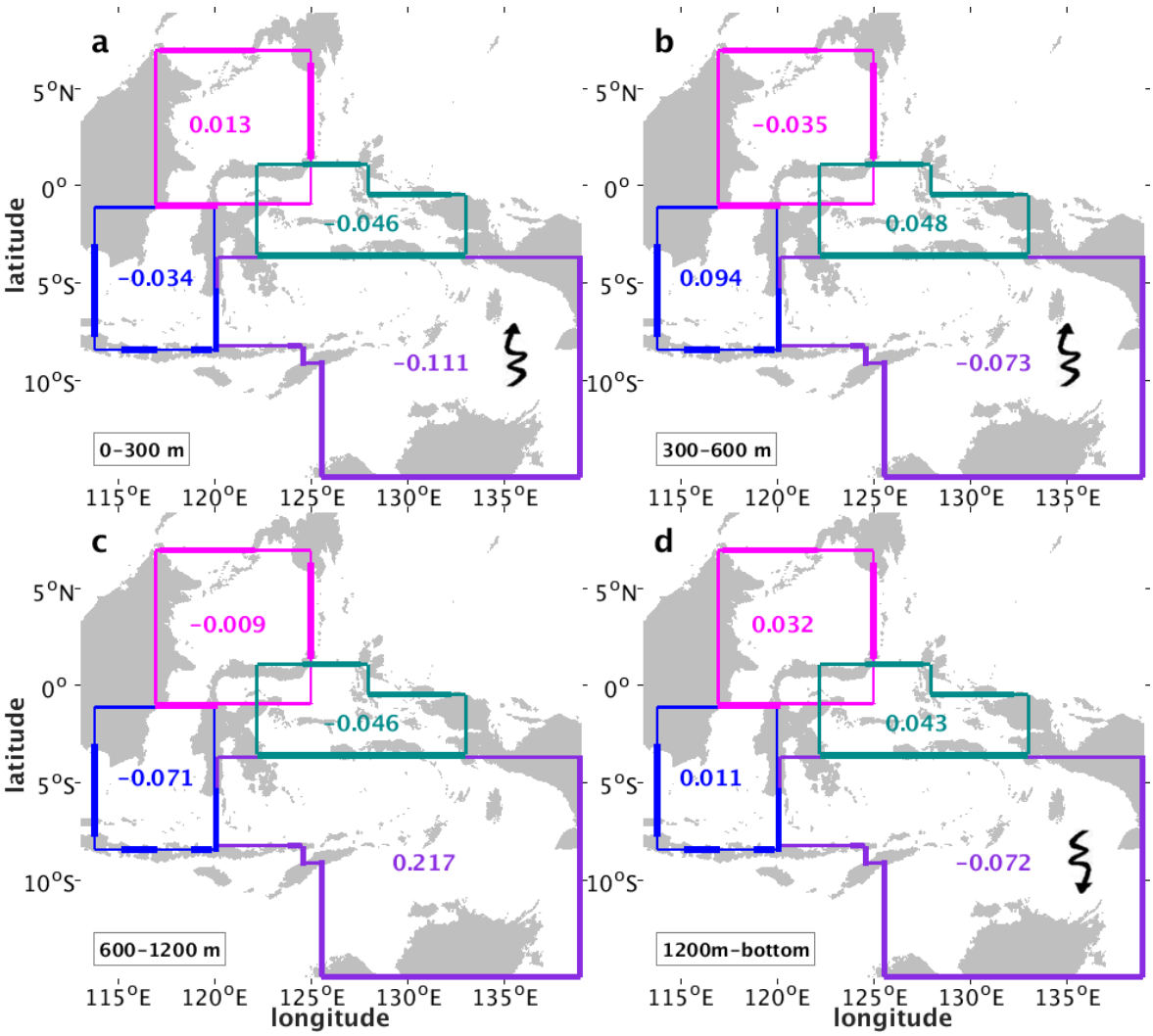

Figure 3.4: Volume budget in four boxes for the layers 0 - 300 m (top layer), 300 - 600 m (intermediate layer), 600 - 1200 m (deep layer) and 1200 m to bottom (bottom layer). The four boxes are defined by the sections in the north of Banda Sea, Celebes Sea, south of Makassar Strait until Lombok Strait and south of Banda Sea including the exit channels Ombai Strait and Timor Passage. The arrows show the direction of the flow divergence.

transport per unit depth (Figure 3.6.a), and maximum velocity of -0.66 m/s. There is also weaker northward velocity at the eastern boundary of the strait that has a distinct subsurface maximum (0.27 m/s) and this northward flow is associated to the local recirculation gyre seen in Figure 3.2.a. Near the bottom (approximately 600 m), upstream of Makassar, velocities are 0.05 m/s but transports are still observed down to a maximum depth of 700 m (Figure 3.6.d).

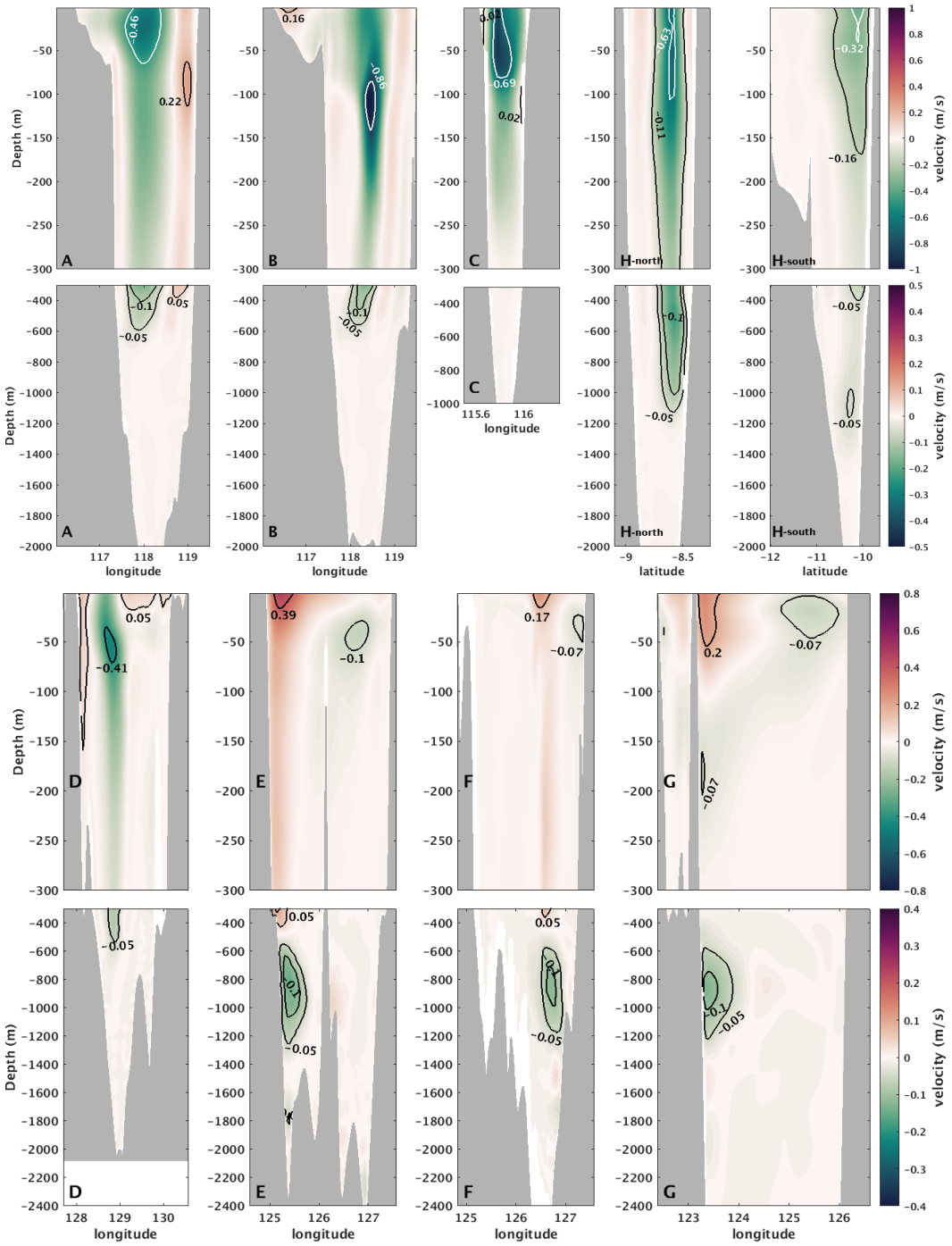

Figure 3.5: Cross-section velocity (m/s) at: (A) upstream at 2°S and (B) downstream at 4°S of Makassar Strait, (C) Lombok Strait, (H-north) Ombai Strait, (H-south) Timor Passage, (E) Maluku Strait, (F) Lifamatola Passage, (G) the total eastern pathway in Banda Sea and (D) Halmahera gap. Transects location are the orange lines on the map of Figure3.2.d. The flow cores consist of a 0.2 m/s envelope. Bathymetry is shown by the grey shaded areas. Note that the vertical axis of the top 300 m are stretched compared to the deeper layers. The aspect ratio is the same excluding Lombok and Ombai Straits that have a 2.5x exaggeration in width.

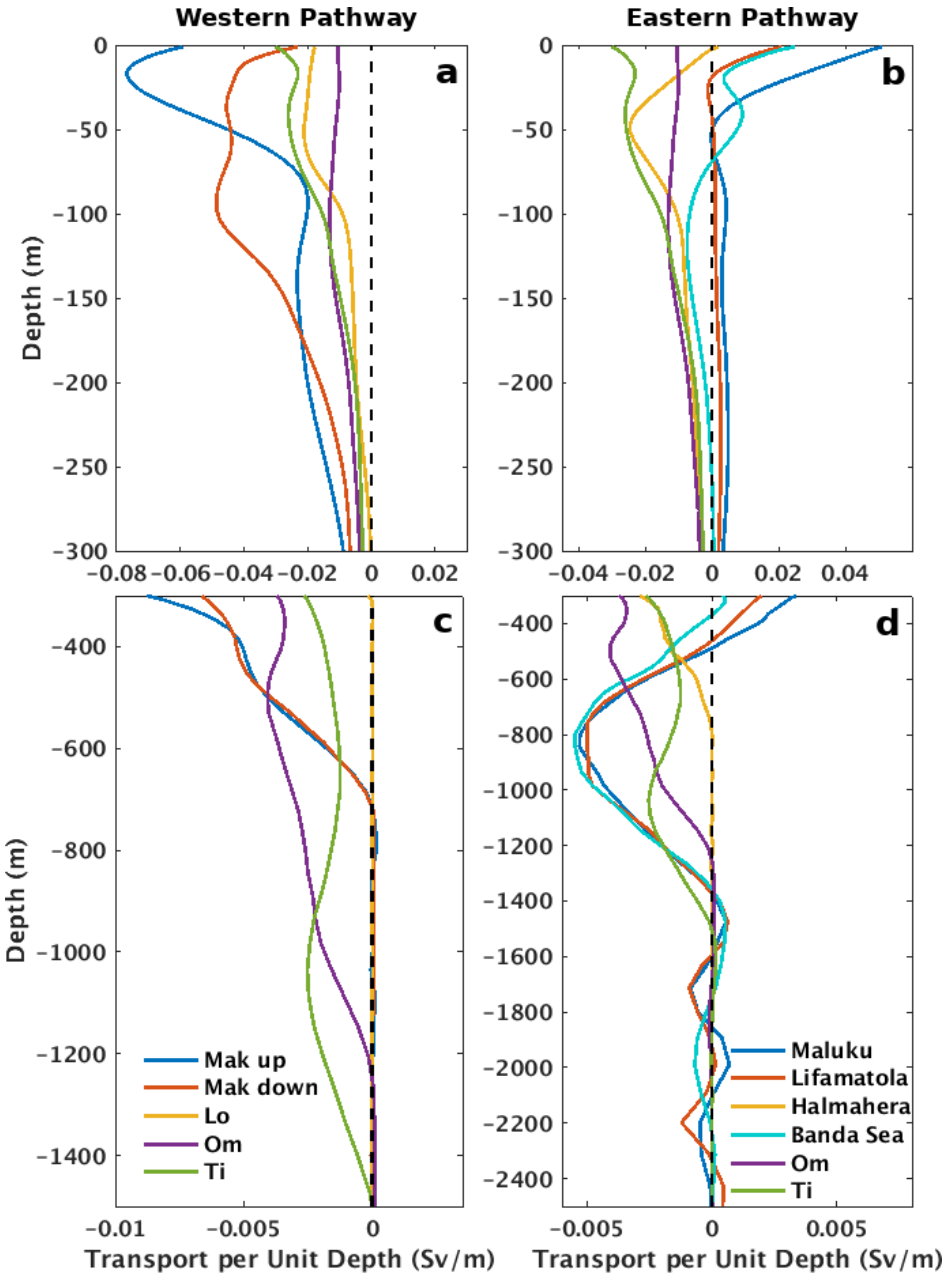

Figure 3.6: Transport per unit depth for the main passages of (a, c) the Western pathway and (b, d) eastern pathway. (a, b) Top panels from 0 to 300 m depth and (c, d) bottom panels from 300 to 1500 m (western pathway, c) and 300 to 2500 m (eastern pathway, d). Note that the axis change for depths and for transports, as transport decrease below 300 m. Different axis for the both pathways as well, as the western pathway has stronger transports than the eastern pathway. Name of the passages in the legends and the transect letters: upstream of Makassar (Mak up - A), downstream of Makassar (Mak down - B), Lombok (Lo - C), Ombai (Om - H-north), Timor (Ti - H-south), Maluku (E), Lifamatola (F), Halmahera (D) and Banda Sea (G). Ombai and Timor are both part of western and eastern pathways and are not inflow passages.

At the Labani Channel, the narrow part of the Makassar Strait, the southward velocity core becomes narrow and deepens with the subsurface maximum now located at 110 m (Figure 3.5 B). The channel constraint changes the structure of the flow and accelerates it. The maximum velocity of the current core increases to -1 m/s and is found at the centre of the channel. The profile of transport per unit depth shows a broad maximum between 15 and 110 m (Figure 3.6.a, red line). Below 300 m, the current is very similar to the upstream structure, with velocities slowly decreasing to zero at approximately 550 m (Figure 3.5 B) and weakening transport per unit depth to maximum depth of 700 m (Figure 3.6.c). The top layer (0 - 300 m) contains 86% of the total net flow in Makassar, leaving just 14% of transport in the intermediate layer (300 - 600 m; Table 3.1).

In Lombok Strait the jet is surface intensified with maximum velocity of -0.9 m/s (Figure 3.5 C; note the aspect ratio is 2.5 times the other channels, except for Ombai Strait that has the same ratio). While the flow at Lombok extends down to 260 m, 69% of the transport is confined within the top 100 m and the maximum transport is found at 60 m depth (Figure 3.6.a). Lombok jet is western intensified with stronger velocities at the western side of the strait, as previously noted by Sprintall et al. (2009), a common feature of a boundary current. Also similar to the INSTANT mooring observations, is the model transport per unit depth profile, with the maximum at the same 60 m depth and intensity close to -0.02 Sv/m.

Along the eastern pathway, a vertical section in the gap at Halmahera Sea shows weaker velocities (-0.41 m/s) than in Makassar Strait (Figure 3.5 D compared to A and B). The strongest velocities here are confined within the upper 100 m with a subsurface maximum. Halmahera Sea brings South Pacific water into the Seram Sea as a subsurface and shallow intensified flow at 47 m (Figure 3.6.b). The transport above 300 m from Halmahera Sea towards Seram Sea is 2.9 Sv which is 82% of the total of South Pacific water at this gap (Figure 3.3 a). That is the strongest southward contribution from the eastern pathway in the upper 300 m as we also observed by the vectors at that layer (Figure 3.2.a). This southward flow is balanced by northward flow in Maluku Strait thus there is only a small net

inflow to the Indonesian Seas (Figure 3.3.a). The structure of the inflow in Halmahera gap is not well known due to limited observations (Cresswell and Luick, 2001) and coarse resolution of models (Morey et al., 1999; Wattimena et al., 2018). Morey et al. (1999) concluded the flow in Halmahera takes place because of the presence of the Halmahera island. The island prevents water from flowing towards Celebes Sea and results in circulation toward the Seram and Banda Seas. They found a transport of approximately 3 Sv, similar to our results. Below 300 m, there is weak flow to 750 m (Figure 3.6.d), similar to the sill depth, transporting 0.5 Sv southward at the intermediate layer (300 to 600 m) and 0.1 Sv at the deep layer (600 to 1200 m; Figure 3.3).

The near surface flow in Maluku Strait is directed northwards with velocities of up to 0.5 m/s (Figure 3.5 E). Above 300 m it transports 2.6 Sv northwards (not shown). On the eastern side of the section there is a weak southward flow with low velocities (-0.14 m/s). In the surroundings, where there is the gap at Halmahera Sea, the transport is 0.7 Sv southward (not shown). A net northward flow of 1.9 Sv is then resultant in Maluku Strait (Figure 3.5 D and Figure 3.3.a). The upper circulation in Maluku Strait has recently been observed by a 4-year mooring array (Yuan et al., 2018). These new observations show a northward mean transport of 1.04 - 1.31 Sv which agrees with the net flow in the upper layer of Maluku Strait from our model results (Figure 3.3.a). At approximately 800 m where the Halmahera transport approaches zero the Maluku Strait, Lifamatola Passage and Banda Sea have a large southward transport maximum (Figure 3.6.d). At depths between 600 to 1200 m the strong flow of 3.1 Sv directed to the south has velocities of -0.15 m/s. Different estimates from previous measurements of the deep layer (7 Sv in Luick and Cresswell, 2001, and 1.8 - 2.3 Sv in Gordon et al., 2003) suggest the observed range in deep transport may be due to seasonal or interannual variability.

The flow in Lifamatola Passage is characterised by a deep contribution to the ITF (Gordon et al., 2010b), similar to Maluku Strait. The vertical velocity structure is weaker in Lifamatola Passage and displaced to the east, where the channel is deeper (Figure 3.5 F and Figure 3.6.d).

It transports 2.5 Sv between 600 and 1200 m (Figure 3.3.c), which is much larger than the net upper layer transport of 0.6 Sv. Weak velocities of -0.12 m/s are found at the jet core between 700 and 1000 m. The jet is narrower than the upstream core in Maluku Strait. No transport is observed below 1400 m in either the Lifamatola and Maluku Straits. Previous observations in the Lifamatola Strait show a deep 0.147 m/s mean jet at 1500 m depth (van Aken et al., 2009), with an estimated mean transport of 2.5 Sv below 1250 m (van Aken et al., 2009; van Sebille et al., 2014). In our model the same transport (2.5 Sv) is found above 1200 m (by integrating to this depth).

Collectively, waters from the Halmahera gap, Maluku Strait and Lifamatola Passage flow into the Banda Sea. Along the west side of the section (Figure 3.5 G) the near surface northward flow is comparable in magnitude to the northward flow in Maluku Strait, but broader and deeper. On the east side the flow is weaker, southward and has a similar magnitude as the near surface southward flow in Maluku Strait. This broader surface jet connects to the western core centered at 180 m and it is clearly seen in the transport per unit depth profile (75 to 200 m; Figure 3.6.b). Most of the southward flow in Banda Sea occurs within the deeper layer (600 to 1200 m) with the same structure and amplitude as the other inflow sections (Figure 3.3.d). The southward transport in the deep layer is 2.9 Sv (Table 3.1). The similarity between the deep layer flow across the Banda Sea and the deep flow in Maluku Strait and Lifamatola Passage suggests the continuity of the flow along these passages. Halmahera Sea surface water recirculates back to the North Pacific within the upper layer. Nevertheless, the connections we see in our maps (Figure 3.1, Figure 3.2, Figure 3.3 and Figure 3.4) suggest that some of the Halmahera flow joins the southward flow in the eastern pathway and not all the water from Halmahera sea recirculates back through Maluku Strait.

The connection between the deep flow in Banda Sea and the outflow through Ombai and Timor flows has been noted before and is evident in our streamfunction analysis (Figure 3.1). We show the deep flow is sourced from the eastern pathway. In the top layer Timor Passage

has approximately 40% of the total from the western pathway (8.7 Sv from Makassar and Java Sea upper flow together), while Ombai and Lombok Straits have equally portions of the upper western pathway flow (30% each). We neglect the small contribution of the small straits, like Flores and Alor Strait, for this calculation. Ombai and Timor have approximately even partitioning of the deep layer flow. When we consider the upper layer (the intermediate plus the top layer) net transport, then the contributions of Ombai Strait and Timor Passage to these upper layer are mostly the same (3.8 and 4 Sv, respectively). Those two layers together contain the transport from Makassar pathway as it does not have deep transport. However, van Sebille et al. (2014) suggests that most of the Timor transport is composed of Makassar Strait sourced waters.

The vertical structure of the flow at Ombai Strait (Figure 3.5 H left; attention to aspect ratio of 2.5 times the other channels) is characterised by a narrow core with very strong velocities (-0.7 m/s) that extent to 120 m. The Ombai jet transports 5.3 Sv westward and a very small reversal transport of 0.1 Sv in the upper layer (seen in Figure 3.5 H as very weak velocities on either side of the main jet). In Timor Passage the flow is much broader and with smaller velocities (-0.35 m/s; Figure 3.5 H right). It has a weak surface jet in the upper 10 m and a subsurface maximum at 40 m (Figure 3.6.a and .b). In INSTANT, the maximum seen in the transport per unit depth profile is at 50 - 60 m. The along-strait velocities in MITgcm have very similar magnitudes to INSTANT.

Below 300 m the only significant velocity is found in the Ombai Strait and Timor Passage (Figure 3.3.b and .c and Figure 3.6.c). Ombai has a secondary maximum around 500 m and Timor has a maximum around 1100 m, which are in agreement with INSTANT. The net transports for the deep layers (300 to 1600 m) are 2.5 Sv in Ombai and 2 Sv in Timor, corresponding to 47% of the total net transport in Ombai Strait and 33% of the total net transport in Timor Passage, respectively.

The vertical analysis of the ITF velocity and transports showed that there is a clear

west/east and shallow/deep flow separation and little communication between these two components of the ITF. There is a considerable flow in Halmahera gap at approximately 600 m depth. Some water is recirculated but not all of it, which contributes to the eastward pathway and composes the outflow ITF. However, we acknowledge there are uncertainties about the contribution of the eastern pathway to the shallow circulation. In summary, any transport contribution below Makassar Strait's sill depth must come from the eastern pathway. The deeper flow of the eastern pathway show a complicated structure, with deep gyres and meanders. Lombok Strait is directly related to Makassar Strait with similarities on the channels structure and also in the current structure and geometry.

3.3 Discussion

We detailed the two pathways of the ITF in the Indonesian Seas regional model. We find that the ITF is composed of a western and an eastern pathways and dominated by flow in the upper (0 to 300 m) and deeper (600 to 1200 m) layers. The ITF western pathway provides a more direct route for Pacific water to reach the Indian Ocean and it is surface intensified. Lombok Strait is directly related to Makassar Strait as it is located just downstream of it. Although the three outflow passages receive water from Makassar Strait, Ombai Strait and Timor Passage also receive water from the more complicated eastern pathway which is the main contribution to the deep transport in these outflows. The flow in Halmahera is the only surface portion of the eastern pathway, but recirculation via Maluku Sea suggests little net upper transport from the eastern pathway. The upper layer recirculation of the eastern pathway, with the inflow from Halmahera Sea was previously measured (Gordon, 2005) and modeled (Potemra et al., 2003; Koch-Larrouy et al., 2008) but the contribution to the Banda Sea southward flow as surface South Pacific waters was unknown. We still do not have a clear quantitative understanding of this contribution but our model showed it is very likely to happen.

This study suggests that the flow in the upper layer (0 to 300 m) and deep layer (600 to 1200 m) are separated by a relatively steady intermediate layer (300 to 600 m). van Sebille et al. (2014) identify two separated cores in the Indian Ocean (at 110°E and 10°S), a large core in the upper 300 m and a smaller core between 600 and 1200 m. These cores are consistent with the separation of the Indonesian surface water from the deeper Indonesian water as found by the tracers study from Talley (2005). Here, we confirm that those two layers not only have different sources and water composition but also the interaction between them is minimum which suggests the ITF may be controlled by different processes. The water composition in van Sebille et al. (2014) seems to overestimate the North Pacific presence in the deep layer and consequently in the eastern pathway, by their choice for the definition of what is North Pacific and South Pacific water. Also the presence of South Pacific water at the Indian Ocean surface cross section might not be realistic, again related to the definition of North and South Pacific source (north or south of equator). While our analysis considers the entry points of the ITF, van Sebille et al. (2014) defines the sources of the ITF at a more distant location. Furthermore, a density layer separation in Koch-Larrouy et al. (2008) was used to highlight the difference between the western and eastern ITF branches, which we identified here by depths checking that the western and eastern pathways are not only horizontally different but also vertically.

Understanding the partitioning of the ITF as observed in INSTANT Sprintall et al. (2009) in this two layer circulation is not straight forward. In Sprintall's partitioning, the total ITF is the sum of the outflows in the three exit straits. However, we know there are different source waters to the flow at different depths and this needs to be taken into account when considering how the total transport is apportioned between the different straits. We suggest a more appropriate way to consider partitioning may consider acknowledge the dynamical relationship amongst the three outflow passages. This partitioning should take into account both the source (western or eastern pathway) but also the layer depth, for example the upper and intermediate layer and western route only. The deep circulation on the other hand does not include Lombok Strait so only Timor and Ombai should be considered. If we consider the

transport in Makassar Strait as the net upper ITF, the partitioning is 31:32:41 (or 27:39:40 for 0 - 600 m) compared to the previous 17:33:50 from INSTANT (Sprintall et al., 2009). Even this alternative definition of partitioning is not that robust, as there is a small and uncertain shallow contribution of the eastern route waters to the shallow cell. Hence, the sum of the three straits adds up to more than 100%, which is also affected by not considering the Java Sea and Flores and Alor Straits that have small contributions. So when it comes to understanding what controls partitioning, an important part of that question continues to be why more of Makassar Strait water does not go out through Lombok Strait directly. Thus, from a dynamical point of view thinking of the ratio of Lombok to Makassar transport may be more useful.

The eastern pathway is complicated and remains largely unobserved. There are numerous unanswered questions including how the eastern pathway partitions between Ombai and Timor, what controls this deep circulation and why there is little or no surface contribution to the ITF through Banda Sea. These are topics for future research. In the next Chapter we focus on this new way of considering partitioning that relates the transport through Makassar and Lombok Straits and try to shed some light as to what controls this western branch of the ITF.

Chapter 4

A Mechanism for the Partitioning Between Outflow Passages

4.1 Introduction

One of the ITF theories describes it as a current driven by the pressure difference between the Pacific and Indian Oceans (Wyrtki, 1987). It also originates from the North and South Pacific low latitude western boundary current (WBC) systems. In this context, Australia and Asia provide the western boundary for the South Equatorial Current (SEC) and the North Equatorial Current (NEC) respectively, in the Sverdrup integration. However, this WBC system is leaky, and in order to close the circulation we need to take into consideration that the western boundary, Australia, is an island, as described by the island rule (Godfrey, 1989, 1996). The North and South Equatorial Currents in the Pacific Ocean feed the Mindanao Current and New Guinea Coastal Current, respectively; the later eventually provide the source waters to the ITF.

Together with the pressure gradient forcing the ITF is also a WBC. However, this current

has an unique behaviour in which most of the outflow water flows eastward and only a small portion flows through the westernmost strait. The expected behaviour would be for all or most of the ITF from Makassar Strait to flow through Lombok Strait, the westernmost gap and the direct connection to the Makassar Strait. The ITF partitioning shows that Lombok Strait has the lowest transport and the remaining water flows eastward along the Nusa Tenggara chain at approximately 8°S, towards Ombai Strait and Timor Passage, which is unusual for a WBC.

The ITF partitioning relates the transport in each outflow strait to the total ITF. Understanding the partitioning and the dynamics that govern it is important as the properties of the water contributing to the Indian Ocean inflow depend on which pathway the water followed. The mixing and water mass modification are different in different areas of the Indonesian Seas (Koch-Larrouy et al., 2015), and therefore, the pathway, as well as which outflow strait the water flows through, influence the heat and saltwater inflow to the Indian Ocean (Vranes et al., 2002). Another reason for better understanding of the ITF partitioning is that it could be used as a proxy for outflow transports, as mentioned in Sprintall and Revelard (2014). For instance, estimating the transport in one of the straits based on the transport in other strait. This could be particularly helpful for planning observational programs, in order to reduce costs and effort.

The controlling mechanism that limits the transport in the narrow Lombok Strait remains unknown. Nof (1995) suggests the ITF flow is choked and only a fraction of a typical western boundary current transport enters the passages. Wajsowicz (1996) using the analogy to an electrical circuit showed that the flow is carried by the westernmost gap (and not the largest), and its limit is set by friction. The remaining transport flows eastward until it finds a wide gap with no resistance. Downstream of the wide gap there is no more transport. Previous studies have investigated partitioning: Sprintall et al. (2009) showed the relation between outflows from observations; Sprintall and Revelard (2014) raised the question about how the partitioning varies according to the phase of climate modes of variability; and van Sebille

et al. (2014) highlighted the complex partitioning of ENSO-induced outflow transports. None of these studies attempted to explain what controls partitioning, and this is the goal at this Chapter. In this Chapter we first illustrate and test our hypothesis in a reduced gravity 1.5 layer model simulating a WBC flowing towards a gap to represent the flow from Makassar Strait towards Lombok Strait. Following that, we explore our ITF simulations and perturbation experiments based on the high-resolution model described in Chapter 2.

By imposing different boundary conditions and exploring the contribution of different terms of the momentum equations in our 4-km resolution ITF regional model, we investigate what controls the partitioning in Lombok Strait. We analyse the differences between model runs to test the hypothesis that the partitioning is determined by the relationship between the structure of the flow upstream of Lombok Strait and the strait geometry. A current upstream of Lombok Strait that is wider than the strait's width may explain why the water takes another pathway eastward along Nusa Tenggara. The analysis of our perturbation experiments in the context of WBC theory for steady flows shows that the transports, the partitioning and the current structure change for different experiments.

4.2 Western boundary current partitioning through a gap in a reduced gravity 1.5 layer model

The ITF western pathway is constrained first at Makassar Strait, with Labani Channel as the narrowest part, followed by Lombok Strait. Between them the flow has enough space to be restructured after the choke point in Labani Channel and before finding the very narrow gap in Lombok Strait. To simulate this interaction between the ITF in Makassar and Lombok Straits we use simple set up with a boundary current flowing towards a narrow gap in a barotropic wind driven gyre model. We run the model as reduced-gravity 1.5 layer model configured according to the Munk linear theory for WBC (Munk, 1950), which uses

Laplacian lateral friction in the boundary current to close the circulation. The model has a 4-km horizontal resolution and nonslip boundary condition. The computational domain of the model is a square basin of 800 km × 800 km. It solves the linear momentum equations for a southern hemisphere anticyclonic gyre where the forcing are the easterly winds at the equator and the westerlies in the south (north and south boundaries respectively in Figure 4.1.a). The boundary current is formed at the western side of the basin.

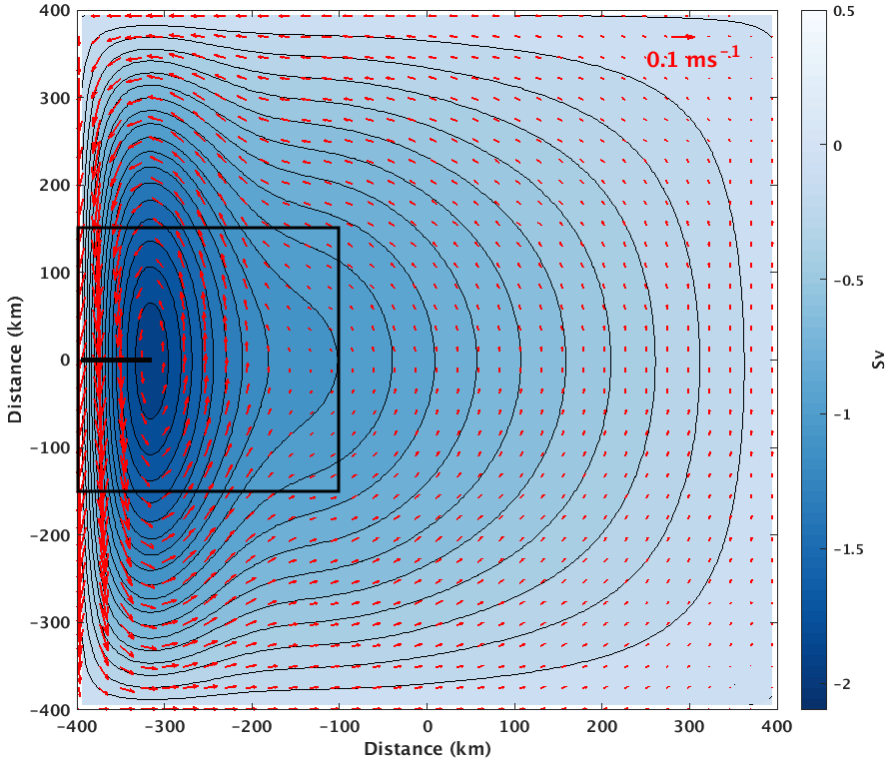

Figure 4.1: The southern hemisphere circulation gyre for the reduced gravity 1.5 layer model with viscosity coefficient of 1000 m^2/s. The WBC is to the left of the domain. Velocity vectors in red. The black square zoom in the area where the streamfunction is maximum and shows the transect (black line) where we extract velocities and measure the current width.

In our reduced gravity 1.5 layer model to explore the effect of current width in the circulation, we first run the model with different viscosity coefficients (A_H; Figure 4.1). The current width can be estimated by the cumulative transport and velocity along a zonal transect on the WBC, where the streamfunction is maximum. A cross section at the center of the gyre (transect at Figure 4.1) shows that the width of the current increases in different runs as we increase viscosity (Figure 4.2), as predicted by Munk's model. Munk described

this relationship between viscosity coefficient and current width with the following relation:

$$\delta_M = \sqrt[3]{\frac{A_H}{\beta}} \quad ,$$

where δ_M is current width and β is the latitudinal gradient of the Coriolis parameter (df/dy).

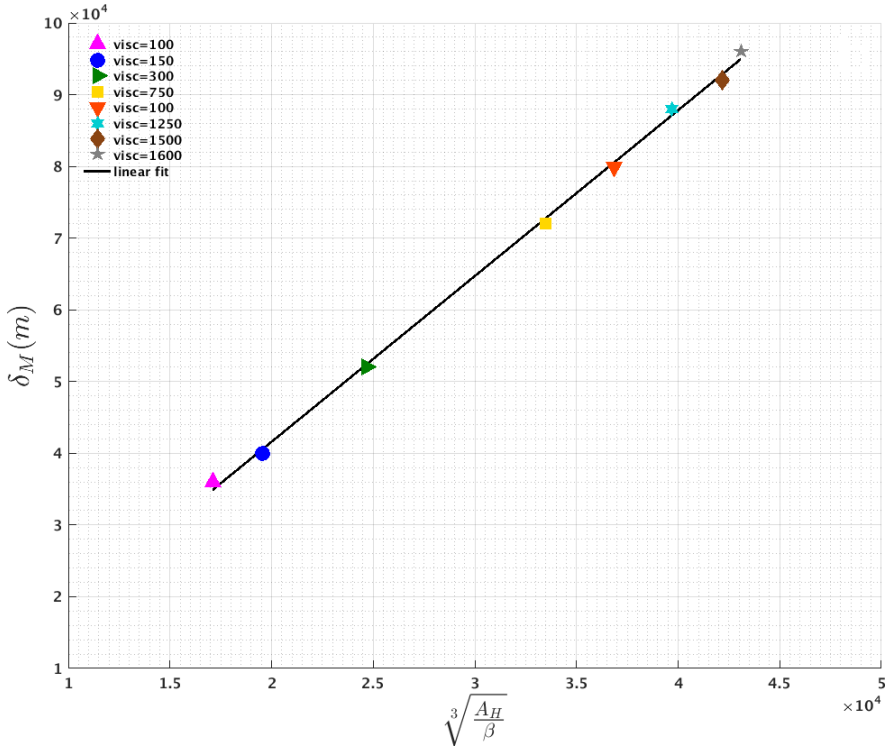

Figure 4.2: WBC width (δ_M, in meters [m]) and viscosity coefficient (A_H, in [m^2/s]) relation in the reduced gravity 1.5 layer model. The linear relation between the cubic root of the viscosity coefficient, A_H over β, from the Munk model, shows the current width increases with increasing viscosity coefficient.

Next, we simulate the partitioning of the ITF by adding an obstacle to the reduced gravity 1.5 layer model. We add a narrow zonal wall (4 km wide and 48 km long) in the center of the domain, leaving a gap of 32 km between the western boundary and the western side of the obstacle (Figure 4.3), which represents the Lombok Strait. We expect the obstacle to interfere with the WBC flow when the current is wider than the gap, as it interrupts the current's pathway. In this case the possibilities are: (1) the current squeezes towards the boundary to fit into the gap; (2) the current splits and part of it flows east and around the wall; (3) the current splits and part of it recirculates when it meets the wall. For a wide

current (larger than the gap, e.g. current width of 40 km), as is the case with $A_H = 1000$ m^2/s, we find the WBC cannot fit in the narrow gap (Figure 4.3.a). Instead, most of the current goes eastward along the obstacle, with some of the flow going around the obstacle (Figure 4.3.b) and a recirculation cell develops north of the wall. Some of the WBC flows into the gap. This split in the flow is similar to observations and modeling of the ITF western pathway.

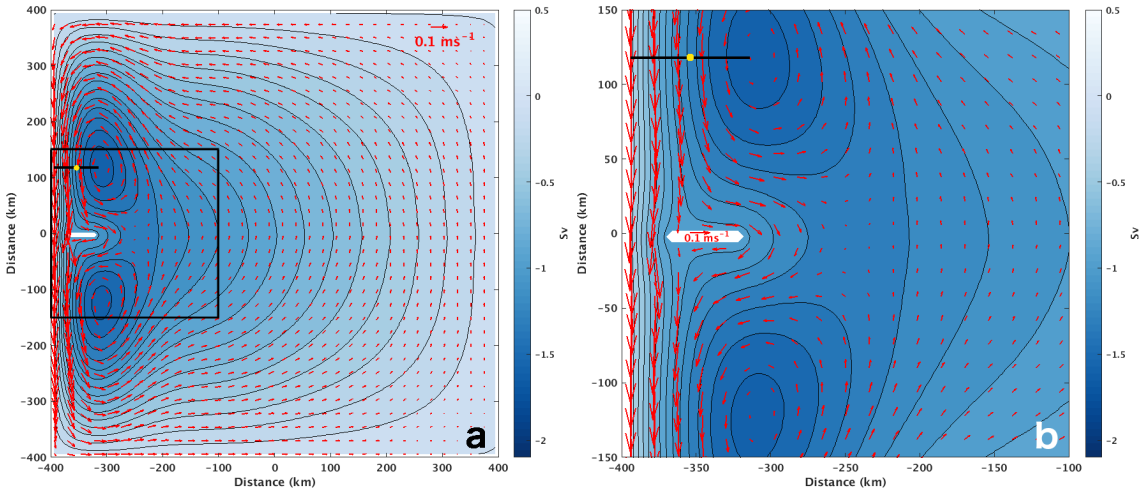

Figure 4.3: (a) The southern hemisphere circulation gyre in the reduced gravity 1.5 layer model with nonslip condition, viscosity coefficient of 1000 m^2/s and a wall with a gap interrupting the WBC. Velocity vectors in red. (b) The black square zoom in the center west of the domain shows the transect (black line) where we measure the WBC width. The limit of extension of the WBC width (yellow dot) excludes the recirculation gyre and the splitting of the WBC.

To explore the effect of current width on the fraction of WBC transport that is able to flow downstream through the gap (partitioning), we again change the WBC width by changing A_H. We find the wider the WBC the smaller the partitioning (a current 60 km wide has a 58% partitioning and a current 32 km wide has a 86% partitioning, Figure 4.4) which shows an inverse relation between those two quantities. In the limit when current width is smaller than the gap, partitioning reaches 100%, that is the entire transport of the WBC can fit through the gap. Indeed, as we hypothesised, the reduced gravity 1.5 layer model shows that the current width upstream affects partitioning at the gap, suggesting a mechanism for the control of transport in the gap. Furthermore, we also see that the portion of flow that does not fit in the gap flows eastward along the northern boundary of the obstacle (island).

The results obtained in the reduced gravity 1.5 layer model show a clear inverse relation between current width and partitioning in a narrow gap. Here we explored this relation by changing viscosity and therefore current width. Larger viscosity coefficients produce wider currents and in turn the portion of water transported by this current that is able to fit in the gap is lower. This happens because the narrow geometry of the gap interrupts part of the flow which then needs to find another route. The similarity between this simple model and the real ITF suggests we may see the same process happening between Makassar and Lombok Strait. That is what we explore in the next section.

WBC theories are built upon the principle of balancing planetary vorticity. For the flow to navigate a complex bathymetry there must be a balance between sources and sinks of planetary vorticity along the pathway. We will explore this later by the vorticity budget analysis. Before that, in order to add complexity to the problem we tackled in the reduced gravity 1.5 layer model, we now investigate the mean outflow ITF in our high-resolution model. Perturbation experiments in which we change boundary conditions and terms in the momentum equation produce variations in the steady ITF and we explore the relationship between partitioning and current width. The real ocean is neither linear nor barotropic, and does not necessarily behave as per non-slip conditions. Therefore, changes in the planetary vorticity as the ITF flows southward along Makassar Strait towards Lombok Strait can be balanced by other processes and not just lateral friction as in the simple reduced gravity 1.5 layer model. The perturbations allow us to explore other ways the flow balances planetary vorticity change and likely changes current width in the ITF western pathway.

4.3 The Perturbation Experiments

WBC theories (Sverdrup, 1947; Stommel, 1948; Munk, 1950; Fofonoff, 1954), build upon Sverdrup balance and recognise the need for a narrow strong boundary current in order to

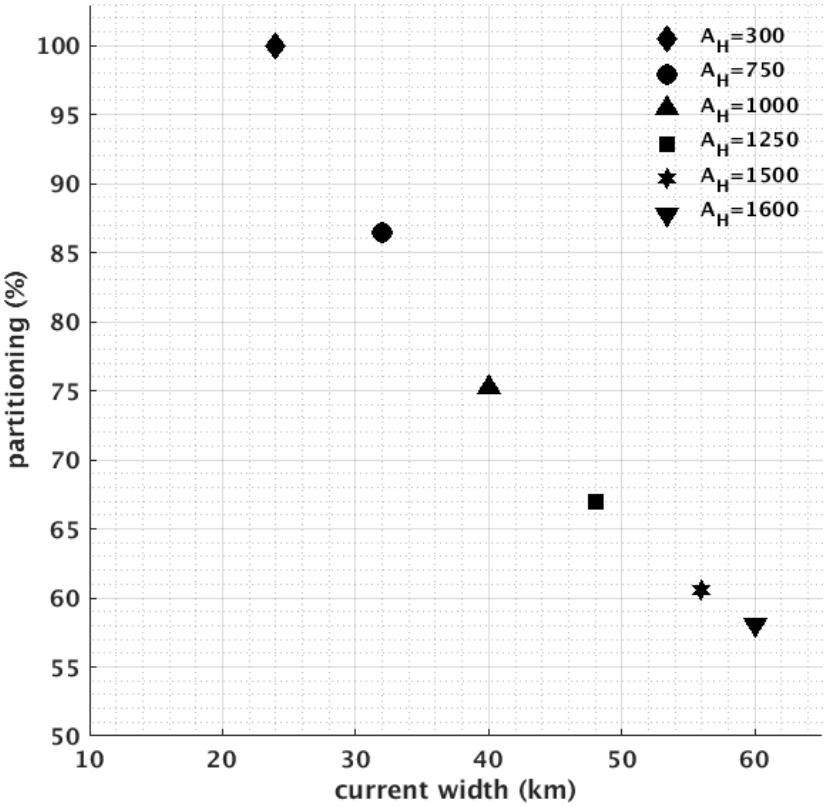

Figure 4.4: Inverse relation between current width and partitioning for different viscosity coefficients A_H (m^2/ s) in the reduced gravity 1.5 layer model with an obstacle and a gap 32 km wide.

close the circulation in the ocean interior. Different models achieve this through various approximations involving bottom friction (Stommel model), lateral friction (Munk model) and non-linearity (the inertial Fofonoff model) to balance changes in planetary vorticity. In all cases the role of the boundary layer is to remove the gain/loss of vorticity as the flow moves south/north, which will be done in different ways depending on the dynamics. The width of the boundary layer, that is the current width, is set in each of these models by the leading order balance terms. These models can be solved for different boundary conditions at the lateral boundaries (slip, non-slip or super-slip walls), without changing the balance of change in planetary vorticity.

In our experiments, and treating the ITF as a boundary current, we will explore the effects of having a viscous boundary layer and an inertial boundary layer using different model configurations. We run linear/non-linear experiments for the steady ITF and also

experiments with increased friction. Because the ITF is strongly constrained by topography, we anticipate significant interactions with the boundary may also play a role in the current dynamics. Thus, we run all our experiments under different boundary conditions, slip and non-slip. Slip walls allow the flow to slide at the boundaries and velocity at the wall is non-zero, while under non-slip walls velocity at the wall is zero.

The six experiments are as follows: (1) a non-linear experiment with non-slip condition, which is the control run (from Chapter 3); (2) a non-linear experiment with slip condition; (3) a linear experiment with non-slip condition; (4) a linear experiment with slip condition; (5) high friction (A_H=1000 m^2/s) non-linear and non-slip; and (6) high friction (A_H=1000 m^2/s) non-linear slip. The linear experiments do not include the advection of momentum terms in the model solution. We also ran an experiment in which we double the magnitude of local winds, but found no significant changes in the transport and ITF dynamics, so this experiment is not discussed any further.

4.4 Perturbation Experiments Comparison

The inflow (A and B on Table 4.1) and outflow (C, D and E on Table 4.1) vertically integrated transports for the perturbation experiments in various ITF straits provide a comparison of changes in transport. All experiments are compared to the control (non-linear, non-slip setup). The two inflows co-vary, balancing each other in such way that if the western pathway increases, the eastern pathway decreases. The only experiment that has increased transport in the western pathway (Makassar Strait; although it is a small change of just 0.19 Sv) as a response to the non-linear slip model configuration. All the others, especially for the larger friction with non-slip boundary condition experiment that shows the most pronounced difference (2.02 Sv), have decreased transport in the western pathway and increase in the eastern pathway. This shows the significance of a slip condition at the boundary, on bringing

the flow to the western side of the Indonesian Seas. Linearity and increased friction both result in increased transport in the eastern pathway.

We clearly see that changes in transport between experiments, especially in Makassar and Lombok Straits, can affect the partitioning (Lombok/total ITF), as the relation between the outflow passages changes. While the total ITF is the same in all experiments, how it is distributed across the different outflow passages varies according to intrinsic factors like boundary conditions, non-linearity and friction. Because these perturbations affect the transport distribution, we expect to see changes in other aspects of the current such as the jet structure including current width. So we now investigate the pathways and circulation for each perturbation experiments to understand the relationship between inflow and outflow passages and explore the vertical structure of the jets.

Experiment	**control**	**non-linear slip**	**linear non-slip**	**linear slip**	**> friction non-slip**	**> friction slip**
Western pathway (A)	-9.7	-9.9 (+0.2)	-8.5 (-1.2)	-8.6 (-1.1)	-7.7 (-2)	-9.3 (-0.4)
Eastern pathway (B)	-4	-3.8 (-0.2)	-5.2 (+1.2)	-5 (+1)	-6.1 (+2.1)	-4.5 (+0.5)
Lombok (C)	-2.6	-3.4 (+0.8)	-3.4 (+0.8)	-5.4 (+2.8)	-1.7 (-0.9)	-2.9 (+0.3)
(C/F) %	19.9	26.6	26	41.5	12.4	22.4
Ombai (D)	-5.1	-4.7 (-0.4)	-7.8 (+2.7)	-6.5 (+1.4)	-4 (-1.1)	-4.9 (-0.2)
(D/F) %	38.9	36.5	59.3	50.2	29.4	37.3
Timor (E)	-5.4	-4.8 (-0.6)	-1.9 (-3.5)	-1 (-4.3)	-7.9 (+2.5)	-5.3 (-0.1)
(E/F) %	41.1	36.8	14.6	8.3	58.1	40.3
Net outflow (F) (F=C+D+E)	-13.1	-12.9 (-0.2)	-13.1 (0)	-12.9 (-0.2)	-13.6 (+0.5)	-13.1 (0)
Partitioning ratio (C/A) %	26.9	34.8	40.3	62.2	21.9	31.7

Table 4.1: Six month averaged volume transports in Sv (10^6 m^3/s) in the main ITF inflows western and eastern pathway, and major outflow passages Lombok, Ombai and Timor). Positive differences in brackets mean transport increases and negative mean transport decreases with respect to the control run. The partitioning is expressed as a percentage of either the total outflow (for each strait) or only the western pathway (for Lombok Strait). See Figure 1.1 for location of inflow/outflow passages.

4.4.1 ITF pathways and circulation in the experiments

The ITF pathway transport for the non-linear slip is very similar to the control run (Figure 4.5.a compared to Figure 3.1 from Chapter 3). The circulation is mostly affected by linearity as we see a significant change in the current, with narrower jets following the shelf more closely (300 m isobath in Figures 4.5.b and 4.5.d) along with increased transport in

Lombok and Ombai Straits (Table 4.1). In the control (non-linear) run we observe that the current overshoots boundaries, and the flow meanders more than in the linear run (Figures 4.5.a). Another difference, is that in the linear runs, flows outside the ITF (the circulation in the Pacific and Indian Ocean portion of the model domain) are mostly zonal and have limited meridional extent compared to the non-linear runs. In the larger friction experiment (non-slip) the flow overshoots past the boundary as in the control run, but it does not follow topography as much as in the other experiments and the jets become wider (Figure 4.5.c).

In the eastern pathway at the Banda Sea, the current just south of 5°S penetrates further to the west into Flores Sea in all experiments, compared to the control except from the larger friction experiment. Particularly in the linear run (Figures 4.5.b) it penetrates far enough west to join the current coming along the western pathway through Makassar Strait at approximately longitudes of 118°E.

To further illustrate changes in the circulation for the perturbation experiments we look at the difference between the mean speed averaged in the top 300 m in the control run (Figure 4.6) and that of each experiment (Figure 4.7). The non-linear slip run shows an intensification of Mindanao current entering Celebes Sea until it reaches Makassar Strait (Figure 4.7.a); stronger velocities are closer to the coastline. The linear runs have much stronger speeds along the whole western pathway: maximum difference of around 3.8 m/s at Mindanao current, 1.9 m/s upstream of Makassar Strait at the northwest of Celebes Sea and 0.8 m/s along Makassar Strait. Away from the western boundary the velocities are weaker as the flow is closer to the boundary. In the larger friction experiment (non-slip) the only significant difference is at Mindanao inflow with the opposite effect; the current is slower closer to the boundary (differences of -0.9 m/s; Figure 4.7.b.). At Makassar Strait, the maximum difference is -0.3m/s. There are no significant differences in the eastern route in the Banda Sea for all experiments. Linearity appears to affect the current the most, in terms of jet position and strength along the western pathway, combined with large changes in transports at the outflow straits.

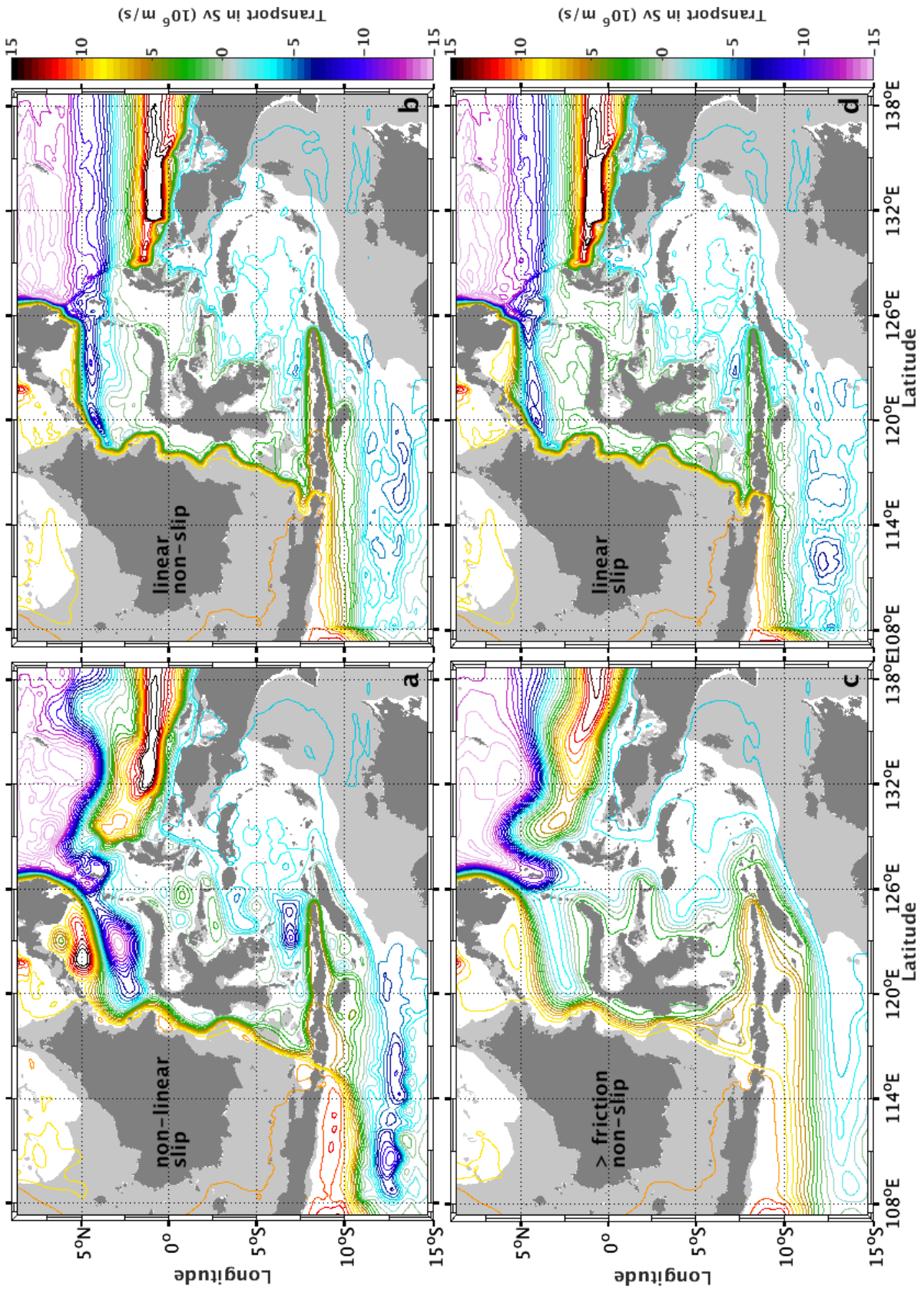

Figure 4.5: Barotropic transport streamfunction in the perturbation experiments: (a) non-linear slip, (b) linear non-slip, (c) >friction non-slip and (d) linear slip. Contour intervals are 1 Sv. Areas in lighter grey are shallower than 300 m.

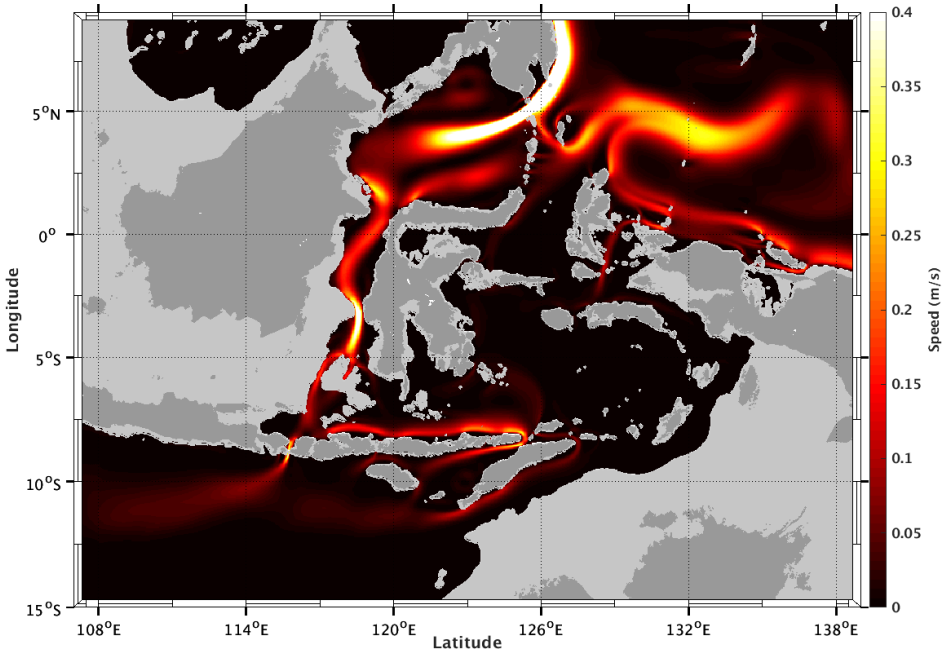

Figure 4.6: Six month mean speed for the control run, averaged in the top 300 m. The areas in lighter grey are shallower than 300 m.

The distribution of the flow amongst the three exit passages is much more complex. For the perturbation experiments that produced increased transports in Lombok Strait, the other straits, Ombai and Timor Passage, do not show a consistent variation that balance changes in Lombok Strait (Table 4.1). Sometimes they combine to balance Lombok Strait changes and other times one co-varies with Lombok Strait and the other strait balances the sum. However, this complicated response at the outflow passages may reflect changes in the upper, intermediate or deep inflow originating from either the western or eastern pathways. In order to understand what controls the fraction of Makassar Strait water that exits via Lombok in the context of WBC theories, we reconsider the term partitioning and calculate it as the ratio of western pathway water that flows through Lombok Strait, rather than considering partitioning as a fraction of the total outflow (C/A % in Table 4.1).

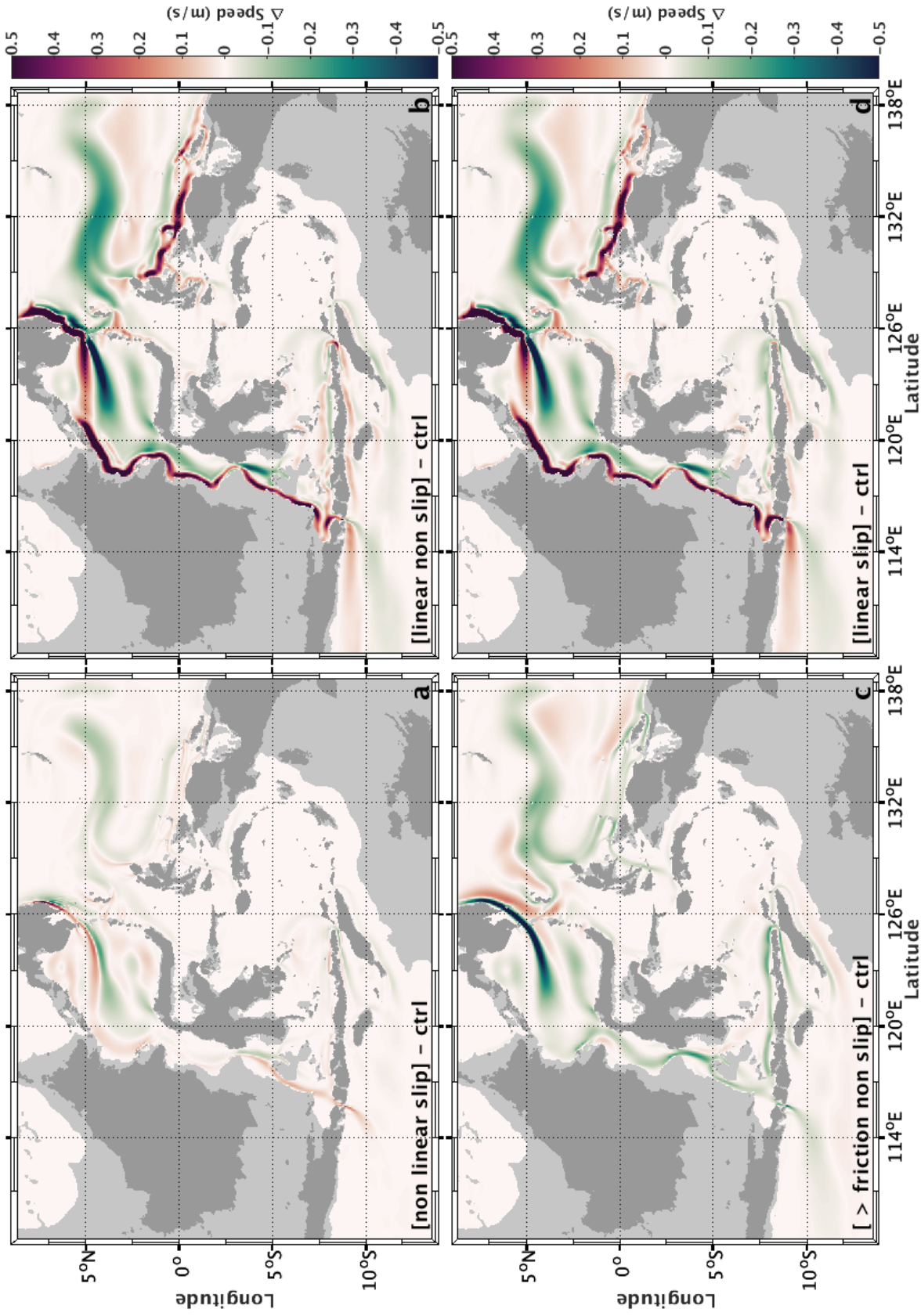

Figure 4.7: Difference in the top 300 m averaged speed between experiments and control run: (a) non-linear slip, (b) linear non-slip, (c) >friction non-slip and (d) linear slip. The areas in lighter grey are shallower than 300 m.

4.4.2 Vertical velocity structure

The vertical structure of the velocity in Lombok Strait jet is constrained by the shallow (maximum of 300 m) and narrow topography. Therefore, changes in the vertical extent of the flow could also affect partitioning without changing current width. We found considerable differences in the top 300 m layer mean speed analysis (Figure 4.7). To complement that analysis, we investigate the jet in the vertical in a choke point of the Makassar Strait, surrounding the Labani Channel. Three cross sections at 2°, 3°and 4°S show the effect of the narrow channel on the flow (Figure 4.8).

In the control run at the northern entry of Makassar Strait (2°S) the jet is located in the middle of the strait and is surface intensified (Figure 4.8.a). After squeezing to fit in the Labani Channel at 3°S (Figures 4.8.e and 4.8.i), with stronger speed reaching almost 200 m, the jet becomes deeper and faster with the core around 100 m at 4°S, however it has similar width as the upstream jet at 2°S. This is the structure of the jet just before reaching Lombok Strait (Figure 4.8.c). In the non-linear slip experiment the upstream current is the same as the control. The jet is similarly affected by the constraint as it is in the control with just a small increase in velocities on the western side of the downstream jet (Figure 4.8.j). The linear runs produce a much different current structure, again highlighting largest changes are related to linearity. The upstream jet is much stronger (1 m/s), narrower and deeper than the control (Figures 4.8.c and 4.8.d). While crossing Labani channel, stronger velocities are concentrated only in the narrower part of the channel and the surface has a decrease in speed (Figures 4.8.g and 4.8.h). Downstream at 4°S, the jet is narrower with a deeper core, similar to the control but now with a much stronger speed shifted to the western boundary (Figures 4.8.k and 4.8.l). For both linear runs, the transition from upstream to downstream of Labani Channel is independent of the boundary condition setup (slip or non-slip).

The outflow passages velocity sections show a western intensified jet in Lombok Strait with a core speed of 0.7 m/s centered at 60 m (Figure 4.9.a). Ombai Strait has a deep and

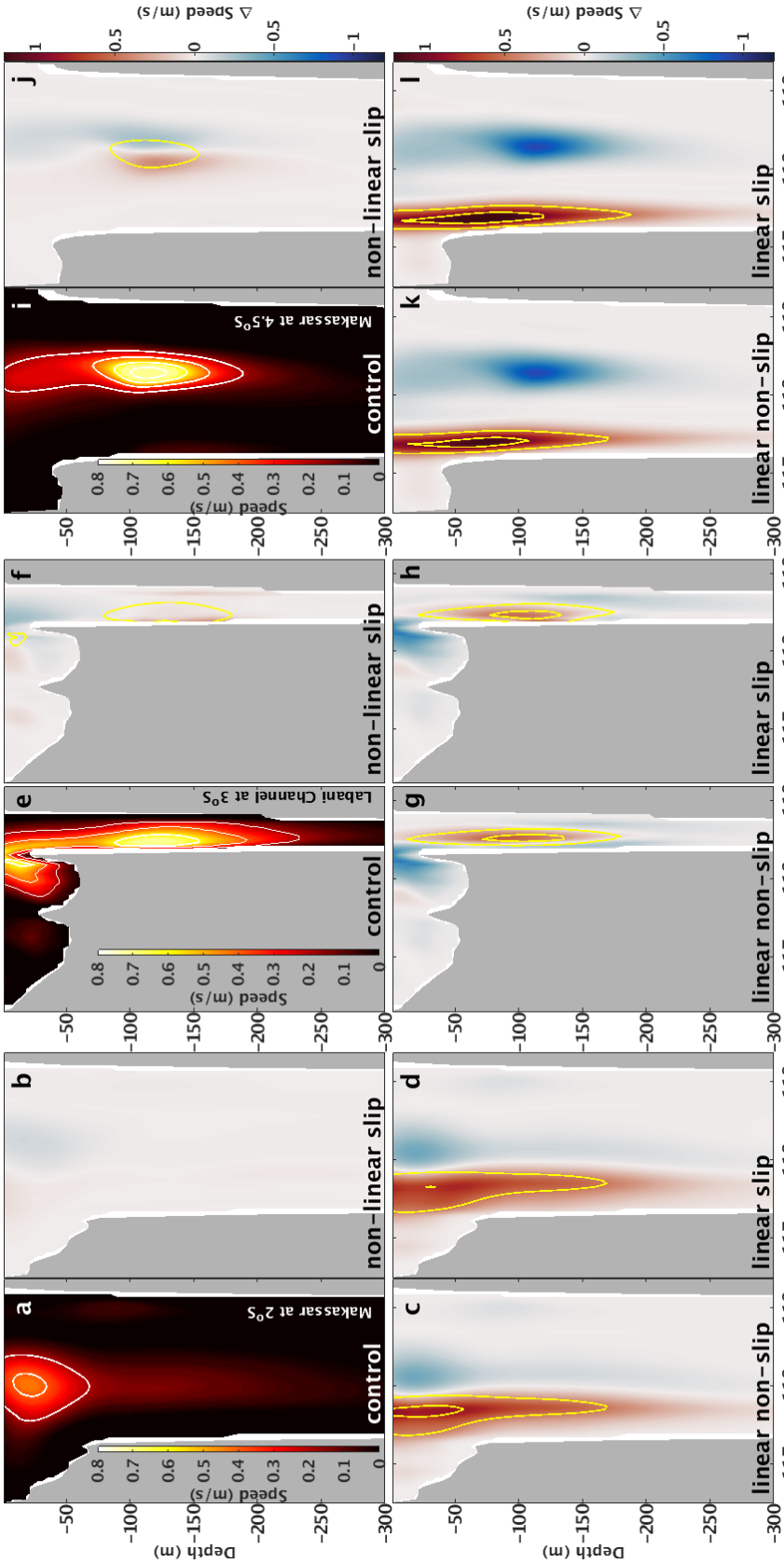

Figure 4.8: The speed in the top 300 m for the control run at (a) Makassar Strait across a zonal transect at latitudes 2°S north of Labani Channel, (e) at 3°S at the constrained Labani Channel and (i) at 4°S south of Labani Channel. White contours interval is 0.2 m/s. (b,c,d,f,g,h,j,k,l) Difference in speed between the three experiments and the control run for the same transects. (b,f,j) are the non-linear slip - control run; (c,g,k) are the linear non-slip - control run; and (d,h,l) are the linear slip - control run. Yellow contours interval is 0.5 m/s.

narrow jet slightly displaced to the northern side. Maximum speed is 0.5 m/s with a core around 100 m, deeper than in Lombok Strait. With slip condition the jet shifts to the west boundary in Lombok Strait seen as stronger speed closer to the wall (Figure 4.9.b). Linearity intensifies the jet cores and bring them closer to the surface (Figure 4.9.c and 4.9.d). The linear slip run shows both effects (attaches to the coast and increased speeds) in the jet that occupies almost the whole strait with a very strong core of 2.6 m/s. The Ombai Strait jet is slowed down in the experiments with slip condition and broadened resulting in velocity increase on the jet edges in the linear non-slip experiment. In Timor passage there are no significant differences.

In summary, in Lombok Strait, the slip condition increases velocities attached to the western boundary but keeps the same jet structure while absence of non-linearity reorganises the flow in a broader jet. Upstream of Lombok Strait, at 4°S (Figure 4.8.c) slip condition shifts the jet to the west but it is still more centered in the channel, while in linear runs the current is narrower and much closer to the coast. This indicates the importance of non-linearity for the ITF at this sector. After crossing Labani Channel at 4°S, non-linearity results in overshoot on the flow (advection of momentum) and the current does not have enough time and distance to adjust and reattach to the coast. When it reaches Lombok Strait, for the current to be dynamically balanced, the flow approaches the boundary. In the linear cases, friction is acting along the entire pathway which keeps the flow attached to the coast even upstream at 4°S. Overall, the vertical structure shows that there are no considerable changes in the depth of the current and therefore the partitioning is not limited by vertical extension.

Lastly, we analyse the transport per unit depth of the jet upstream of Lombok Strait at a zonal transect at latitude 4.5°S (Figure 4.10). The net transport above 300 m is approximately 1.5 Sv for the control, non-linear slip and friction slip experiments and approximately 1.3 Sv for the two linear experiments and the friction non-slip. This difference reflects how the transport is partitioned between the western and eastern pathways, which is

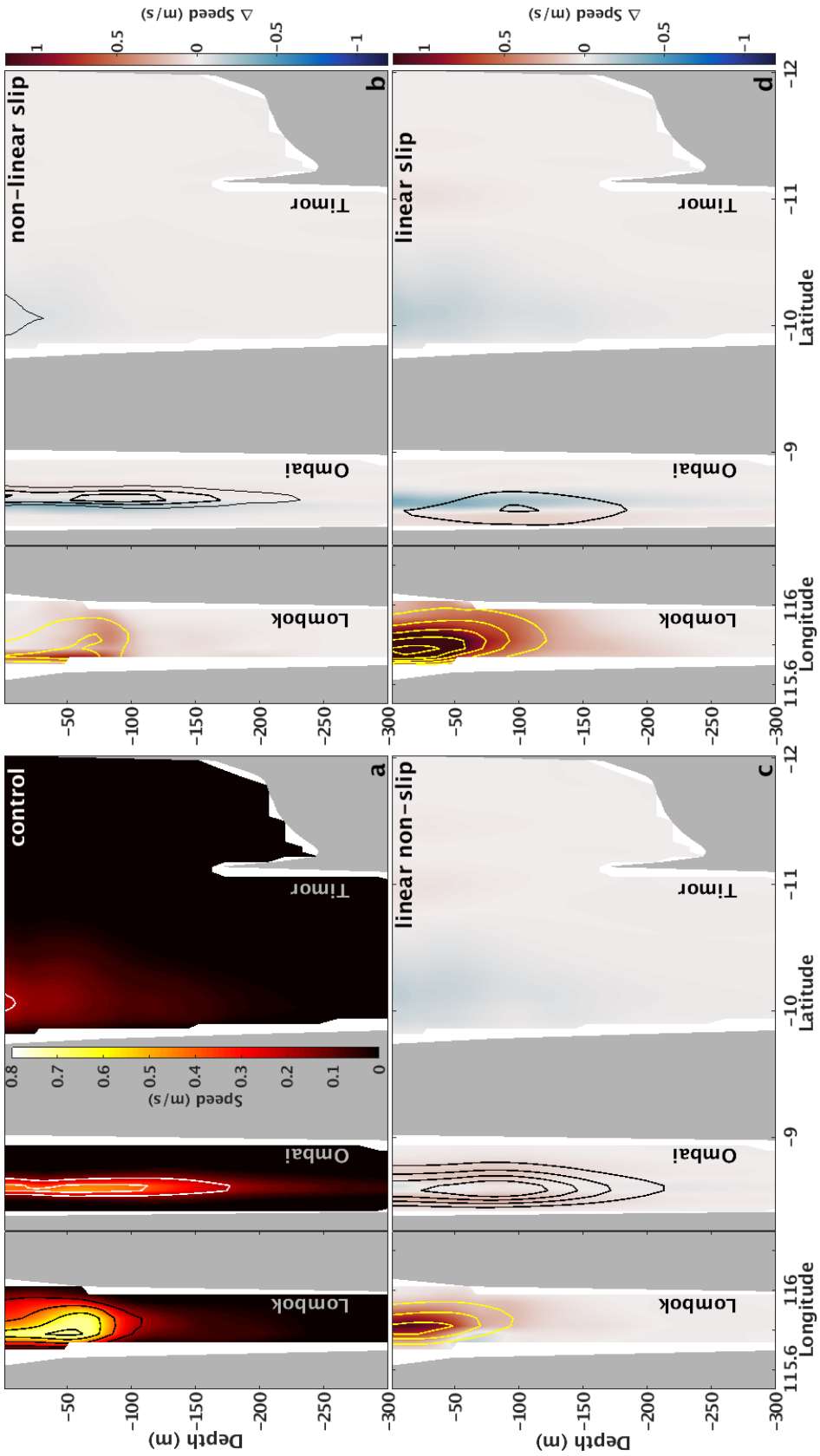

Figure 4.9: (a) Speed for the control run in the three outflow passages cross-section. Difference in speed at the same transects between (b) non-linear slip, (c) linear non-slip and (d) linear slip runs and the control run indicated in the red and blue colorbars. Yellow and black contours are the speed in each experiment and the intervals are 0.5 m/s and 0.1 m/s, respectively.

lower at the western pathway in the second group of experiments (Table 4.1). Therefore, the vertical distribution of transport maxima in each experiment, even showing different depths of maxima, does not seem to affect partitioning. In other words, while there are differences in the vertical structure of the flow, the vertical extent of the current is not deeper than the sill depth of Lombok Strait. Those differences of the flow core depth and the fact that they are all above Lombok Strait sill depth, encourage us to explore this transect further and estimate current width.

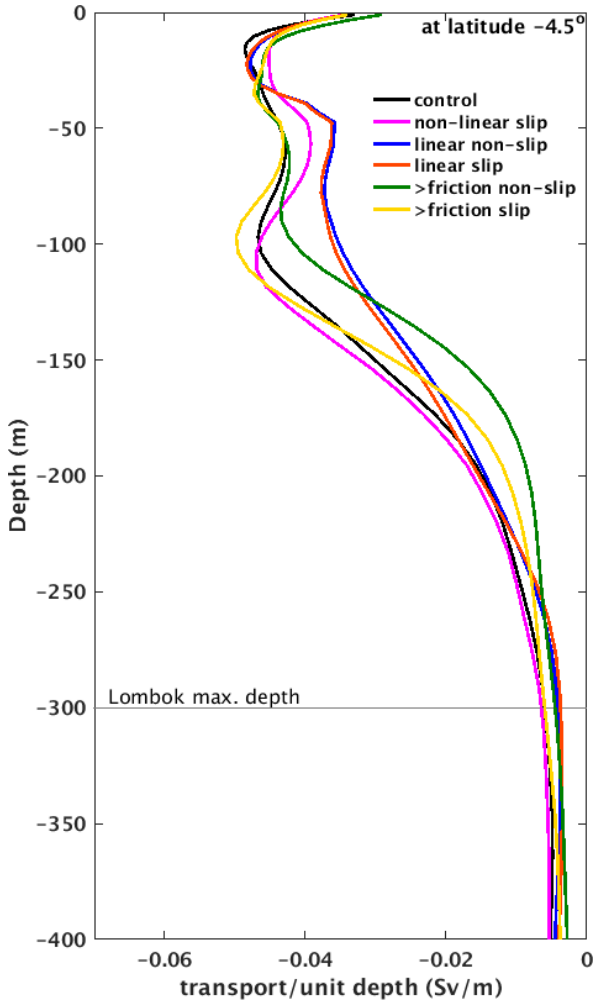

Figure 4.10: Transport per unit depth (Sv/m) for the zonal transect at 4.5°S in the control run and the perturbation experiments. The Lombok Strait maximum depth is indicated.

4.5 Why are there differences in partitioning?

According to WBC theory, the width of the WBC can be controlled by lateral friction and non-linearity. Based on the changes in the jet structures we have observed in the perturbation experiments, we expect changes in current width to occur. The most affected is the Makassar Strait flow structure (at latitude of 4.5°S, Figure 4.11). Despite changes in the depths of maximum speed and transport (Figure 4.8 and Figure 4.10), the most apparent difference between models is the horizontal extent of the current (Figure 4.11).

The streamlines suggest the current is wider in the control and the non-linear slip runs (Figures 4.11.a and 4.11.b). We also see the WBC streamlines cannot all fit in the limited width of Lombok Strait and some are deflected to the east, similar to the behaviour we also observed in the reduced gravity 1.5 layer model. The current splits close to Lombok Strait and also further north at 5°S, where it meets the shallow topography of the Dewakang sill. This shows that the partitioning happens more than once. In the linear experiments, extra streamlines flow through Lombok Strait (represented by the red lines from the control limit and extra black lines in Figure 4.11.b, 4.11.c and 4.11.d), which correspond to 1 Sv in the linear non-slip and 3 Sv in the linear slip. The boundary current has a smaller width and more water flows through Lombok Strait in the linear runs. This suggests a direct relation between the current width and the partitioning where the wider the current the lower the transport in Lombok Strait.

To investigate if a WBC width and partitioning relation exists we measure the current width in the 4.5°S transect (marked in Figure 4.11). We chose this location because it is where the current has time and space to be restructured after squeezing through the Labani channel. We use the cumulative transport and vertical integrated velocity along the transect to define the edges of the WBC (Figure 4.12). First we check the maximum transport that can flow within 35 km distance, which is the same width of Lombok Strait, using the vertical

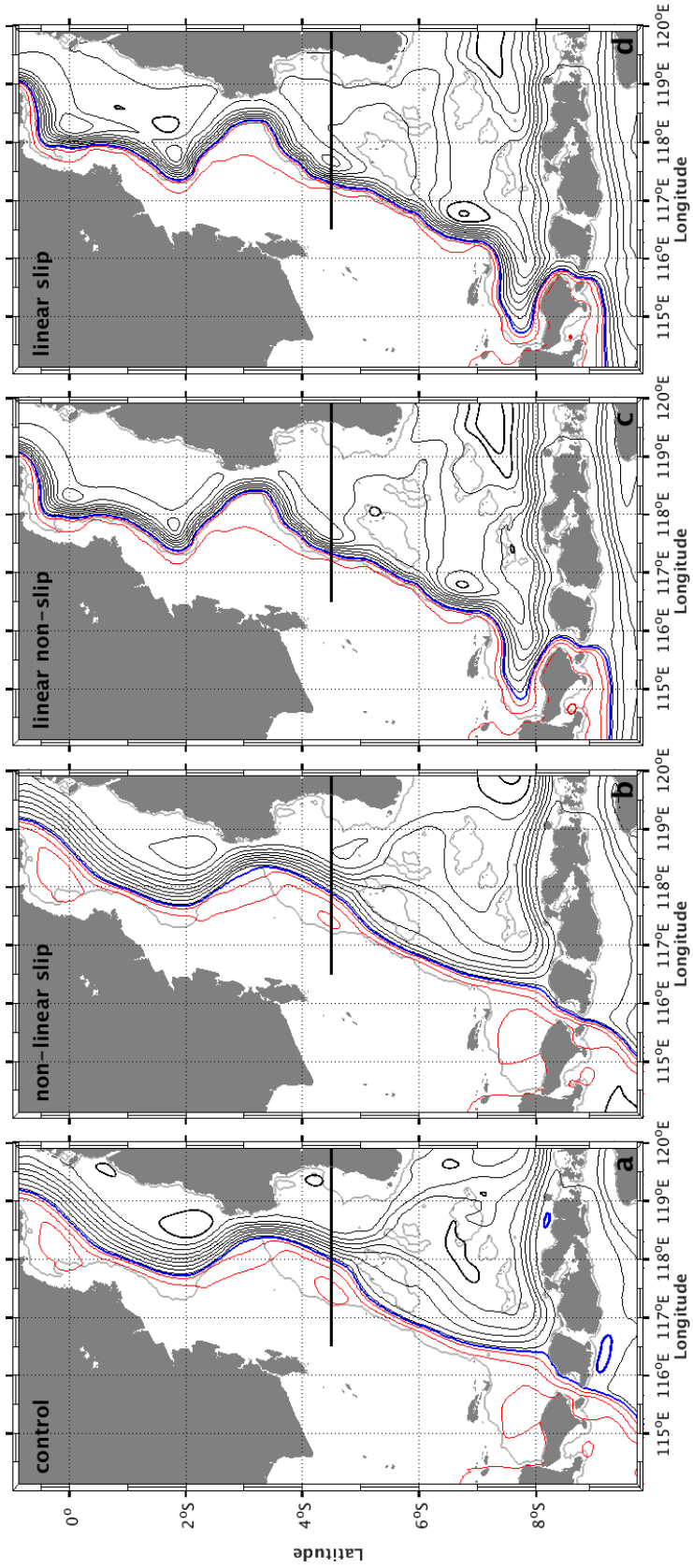

Figure 4.11: Barotropic transport streamlines along Makassar Strait for (a) the control, (b) the non-linear slip, (c) the linear non-slip and (d) the linear slip runs. Contour intervals are 1 Sv and the transport is the difference between isolines, decreasing towards the east as the transports are southward. In the control run, streamlines that flow through Lombok Strait are in red, the streamline limit is in blue and the streamlines that do not flow through Lombok Strait are in black. In the experiments, the same colors are kept for the same values of streamlines. The 200 m isobath is shown in light grey. The transect line in black at 4.5°S is where we measure the WBC width.

integrated velocity (dashed line in Figure 4.12) for the control run. We estimate how much of the total current transport, at that location, fits in 35 km; we find that 53% of the total southward transport in the control run fits in an extension similar to the Lombok Strait width (indicated in Figure 4.12.a as the percentage in grey between the two dotted lines that represent the 35 km width). Based on the 53% of total transport carried in 35 km, we use a rounded quantity to the 53% (only for approximation purpose; 55%) of the total southward transport (the 55% is more than the half of the total southward transport and is approximately the total carried in 35 km extension for the control run) to determine the current width.

We test two methods for measuring the current width based on our 55% criteria, these consider different locations along the zonal section of the current where we measure it. One is closer to the western boundary and we delimit if from the 5% of total transport, to exclude the effect of interaction with the boundary, until the 60% of total transport. The current width is the distance between these two locations (larger dots with percentages in Figure 4.12). The other method also uses the 55% of total transport but we displace it to the east so the center coincides with the maximum vertical integrated velocity. We project it on the cumulative transport curve and delimit the edges of the current (red dots in Figure 4.12). That way we measure current width centred around the strongest part of the jet. Both methods give similar current width for the same experiments and the small differences do not alter our main results. Thus, we chose the first method described, as the current closer to the boundary is meridionally aligned with Lombok Strait and likely the further to the east, the less of that transport will flow towards Lombok Strait. The estimated current width are presented in Table 4.2.

The width of the Makassar Strait WBC in the control run at 4.5°S is 53 km (Table 4.2). This is 18 km wider than the Lombok Strait. The transport carried in this 18 km just upstream of Lombok Strait cannot physically fit in the strait. The WBC narrows in the linear experiments, it is 35 km for both non-slip and slip runs. Those experiments also

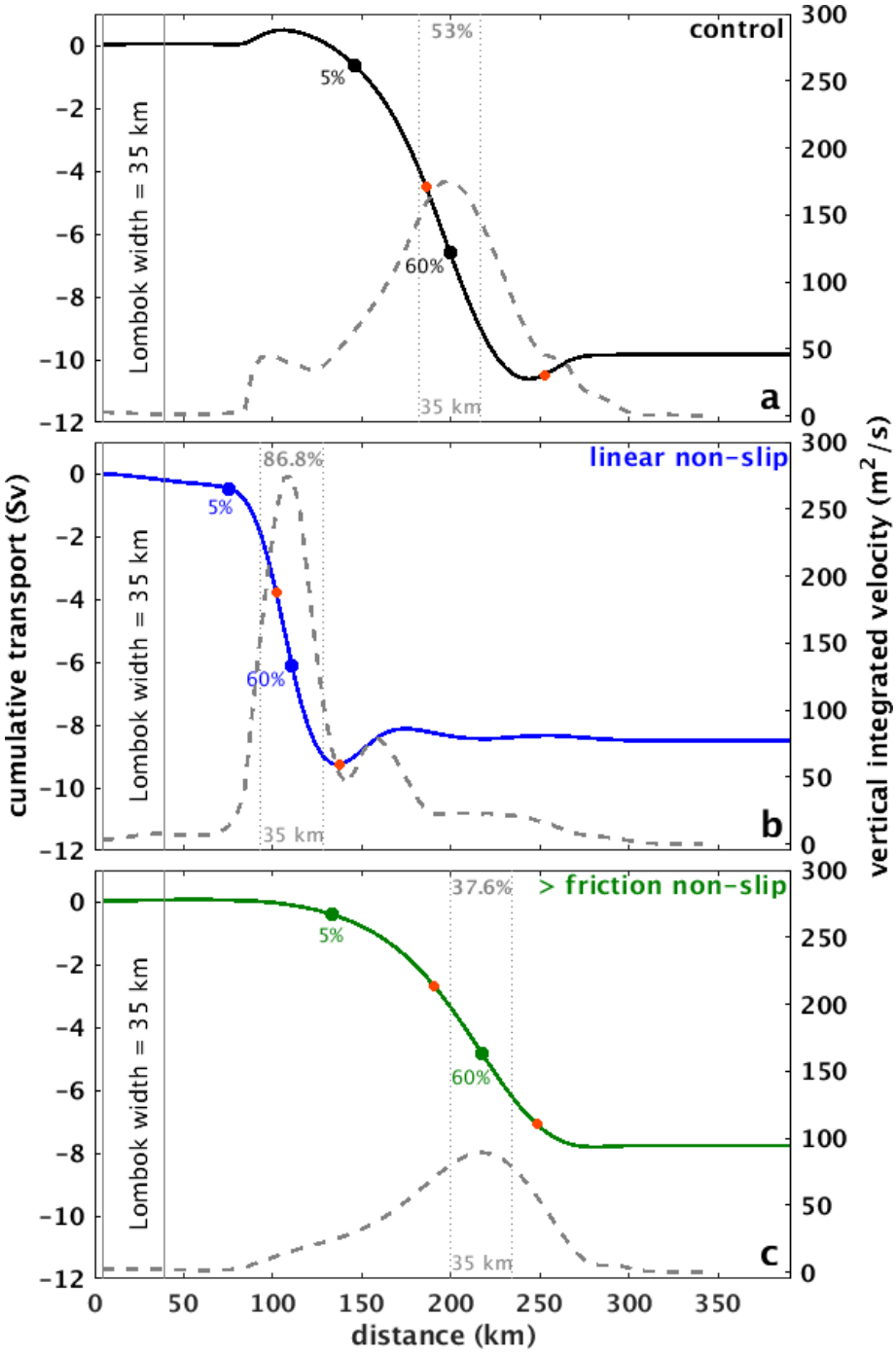

Figure 4.12: Cumulative transport integrated from west to east along the zonal transect at 4.5°S (solid lines in color), along with vertical integrated velocity (dashed lines in grey) to illustrate our current width definition for the (a) control, (b) linear non-slip and (c) >friction non-slip runs. Percentages in larger dots show the edges of 55% of the total transport considered to measure current width closer to the boundary. The red dots show the edges of the 55% (starting at 5% until 60%) of the total transport considered to measure current width at the centre of the jet. In grey, the percentage transported within 35 km which is limited by the two grey dotted lines. Lombok Strait width and position in reference to this transect at 4.5°S are shown.

have the largest partitioning for Lombok Strait as the ratio from Makassar transport (40% when boundary is non-slip and 62% when slip), which clearly show the relation from our hypothesis, where WBC width controls partitioning. We highlight that even if the current width has the same width of the channel (35 km), not all of it fits in Lombok Strait because of limitations of our method to measure current width, that does not consider 100% of the current transport, but only 55%. Other indications that support the partitioning control by current width is shown by the experiments: non-linear slip with a slightly wider current, 58 km; and the two friction experiments with an even wider current, more than 80 km). The partitioning in these three experiments decreases being the lowest with a wider current. In Table 4.2 we also see how the previous partitioning, as the percentage of the total ITF outflow, does not follow the same relation with current width.

Experiment	**control**	**non-linear slip**	**linear non-slip**	**linear slip**	**> friction non-slip**	**> friction slip**
Current width (km)	53.17	57.6	35.45	35.45	84.19	88.62
Lombok (Sv)	-2.62	-3.45	-3.43	-5.37	-1.69	2.95
Makassar (Sv)	-9.72	-9.91	-8.51	-8.63	-7.7	-9.3
Lo/Mak (%)	26.9	34.8	40.3	62.2	21.9	31.7
partitioning (%)	19.95	26.63	26.08	41.46	12.41	22.42

Table 4.2: Current width measured at the 4.5°S zonal transect, the transports in Makassar Strait (upstream) and Lombok Strait (downstream), the relation between both and the partitioning.

The reduced gravity 1.5 layer model and our results from the perturbation experiments, together help to explain the relation between current width and partitioning (Figure 4.13). The changes in current width with different viscosity coefficients in the reduced gravity 1.5 layer model and partitioning are comparable with what we observe in the perturbation experiments. We find relationships, one for each of the two regimes at the boundary condition that we have in the experiments, non-slip and slip. Considering them separately, linearity is what narrows the current, and consequently increases partitioning. While larger friction widens the current and decreases partitioning, in the same way that we showed for the reduced gravity 1.5 layer model (Figure 4.13).

We find an inverse linear relationship where current width decreases and partitioning increases (Figure 4.13), assuming the magnitude of the vertical integrated velocity (V) does

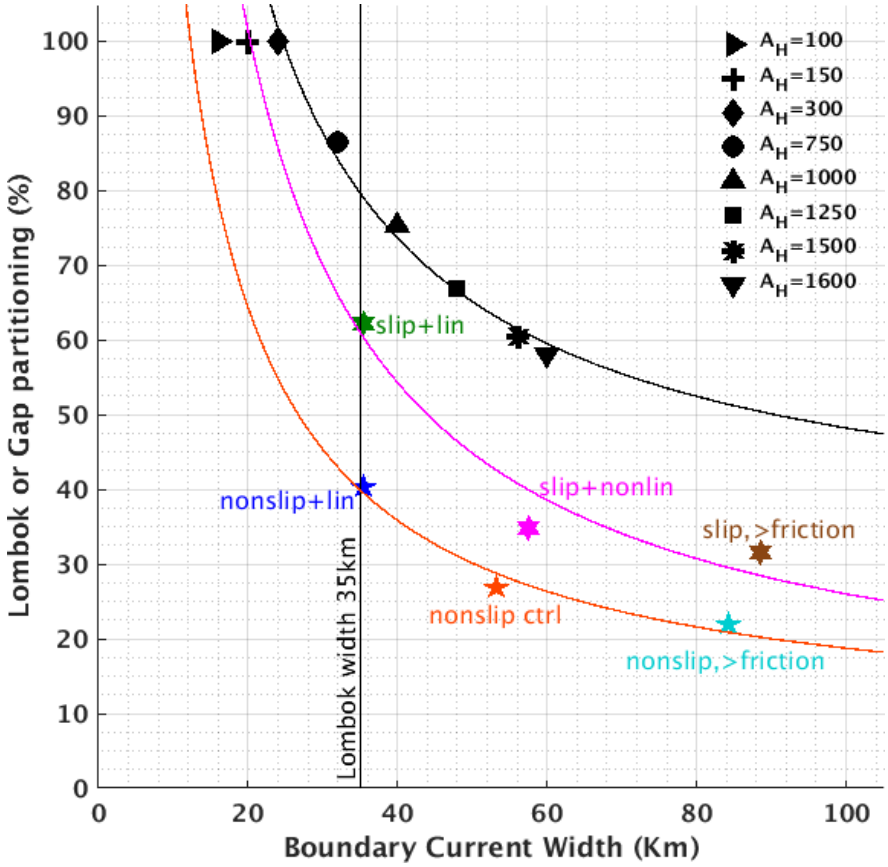

Figure 4.13: Partitioning as a function of boundary current width. Colored stars represent the perturbation experiments. Black markers show the results from the reduced gravity 1.5 layer model for the range of viscosity coefficients explored.

not change between Lombok and Makassar Straits, L is the width and partitioning (**P%**) is the ratio between transport in Lombok (T_{Lo}) and in Makassar Straits (T_{Mak}):

$$\mathbf{P\%} = \frac{T_{Lo}}{T_{Mak}} = \frac{\cancel{K}.L_{Lo}}{\cancel{K}.L_{BC}} = \frac{L_{Lo}}{L_{BC}} \sim \mathbf{L_{BC}^{-1}}$$

The **P%** is directly proportional to the inverse of the current width ($\mathbf{L_{BC}^{-1}}$; BC means boundary current). Given that Lombok Strait width (L_{Lo}) does not change and velocities are similar in both upstream and gap (or at the 4.5°S zonal transect and Lombok Strait), the partitioning is only a matter of the width of both (Lombok Strait and WBC).

Now we evaluate what sets the current width and if this is the only factor that limits the

transport in Lombok Strait, by investigating the vorticity balance for the control and the perturbation experiments in detail.

4.6 Vorticity Budget in the ITF's Western Pathway

Here like in the simpler WBC models, we can use the vorticity budget to help with understanding the ITF dynamics. To investigate that we use the vertical integrated vorticity equation (Equation 4.1). The western pathway of the ITF is a thermocline layer circulation (most of the flow is concentrated at the thermocline layer) so the equation does not include the interaction with the bottom (no bottom friction term). The effect of the wind curl term is restricted to the surface grid cell so it has minimal contribution to the vertical integrated balance. The wind curl term is then not considered in our vorticity equation and is included as a residual. The final equation for the vorticity balance in the outflow ITF is

$$\underbrace{\frac{\partial \xi}{\partial t}}_{(1)} + \underbrace{\mathbf{u}.\nabla_H \xi}_{(2)} + \underbrace{\beta V}_{(3)} - \underbrace{f w_z}_{(4)} = \underbrace{\frac{1}{\rho_0}\nabla_H \times \tau_z}_{(5)} + \underbrace{A_H \nabla^2 \xi}_{(6)} \tag{4.1}$$

where the terms are: (1) change in total vorticity - $\Delta\xi$; (2) advection - ADV; (3) planetary vorticity - βV; (4) stretching; (5) wind curl; and (6) friction - FRI. The variables are: vorticity (ξ), horizontal velocity vector ($\mathbf{u}$= (u, v)), Coriolis parameter(f), latitudinal gradient of f ($\beta = df/dy$), meridional component of velocity (V), vertical velocity (w_z), constant reference density (ρ_0), wind curl (τ_z) and viscosity coefficient (A_H).

We quantify the balance between the terms in the vorticity equation for the flow along Makassar Strait towards Lombok Strait in the control run. From the WBC models, we expect the friction term and non-linear term to be the dynamical factors balancing planetary vorticity along the western pathway of the ITF.

We use the momentum equation terms given as outputs from the control run to calculate the vorticity terms. These terms are provided as model products by the following: advection terms, Coriolis terms, lateral friction dissipation terms, vertical friction implicit terms, sea level height (η), pressure gradient and external forcing terms. We calculate the curl of those terms to obtain the vorticity equation terms and integrate in the vertical. The subdomain considers the balance only at the western pathway and its connection to Lombok Strait (Figure 4.14).

We do not show vertical friction (or stretching) and external forcing (wind curl) terms as they are small when considering the vertically integrated vorticity. The residual includes these two terms and therefore the final budget shows that the leading order terms of the vorticity balance for the western ITF outflow area are ADV (which can also be seen as relative vorticity), βV and FRI (Figure 4.14). It is important to highlight that actually ADV and BV have opposite signs in terms of what they are actually doing to the vorticity change. Here we consider the relation in Equation 4.1 which says a positive βV means a decrease in planetary vorticity.

Along the meridional flow from Makassar to Lombok Straits in the control run, ADV plays the dominant role in balancing βV but at times with reversing sign (which means going from source to sink) while the effect of FRI is localised and very large at the Labani Channel (Figure 4.14). That means the input of positive vorticity from βV as the flow moves southward is balanced by ADV at the upstream portion of Labani Channel. Where the channel gets narrower, around 2.5°S, FRI becomes the leading order balancing vorticity in the system, likely through higher friction produced by the walls of the narrow channel. Downstream of Labani Channel FRI is not important. Around 3.5°S where the channel becomes wider again, the ADV term begin to balance βV. From there on, the FRI term remains negligible until reaching Lombok Strait.

The mean ITF in our reference run (the control) has the ADV and FRI terms playing

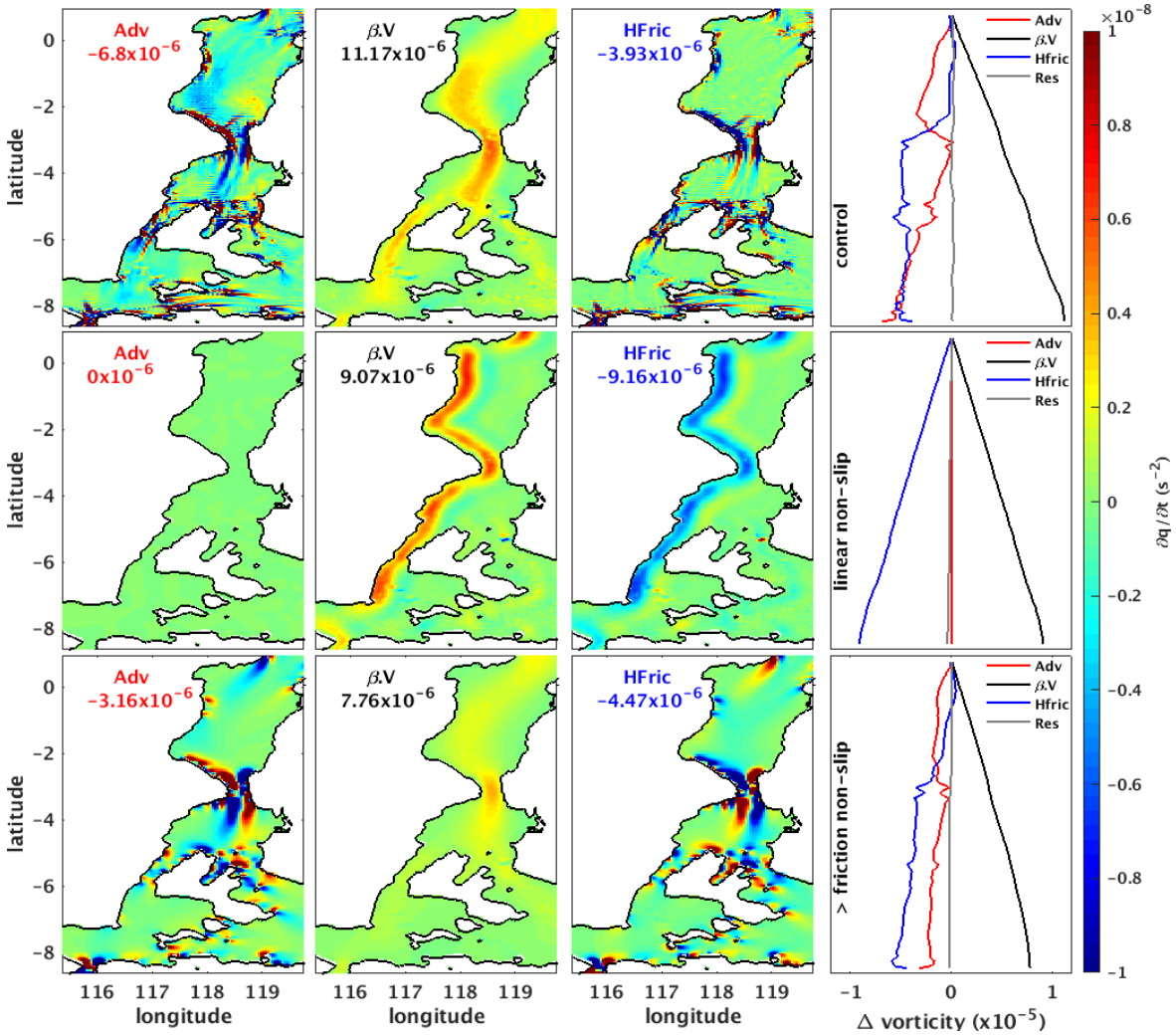

Figure 4.14: The leading order terms in the vorticity balance along the ITF's western pathway for the control run (top panels), linear run (middle panels) and larger friction run (bottom panels). The values for each term are the total integration for the whole sub-domain to show a quantitative comparison between the terms. The terms are advection (Adv), planetary vorticity (βV), friction (HFric). Change in vorticity along latitudes as a cumulative sum of the longitudinal integrals are presented in the lines graphic (right panels).

important roles on balancing the positive change in vorticity from the planetary vorticity term. Depending on the friction along the pathway the balance switches between ADV and FRI.

One difference between zonal and meridional flows is the gradient of planetary vorticity (βV). For meridional flows, as there is latitudinal variation, βV changes. Some other term in the vorticity equation needs to counterbalance it. In the linear cases there is no advection of vorticity. Therefore, the only way the current has to balance the increasing planetary vorticity (as it flows south in Makassar Strait for example) is by friction with the boundary (Figure 4.14). For zonal flows, planetary vorticity is constant. If there is no advection of vorticity, friction is not important as it is not needed to balance the constant βV. That is why the flow is not as attached to the boundary and flows like a straight jet. In the non-linear cases, ADV and FRI can alternate to balance βV (Figure 4.14). In the meridional flow we see the advection of vorticity acting by the meandering current and friction only where straits are narrow and interaction with topography is unavoidable.

The vorticity budget in the control run shows the importance of ADV and FRI on the ITF dynamics. We now investigate the changes the perturbations produce in the vorticity budget. This analysis helps to understand the difference in current width as well as how it affects the partitioning between the exit passages.

In the non-linear experiment with slip walls (not shown) the vorticity balance is similar to the balance in the control (Figure 4.14) yet with smaller friction. Therefore the vorticity balance is mainly between ADV and βV with a small contribution from the FRI term. In general, the changes on boundary condition produce variation in the balance, swapping to ADV as the FRI becomes more and less important for the vorticity compensation. Planetary vorticity is always present, so we evaluate how the balance changes between ADV and FRI terms considering that we have different conditions in terms of interaction between flow and side walls.

In the linear experiment with non-slip condition at the walls, as non-linearities are absent the ADV term is zero (Figure 4.14). The only term left to balance βV is the FRI term, and hence the flow moves closer to the wall where friction can balance vorticity. The linear and slip run has a similar balance (figure not shown) to the linear with non-slip walls. FRI is still the only way to balance the planetary vorticity. The larger friction experiment shows a stronger relation between advection and friction terms balancing each other. As expected, FRI is largest in the Labani Channel.

The boundary current width is related to the amount of water that crosses Lombok Strait. It is determined by slip/non-slip boundary conditions and non-linearity like in the theoretical Stommel and Munk models ultimately by the scaling relations (described below). Therefore, the vorticity budget by the analysis of the terms in the vorticity equation can be a helpful tool to understand how the current width is set. From the vorticity budget we find out which term is important for the dynamics. It provides a quantitative estimation of what balances the vorticity.

We measure the current width at 4.5°S, just upstream of this location is the narrower part of Makassar strait. At that point, considering the vorticity terms, friction and advection of vorticity are the important terms in determining the current width. When we have no non-linearities, which is the most important current setup factor in the ITF case, the current width becomes very narrow as the flow cannot move away from the coast because it needs friction to balance planetary vorticity.

In general, friction makes the current width larger but anchors the flow to the coast while the absence of advection makes the current width thinner. In the ITF case, non-linearity is crucial on determining the current width.

As previously mentioned in WBC theories for the Sverdrup balance to be achieved in the interior we need the terms related to planetary vorticity and vortex stretching (both in bold)

in the homogeneous model governing equation 4.2 to be balanced.

$$\frac{\partial}{\partial t}\nabla^2\psi + J(\psi,\nabla^2\psi) + \boldsymbol{\beta\frac{\partial\psi}{\partial x}} = \boldsymbol{\frac{f_0}{D}w_E} - r\nabla^2\psi + A_H\nabla^4\psi \tag{4.2}$$

The second term on the left side of equation 4.2 is the Jacobian of the stream function with the relative vorticity ($\xi = \nabla^2\psi$) and represents the advection of relative vorticity by the motion field. The second term on the right side of equation 4.2 represents the effect of the vorticity change due to vortex stretching produced by the vertical velocity pumped out of the bottom boundary layer, referred as the bottom friction term. The r coefficient is an inverse time scale for vorticity decay due to bottom friction, D is the layer thickness and w_E is the Ekman velocity pumped out of (or into) the upper mixed layer. Scaling the balance of those two terms (in bold) we obtain:

$$\frac{\partial}{\partial t}\nabla^2\psi + \varepsilon J(\psi,\nabla^2\psi) + \frac{\partial\psi}{\partial x} = w_E - \mu\nabla^2\psi + E\nabla^4\psi \tag{4.3}$$

and the resulting scaling for each theory are:

1. inertial theory: $\varepsilon = \frac{U}{\beta L^2} = \left(\frac{\delta_I}{L}\right)^2$ which measures the importance of non-linearity. It is written as a ratio of length scale δ_I for the boundary layer (Charney, 1955; Carrier and Robinson, 1962);

2. Stommel's boundary layer thickness: $\mu = \frac{r}{\beta L} = \left(\frac{\delta_S}{L}\right)$ which measures the importance of bottom friction. It contains the scale δ_S (Stommel, 1948);

3. Munk's theory: $E = \frac{A_H}{\beta L^3} = \left(\frac{\delta_M}{L}\right)^3$ which measures the importance of lateral diffusion and has the scale for the boundary layer of thickness δ_M (Munk, 1950).

These three non-dimensional terms represent the boundary current width. The last scaling relation was introduced in section 4.2 when we analysed the relation between the changing friction coefficient and the width of the boundary current. This is valid for a frictional regime where the vorticity balance is made by the friction term. This is the dominating balance in our linear experiments (Figures 4.14). However, when the balance changes and is controlled by non-linearity, we need to consider another scaling. In this case, the width of the current is directly proportional to the velocity. This is valid for our non-linear experiments when the advection term is the controlling term in vorticity balance (Figure 4.14). We do not evaluate the bottom friction scaling relation in this study as the ITF is a surface current and we can neglect the bottom interaction. Both scaling, 1 and 3, depend on the physics and conditions of the boundary layer which are reflected in the vorticity balance. So we can have an inertial boundary layer as in the non-linear cases or we can have a viscous boundary layer as in the linear cases.

As a conclusion we observed that non-linearity is what affects current width the most. So now we use the inertial scaling relation

$$\delta_L = \sqrt[2]{\frac{U}{\beta}}$$

that shows the dependency in velocity (scale U) on determining the current width (δ_L). Our perturbation experiments are not enough to demonstrate this relation once our non-linear experiments have different regime setups (slip and non-slip boundary conditions) that therefore cannot be compared. For that to be tested, we need to compare experiments with different velocities but in the same non-linear setup with the same regime, either slip or non-slip boundary condition.

4.7 Summary and Conclusion

The ITF partitioning as the ratio of transport in Lombok and Makassar Straits is controlled by the ITF current width, as we hypothesise and demonstrate with the reduced gravity 1.5 layer model. Depending on how wide the current is, which is limited by the width of Lombok Strait, some portion of the current may not fit and therefore do not flow through Lombok Strait. If the current is wide, not all of its water crosses Lombok Strait and the remaining water flows eastward, searching for the next gap to the Indian Ocean. As a simple way of changing current width we use different viscosity coefficients in the reduced gravity 1.5 layer model and observe different portions of the total boundary current transport flowing through a gap.

Our perturbation experiments show similar behaviour to the reduced gravity 1.5 layer model. We find that the main partitioning controller is non-linearity as it is the main factor influencing the boundary current width, upstream of Lombok Strait. By the vorticity budget analysis, along with the perturbation experiments results, we conclude that a linear current can make the partitioning increase, and thus more transport flows in Lombok Strait. This is because a linear current has narrower current width.

We did not prove current width relation with transport itself, for instance if a wider current width necessarily transports more water. From our results, we see this relation is not true, given that we have considerable changes in current width but the Makassar transport does not change significantly. We also observe that not only the structure of the jets changes, but velocities are also affected. That way, the flow accelerates and can transport more water, not necessarily affecting current width. A linear current has a narrower width. Increased velocity makes the same amount of water to flow in a narrower jet. More volume of water needs larger velocities to keep the same current width. So, if the ITF volume changes between seasons, the monsoons for example, it can affect the current width, and consequently change

the partitioning. Linearity can also be affected by increasing velocity for example, while friction can be dominant in slower flow conditions, and these may be observed when the ITF has variability.

To investigate further how the transport and current width relate, an ITF with variability should then be considered. We raise the hypothesis that the partitioning in Lombok Strait might be a much smaller proportion of the real initial WBC Mindanao and NGCUC in the west Pacific. This is a topic that needs to be investigated, considering a proper transport from the outside of our boundaries in the west Pacific. For example, Wang and Yuan (2012, 2014) found different penetrating/choking rates for different gap widths at the ITF entrance in numerical experiments. Yuan et al. (2018) reported the importance of non-linear dynamics of the quasi-geostrophic vorticity equation on controlling the WBC at the ITF entrance, which is in alignment with our findings on how linearity affects the current width significantly. The control of Lombok Strait transport by current width suggests similar dynamics may be at play at other upstream locations along the ITF pathway.

One expectation on exploring partitioning is if the ratio between Lombok and Makassar Straits transports could be used to plan observational programs, or even reduce sampling efforts. As a proxy, the partitioning could, for example, be used to predict the transport in Lombok Strait based on measurements at Makassar Strait. However, this is inconclusive, given the complexity of the pathways and how the flow splits between the outflows. Also, our idealised experiments do not indicate how the partitioning behaves in more realistic conditions, with all the variables of the system.

In the next Chapter we will explore the variability modes that affect partitioning and test the relationship we found in this Chapter, where the narrower the current is the larger the transport is in Lombok Strait. We already know that the seasonal regime of southeast and northwest monsoon has great impact on the ITF transport (Sprintall et al., 2009). Inter-annual variability is also important in the Indonesian Seas due to the influence of

climate modes of variability like El Niño/La Niña and IOD (Wijffels and Meyers, 2004; Liu et al., 2015) as it is strongly connected to the Pacific and Indian Oceans. Our next question is if and how the partitioning responds to variability. In the case that it does respond, we will then check if the current width changes with variability. This will allow us to verify our results that a wider ITF means a lower partitioning for Lombok Strait.

Chapter 5

The Indonesian Throughflow upstream control and relation with inter-annual variability

In this Chapter we discuss the effect of ITF inter-annual variability on partitioning. Our main goal is to verify if the relation we found in Chapter 4, between boundary current width at Makassar Strait and partitioning at Lombok Strait, is appropriate when variability is considered. We briefly introduce the main modes of variability in the ITF region and then focus on the inter-annual timescale, which best represents an equilibrated system. Last, we show how the same process regulating the partitioning between Makassar and Lombok Straits applies to the inflow of Mindanao Current waters into Makassar Strait and the implications for the ITF eastern pathway.

5.1 ITF inter-annual variability

It is well documented that the ITF circulation varies on different time scales (Wijffels and Meyers, 2004; Sprintall et al., 2009; Schiller et al., 2010; Sprintall and Revelard, 2014). The main modes of variability acting on the ITF are: (1) the monsoons, which characterises the seasonal variability; (2) the El Niño/La Niña - Southern Oscillation (ENSO) and (3) the Indian Ocean Dipole (IOD) both introducing variability in the ITF at inter-annual timescale; and (4) the Madden-Julian Oscillation (MJO), which actively influences the strength of the ITF at intra-seasonal timescales (Schiller et al., 2010).

Monthly average outputs of 18 years (1997 to 2014) from the global model OFAM3 (presented in Chapter 2) show that the dominant mode of variability in Makassar and Lombok Straits transports is at the seasonal timescale (Figure 5.1). The seasonal mode is expected to be the strongest signal, since the monsoons are responsible for most of the ITF variance and it also produces variability in the partitioning (Figure 5.2.d). However, this short timescale is not long enough to allow the system to reach equilibrium (simulations of our regional model take one year to reach equilibrium, Chapter 2), thus the dynamics that control the steady circulation, and hence underpin our theory about partitioning (Chapter 4), are unlikely to hold seasonally.

England and Huang (2005) showed a 4-7yr period as a dominant inter-annual variation on the ITF anomaly, when removing the seasonal cycle from a 50-yr experiment of the Simple Ocean Data Assimilation (SODA). They also relate this inter-annual variability with ENSO pattern and suggest an ITF response lag of 8-9 months. That explains why the inter-annual signal is not as evident in the 18 years of OFAM3 monthly outputs (Figure 5.1), as we only represent approximately two repetitions of this cycle in this dataset.

When considering annual averages, we observe a different relation between partitioning

in Lombok and Makassar Straits than inferred from monthly means (grey dots compared to black dots in Figure 5.3.a), suggesting that timescales affect partitioning differently. So, we will focus on this lower frequency variability, for which our theory on the control of partitioning derived for the steady state circulation may hold.

We know there is variation in the partitioning of the total ITF transport through each of the main exit passages related to the phase of the IOD or ENSO (Sprintall and Revelard, 2014), characterising the partitioning inter-annual variability. It is important to note that the partitioning considered in Sprintall and Revelard (2014) relates the total outflow with the three exit passages. In this work, we discuss partitioning as the ratio between transports in Lombok and Makassar Straits, so our results may differ from theirs.

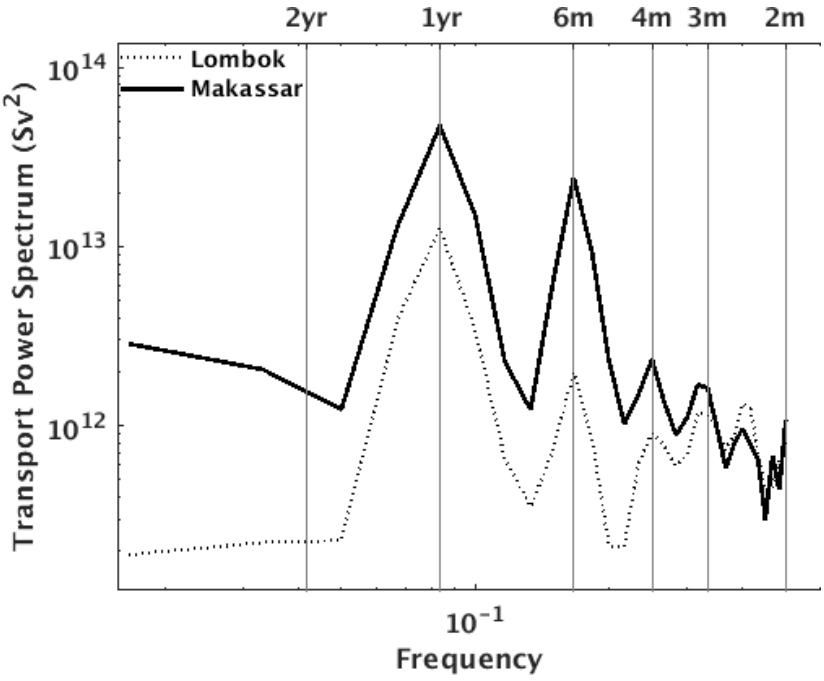

Figure 5.1: Spectra analysis of 18 years of monthly averaged transports in Lombok and Makassar Straits.

On inter-annual and longer timescales the main source of variability in the tropical Pacific are the trade winds. Variations in the wind lead to changes in sea level in the western Pacific, such that a weaker sea level gradient between the Pacific and Indian Ocean develops during El Niño years. This decreases the pressure gradient between both oceans and therefore

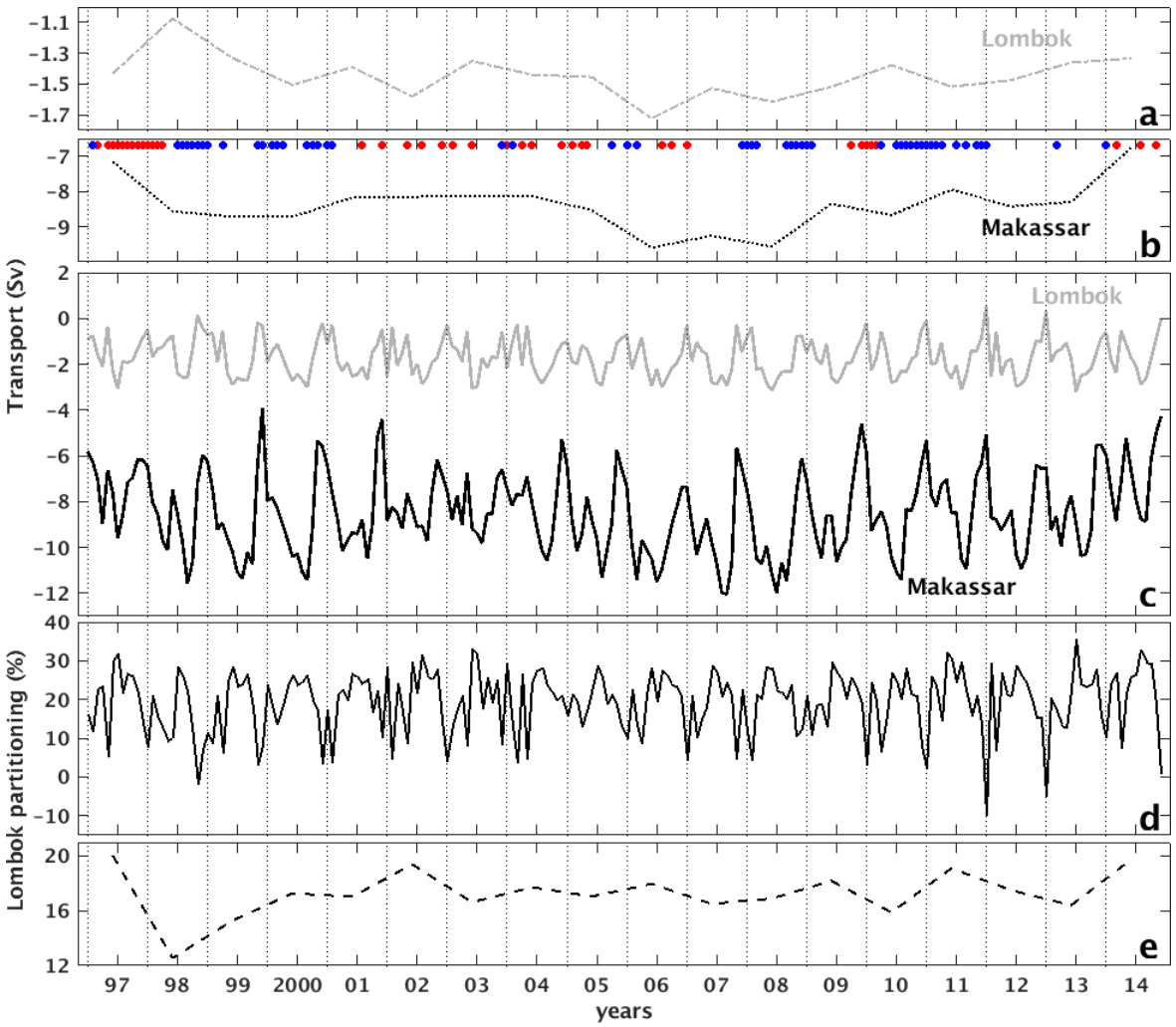

Figure 5.2: OFAM3 annual and monthly averages of 18 years of transport and partitioning for Makassar and Lombok Straits. Inter-annual timeseries for transport in (a) Lombok and (b) Makassar Straits and (c) the respective monthly averages. Partitioning (the ratio Lombok/Makassar transport) timeseries of (d) monthly outputs and (e) annual averages. El Niño (La Niña) months, with SOI lower than -1.5 (higher than 1.5) are highlighted in red (blue).

the ITF weakens. On the contrary, during La Niña, the sea level is higher in the Pacific Ocean, which increases the pressure gradient between the two ocean basins and results in a stronger ITF (Lee et al., 2015). Observations also show that the transport in the Makassar Strait is reduced and the thermocline becomes shallower during El Niño events (Gordon and Fine, 1996). But it is not only the flow in Makassar Strait that responds to the ENSO cycle. Models suggest that during strong La Niña events, the ITF transport is larger and more Southern Hemisphere origin water flows through the Makassar, Maluku, Ombai Straits

and Timor Passage (van Sebille et al., 2014). However, the ENSO-ITF interaction is much more complex than these simple relationships suggest. The outflow straits show remarkable similarities as a response to inter-annual variability (Sprintall et al., 2009), possibly implying changes in partitioning. Although, what the nature of these changes in partitioning is and what the implications for the ITF as a whole are, remain open questions.

In Chapter 4 we proposed and tested the relation that showed the partitioning (as the ratio of Lombok and Makassar transport) is controlled by current width in a steady state of the ITF. We now explore how this relation is affected by the inter-annual variability. To investigate longer term inter-annual variability the observational records are generally not long enough. This is an advantage of using model outputs, which allow a detailed study of the partitioning inter-annual variability. Here we use the OFAM3 18-year velocity and temperature outputs, using the annual means for the velocity field, to calculate transports in the straits, derived from the monthly average outputs.

5.2 Effect of inter-annual variability on the ITF partitioning

We first explore how the inter-annual variability affects partitioning. The annual averages from OFAM3 show partitioning changes by about 5% over the entire 18-year period and has a mean value of 20% (Figure 5.3.a). For a change of 35% in Makassar transport we only see a change in partitioning of 5%, showing there is little influence of the inter-annual variability on the partitioning between Lombok and Makassar Straits. In our theory partitioning is controlled by current width, so we expect that little change in partitioning result from small changes in current width.

To verify the relation: a wider current width results in lower partitioning, or in this

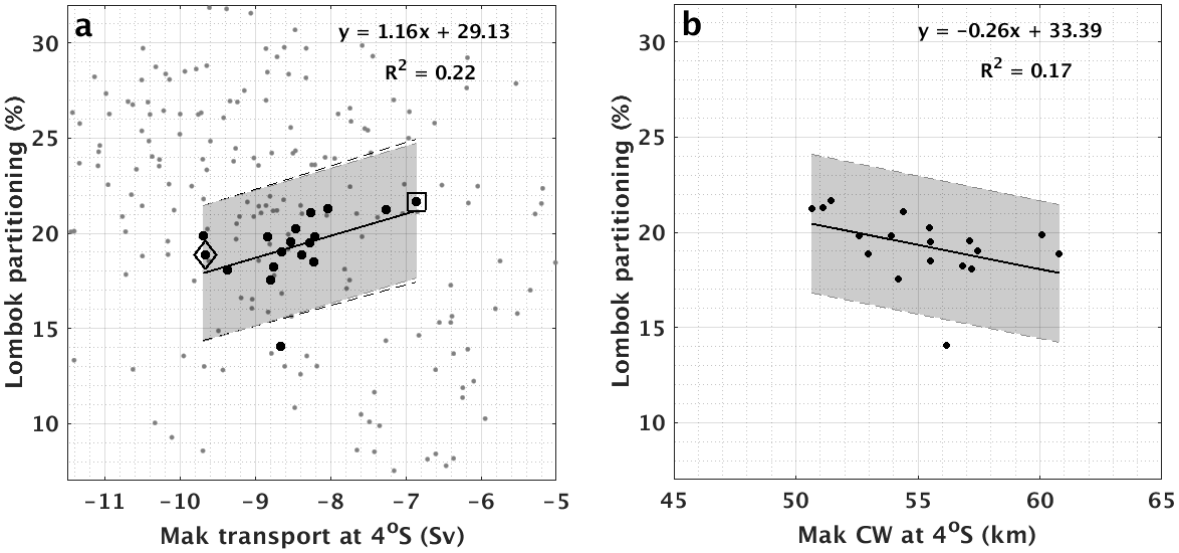

Figure 5.3: (a) Makassar Strait (Mak) transport at 4°S and partitioning in Lombok Strait for the 18-year of OFAM outputs. Black larger dots show annual averages and monthly averages are shown in grey smaller dots). Years of higher (2008) and lower (2014) transports in Makassar Strait are highlighted with a diamond and a square, respectively, representing extreme conditions. (b) Annual averages of Makassar current width at 4°S and partitioning in Lombok Strait. The equation for the best fit line and the R^2 are shown, and the 95% prediction interval is shaded.

case little changes in partitioning mean little changes in current width, we need to consider the current width for the Makassar boundary current in the OFAM3. Because OFAM3 has lower resolution (10-km) compared to our higher resolution model (4-km) from Chapter 4, we cannot use our previous method for estimating current width. Previously, we used the zonal integral of the transport along the current cross section and define current width as the distance where 55% of the transport occurs. At 10-km this method is not very accurate so instead we estimate current width in the 10-km model using transport streamlines (Figure 5.8) to define the boundary current limits. We measure the distance between the minimum and maximum streamfunction in Makassar Strait.

The current is measured in two different locations, upstream (at 1°S) and downstream of Labani Channel (at 4°S, approximately the same location we used in Chapter 4, transect at 4.5°S in Figure 4.11). For both locations, current width shows smaller variation (around 20% of change) relative to transport (around 35%) with a range of 20 km at the upstream location and 10 km at the downstream location (Figure 5.3.b). Thus, given that partitioning

and current width do not have considerable change, we verify the relation we obtained in Chapter 4 at inter-annual timescale. This suggests that current width controls partitioning as Lombok/Makassar is constant at inter-annual timescale even given the much larger changes in transport at Makassar Strait.

Although the Lombok/Makassar Strait partitioning and current width are approximately constant (Figure 5.3.b), transport in Makassar Strait has significant inter-annual variability (Figure 5.3.a). This suggests changes in transport are not related to changes in current width. To explore this further we focus on years 2008 and 2014; they have the highest (-9.7 Sv, diamond in Figure 5.3.a) and the lowest (-6.9 Sv, square in Figure 5.3.a) transport in Makassar Strait, respectively. Comparing the along-strait velocity for those years, we see the jet has a very similar width despite an almost 3 Sv difference in transport (a 33% change relative to the mean transport; Figure 5.4). This transport increase results from an increase in velocity between these extreme years, and yet the current width is relatively constant (Figure 5.5).

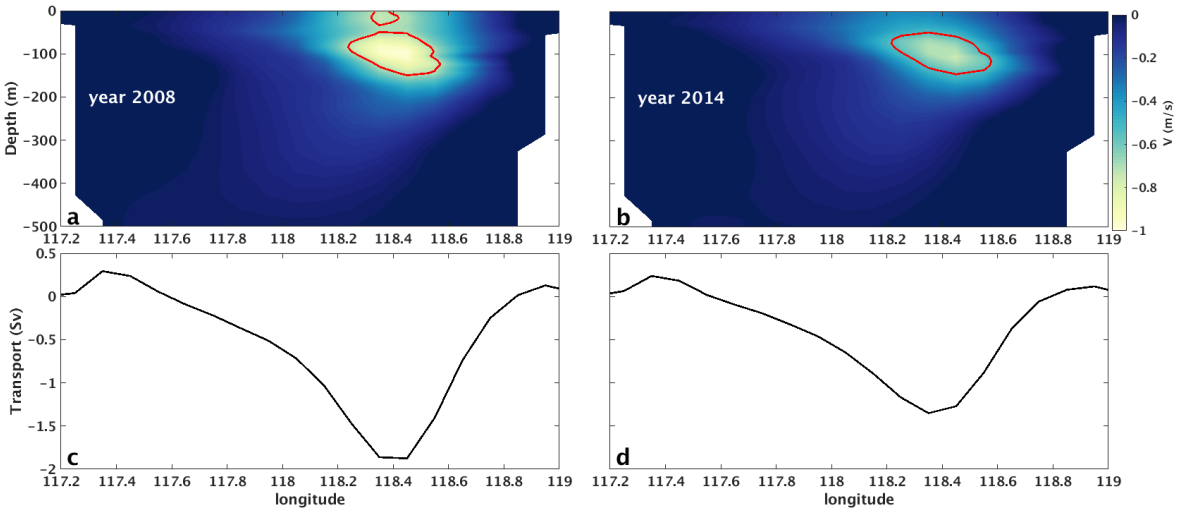

Figure 5.4: Illustration of the jet structure in Makassar at 4°S. (a) 2008 has higher transport and (b) 2014 has lower transport, although the jets have similar current width. The bottom plots (c) and (d) show the vertical integrated transport for the same years.

The approximately constant partitioning in Lombok Strait (Figure 5.3.a) raises the hypothesis that the Makassar Strait flow might be saturated in terms of current width as

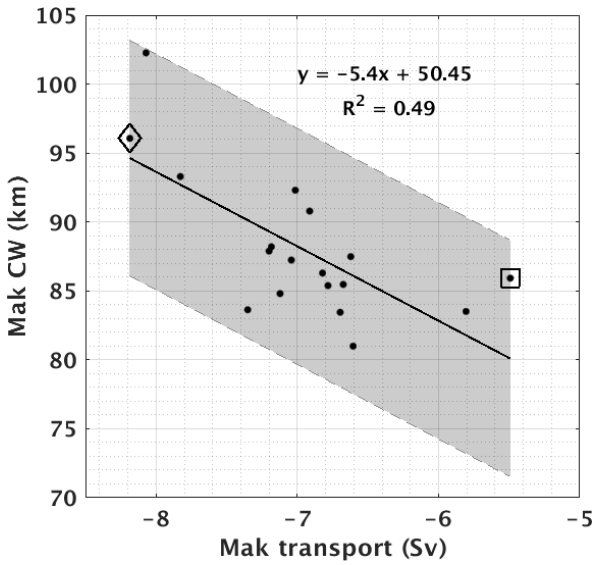

Figure 5.5: Transport and current width (CW) in Makassar Strait (Mak), at the upstream location at latitude 1°S. Note that the location changed from the previous at 4°S and transports are slightly different. The years of high (diamond) and low (square) transports in Makassar Strait are highlighted. The equation for the best fit line and the R^2 are shown, and the 95% prediction interval is shaded.

the strait constrains the current. To understand why Makassar Strait is saturated in current width next we look at the source flow of Makassar, the Mindanao Current.

5.3 Current width saturation in Makassar Strait

The transport in Makassar Strait measured upstream of Labani Channel ranges from -8 to -5.5 Sv in the 18-year OFAM3 run and we do not see considerable changes in current width (Figure 5.5), measured by the streamline method. The current width of the Mindanao boundary current, on the other hand, exhibits significant inter-annual variability with a range of approximately 60 km, comparable to the mean current width at Mindanao and three times the variation in Makassar Strait current width (Figure 5.6.a). We also see that the highest and lowest transport years in Makassar Strait (diamond and square in Figure 5.6.b) correspond to a wider and narrower current width in both Mindanao Current, although not the largest/smallest current width. Mindanao Current transport shows large changes in

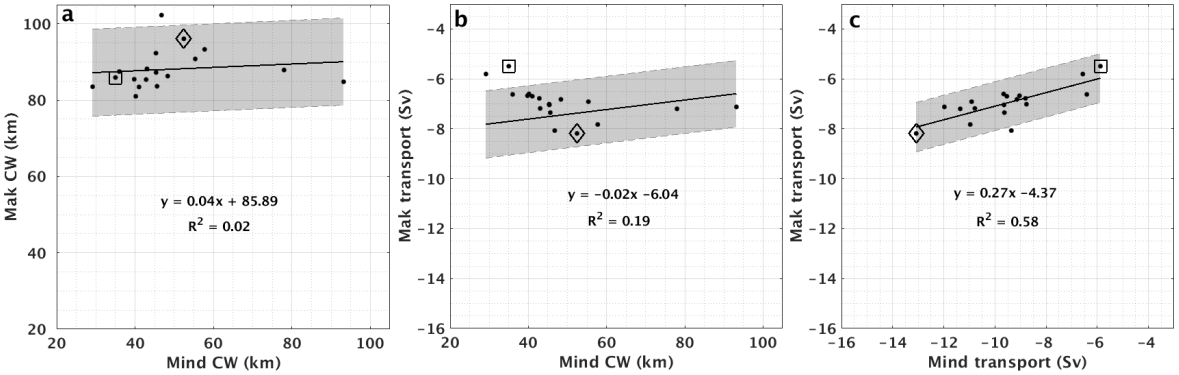

Figure 5.6: Annual averages of (a) Mindanao (Mind) current width (CW) compared to Makassar (Mak) current width; (b) Mindanao current width compared to Makassar transport; (c) Mindanao transport compared to Makassar transport. The years of high (diamond) and low (square) transports in Makassar Strait are highlighted. The equation for the best fit line and the R^2 are shown, and the 95% prediction interval is shaded.

the 18-year averages with a range of 7.2 Sv (Figure 5.6.c). When comparing Mindanao and Makassar transports we observe a direct relation where both transports increase together (Figure 5.6.c). However, we also see the effect of the constrained topography in Makassar Strait, while Mindanao current is free to expand towards the east increasing its width, Makassar Strait is constrained by topography and can change current width much less (Figure 5.6.a).

Most of the Mindanao Current enters Celebes Sea. Because Makassar Strait is constrained by topography a portion of the total Mindanao inflow ITF is not able to fit in the strait. The fraction of the current that does not fit has to flow eastward in the Celebes Sea, in a similar manner to what we see in Lombok Strait where water that does not fit in the strait turns eastward along the Nusa Tenggara. We calculate the partitioning in Makassar Strait, as we did for Lombok Strait in Chapter 4, as the ratio between transports in Lombok and Makassar Strait. The comparison between Mindanao current width (Figure 5.7.a) to the Makassar Strait partitioning shows that a wider current relates to lower partitioning and we confirm what we hypothesised, that partitioning at Makassar Strait follows the same theory than in Lombok Strait. We also see that years of higher and low transports in Makassar Strait do not correspond to a wider and narrower Mindanao current width (diamond and

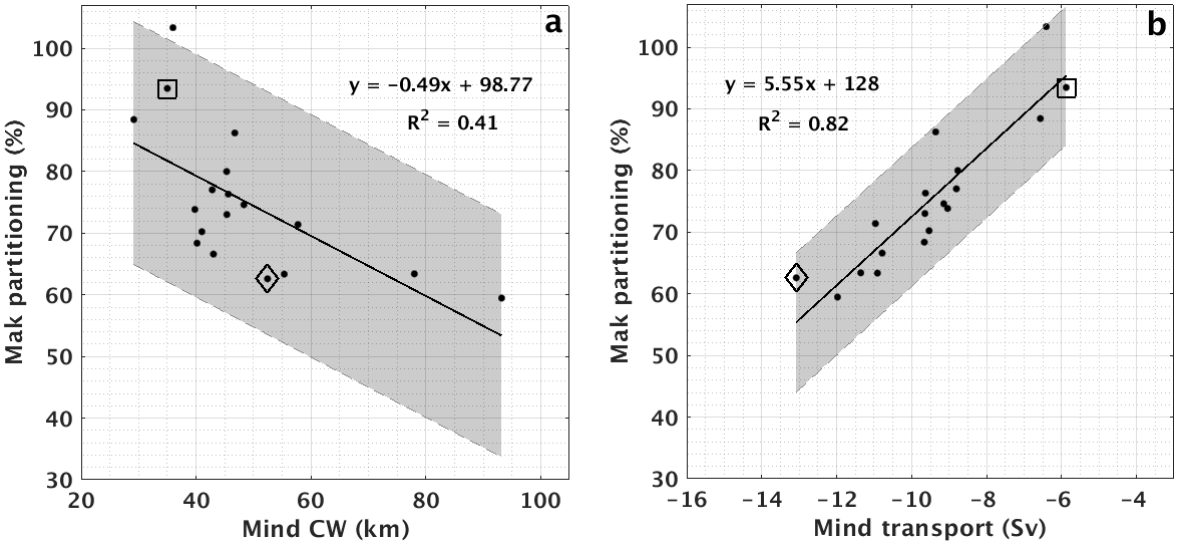

Figure 5.7: Annual averages of Mindanao (Mind) current width compared to partitioning in Makassar Strait (Mak). The years of high (diamond) and low (square) transports in Makassar Strait are highlighted. The equation for the best fit line and the R^2 are shown, and the 95% prediction interval is shaded.

square in Figure 5.6.b, respectively), highlighting uncertainties regarding the relation between transport and current width. Interestingly, the comparison between Mindanao transport to the Makassar Strait partitioning show a good relation but we do not explore that in this study.

So we ask what is the fate of the Mindanao Current waters that do not fit in Makassar? During years when Mindanao current width is wide, a portion of the water that does not fit in Makassar Strait, after exiting the Celebes Sea, flows towards the Pacific Ocean. However, a considerable amount flows through Maluku Strait into the Banda Sea via the ITF eastern pathway (Figure 5.8). This North Pacific water is traditionally assumed to contribute to the western pathway, enhancing the eastern pathway transport instead. We choose four years that represent extreme cases of wider (93 and 58 km) and narrower (29 and 36 km) Mindanao current width. For the years with narrow current width (years 1997 and 2002), there is less flow reaching the Banda Sea (Figure 5.8.a and 5.8.b) while years of wide current width (1998 and 2007), more of the flow continues on to the Banda Sea (Figure 5.8.c and 5.8.d). This variation in transport of North Pacific water to the eastern pathway through Celebes Sea

ranges from approximately 0 to -4 Sv. Note this transport refers only to the inshore portion of the black streamline towards the west coast and not the entire transect in Maluku Strait.

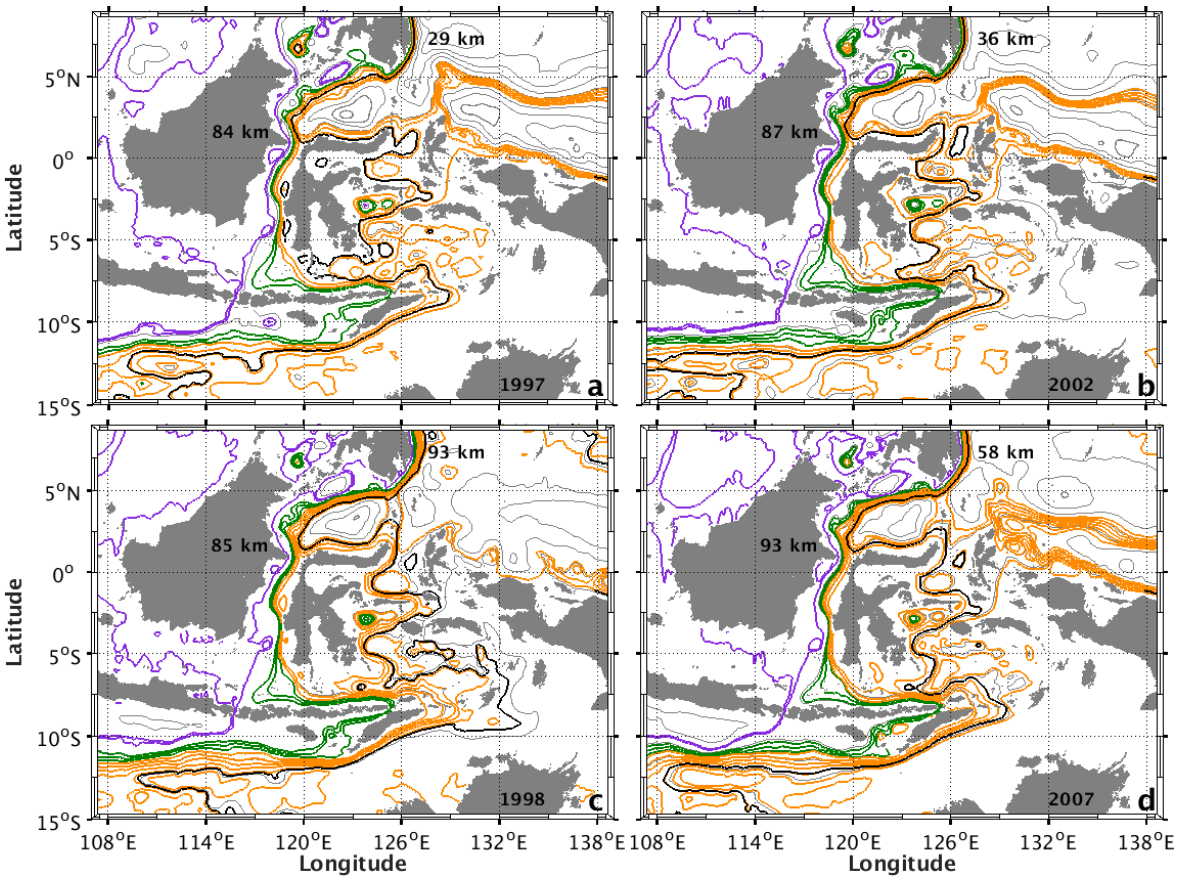

Figure 5.8: Vertically integrated transport streamlines for four chosen years of the 18 years from OFAM3 outputs that illustrate the inter-annual variability in current width. Years (a) 1997 and (b) 2002 have narrower boundary current in Mindanao. Years (c) 1998 and (d) 2007 have wider Mindanao Current. Colors show the streamlines in each outflow strait (purple in Lombok, interval is 0.4 Sv; green in Ombai, interval is 1 Sv; and orange in Timor, interval is 1.5 Sv). The black line highlights the easternmost streamline that flows from Mindanao to Timor Passage through the Banda Sea and illustrates the North Pacific water contribution to the eastern pathway. Grey lines show streamlines at 5 Sv intervals. Current width in Mindanao and Makassar Strait are shown in km (black numbers close to the respective current).

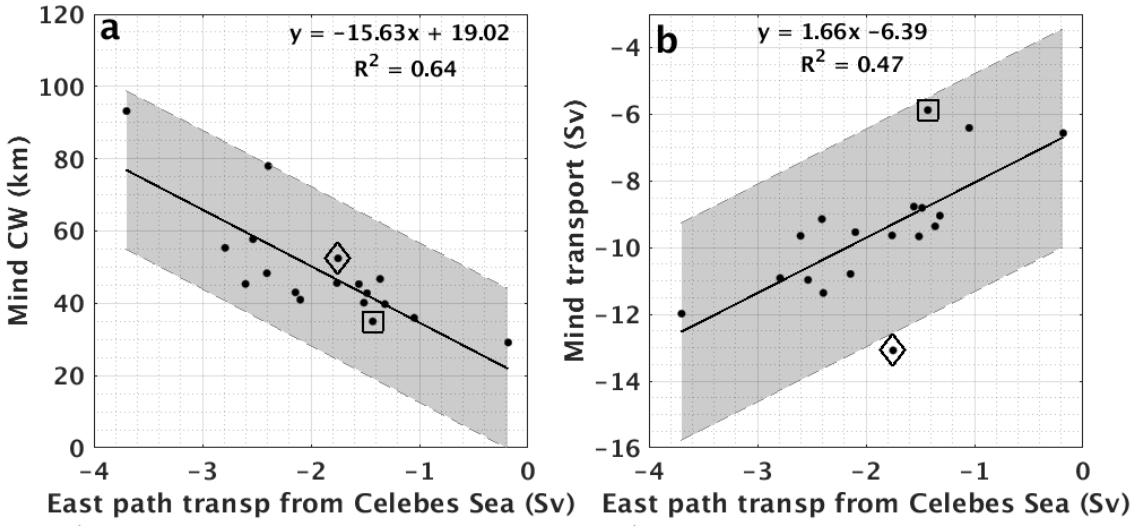

Figure 5.9: Annual averages of eastern pathway transport from Celebes Sea, only the west portion of the transect in Maluku Strait compared to (a) current width (CW) in Mindanao (Mind) and to (b) transport in Mindanao. The years of high (diamond) and low (square) transports in Makassar Strait are highlighted. Negative transport represents southward flow. The equation for the best fit line and the R^2 are shown, and the 95% prediction interval is shaded.

5.4 Inter-annual variability in the eastern pathway and relation to changes in Timor Passage

We find that the ITF inter-annual variability at the inflow Mindanao current width produces changes in Makassar Strait transport (Figure 5.6.b) and partitioning (Figure 5.7) but these are not linked to current width in Makassar (Figure 5.6.a). Mindanao Current inter-annual variability influences the inflow to the eastern pathway (Figure 5.8) as an effect of current width saturation in Makassar Strait. Increased transports in the eastern pathway result from a wider Mindanao current width (Figure 5.9.a; R^2 =0.64). The inflow in the eastern pathway eventually reaches Timor Passage, as shown by the streamlines that cross the entire Banda Sea basin and exit through Timor Passage (black line in Figure 5.8).

To understand at what depth is the Celebes Sea water from the North Pacific contributing to the Banda Sea circulation we examine the vertical profile of transports located inshore of the west of the black streamline in Figure 5.8. Higher transport variance is found in the

layer between 500 and 1000 m, and shows an intermediate flow that is likely coming from Celebes Sea. This shows that North Pacific water enters the Banda Sea above 1000 m, more specifically between 400 and 1100 m, joining the eastern pathway. Unlike the steady ITF described in Chapter 3, that shows only a deep inflow (below 600 m) to the eastern pathway, when inter-annual variability is considered the eastern pathway has significant intermediate (400 - 1100 m) contributions as well. This contribution varies (Figure 5.10) depending on the Mindanao current width, which controls how much of the water fits through Makassar Strait and how much leaks to the eastern pathway. This intermediate layer contribution of North Pacific water to the eastern pathway has not been previously documented. Recent observations in Maluku Strait (Yuan et al., 2018) show an upper southward flow that develops as a function of the Mindanao Current location and the shift of the bifurcation at the Pacific Equatorial currents system.

We now consider how the changes in the eastern pathway relate to the changes in the upstream ITF inflow in Mindanao Current, and consequently translate into changes in Timor Passage, the end of the pathway (Figure 5.11.a). We find that when the transport in the eastern pathway increases the transport in Timor Passage also increases (Figure 5.11.b), and that larger transports in Timor Passage are associated with a wider current width in Mindanao Current (Figure 5.11.a). The intermediate layer contribution from the North Pacific water show higher variability than other layers, and suggests that these waters are from the remaining water that did not fit in Makassar Strait, bringing warmer and fresher North Pacific water to the interior of the Banda Sea.

5.5 Discussion

We find that the partitioning of the ITF between the straits is strongly controlled by the current width of the source boundary currents. In Chapter 4 we show this partitioning control

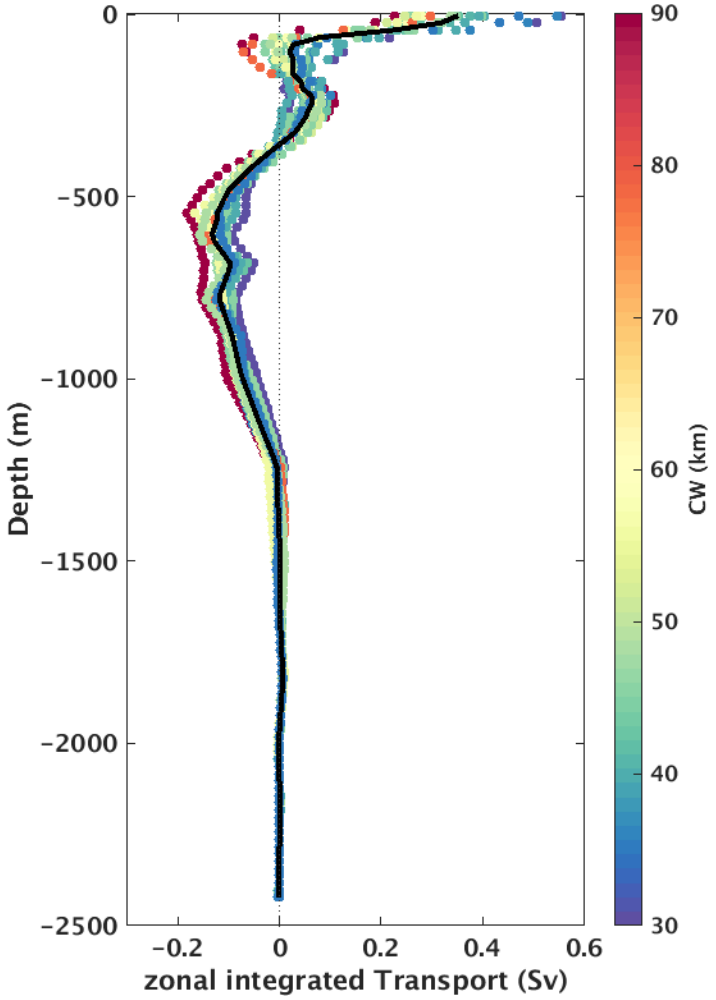

Figure 5.10: Profile of zonal integrated transport of the inflow to Banda Sea time averaged, the jet that joins the ITF eastern pathway. The integration is from the west coast to the black streamline in Figure 5.8 and considers just the inshore part of the inflow. The colorbar shows current width (CW).

for the steady ITF in Lombok Strait, and in this Chapter we also show the same control holds for the ITF subject to inter-annual variability. In this case, we detect partitioning in Lombok Strait is also controlled by current width. But the current width in Makassar Strait is steady, so partitioning in Lombok Strait is steady too. The control happens upstream of Makassar Strait, in the western pathway, by the current width upstream of it, in Mindanao Current.

When considering inter-annual variability, we find that partitioning as the ratio in Lombok Strait from Makassar Strait can be a helpful quantity for ITF study. If this is fixed and does not change considerably inter-annually, then there is no need to measure all the straits

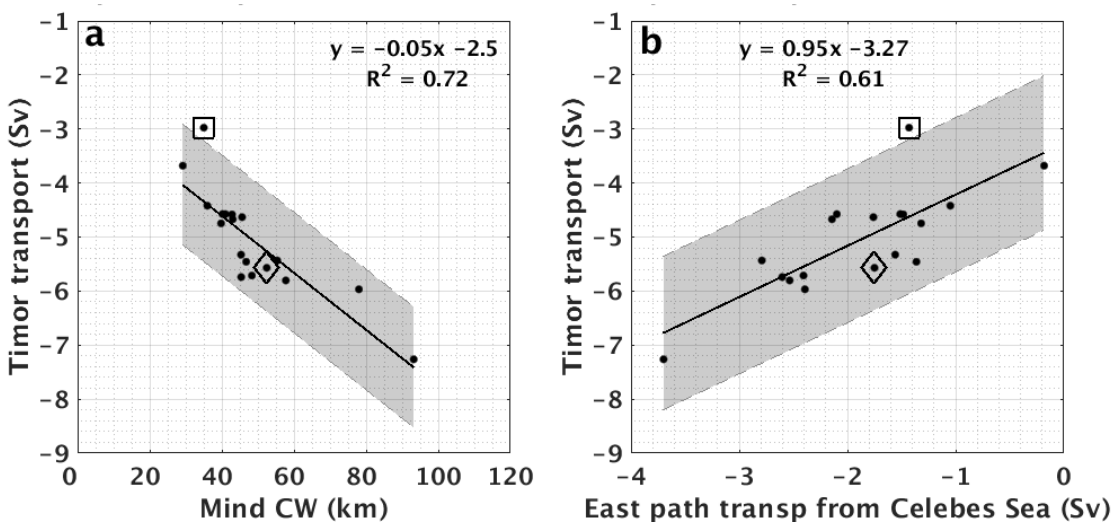

Figure 5.11: Annual averages for comparison between (a) current width (CW) in Mindanao (Mind) and Timor transport and (b) eastern pathway transport from Celebes Sea, only the west portion of the transect in Maluku Strait and Timor transport. The years of high (diamond) and low (square) transports in Makassar Strait are highlighted. Negative transport represents southward flow. The equation for the best fit line and the R^2 are shown, and the 95% prediction interval is shaded.

to estimate the total ITF. This is useful for sampling planning, especially because it is challenging to obtain long term records and have all the straits sampled, as it can be costly. Lombok Strait could be excluded from having its transport measured, meaning less cost and observational effort.

The Mindanao current provides the source water for the ITF at the entrance of the Indonesian Seas and carries North Pacific water. Traditionally, the North Pacific waters have always been thought to flow only via the western pathway. Our findings suggest that there is a contribution of North Pacific water to the eastern pathway. The volume of this North Pacific water contribution to the eastern pathway is subject to inter-annual variability and can have implications for the heat transport to the Indian Ocean at the outflow passages. The warmer and fresher North Pacific waters exposed to the strong mixing and water mass modification in the Banda Sea (Koch-Larrouy et al., 2015), will have different properties than North Pacific water flowing through the western pathway. This is because transport through Makassar Strait provides a more direct route to the Indian Ocean with less modification and no interaction with waters of South Pacific origin.

Our analysis shows there is a relation between transport in Timor Passage and Mindanao current width, such that transport in Timor increases in years that Mindanao current width is wide, as a consequence of increased inflow to the eastern pathway. Outflow straits are known to have relatively warm temperature compared to upstream waters, the transport weighted temperature (TWT) estimated from INSTANT is 21.5°C in Lombok Strait, 15.2°C in Ombai Strait and 17.8°C in Timor Passage (Sprintall et al., 2009). This is explained by the heat contribution from surface fluxes, discussed in Wijffels et al. (2008) and Gordon et al. (2010b) that show waters warm up when crossing the Banda sea. Tidal mixing also contributes to cool down intermediate and deep waters in Banda Sea (Koch-Larrouy et al., 2009). An extra input of warmer waters, coming from the North Pacific through Mindanao and Celebes Sea, could impact on the heat content at the outflows. This is true not only for Timor Passage or Ombai Strait that take water from Banda Sea, but also for Lombok Strait due to change in the contribution from Makassar Strait. The heat budget itself is not our goal in this study, indeed our regional model at previous Chapters does not have a robust mixing setup, and due to time constrains, further detailed study on this topic are not considered here.

The eastern pathway is generally expected to be composed of mostly colder and saltier South Pacific water. It is also a deep waters pathway, as we showed in Chapter 3 and as described in Gordon et al. (2010b), with little shallow or intermediate water contribution. We find here that the inflow to the eastern pathway, as remaining from what did not fit in the western pathway, is composed of an upper and intermediate flow, in addition to the deep flow (Figure 5.10). As noted in Yuan et al. (2018) variability affects the upper flow in Maluku and they suggest this is related to the shifting of the Mindanao WBC. This is in alignment with our results here, where the Mindanao current width affects how much water flows towards the eastern pathway through the Maluku Strait and as a flow above 1000 m.

The modifications the waters to the Banda Sea (the eastern pathway) and along Makassar Strait (the western pathway) are different. Banda Sea waters have a longer residence time and allow waters to go through strong mixing processes. Makassar Strait is a more direct route,

and promotes transfer of waters with little modification, which means physical properties are maintained. This is all reflected in the outflows, where we see different property characteristics in each of the three outflow straits. Thus, we suggest the current width in Mindanao may have implications on defining which pathway the ITF takes, or the portions in each inflow pathway, and ultimately define the heat content exchanged with the Indian Ocean. This is an important finding, that the contribution to the Indian Ocean is highly dependant on which route the ITF follows, and which outflow it exits. This could be reflected in the inter-annual transport weighted temperature (TWT) at Timor Passage and therefore the total heat contribution to the Indian Ocean, but how exactly this happens cannot be clarified with our results.

Related to inter-annual variability modes, El Niño means a weaker ITF. Tillinger and Gordon (2010) mention the ENSO signal is transferred from the Pacific to Indian Ocean not by changes in temperature, but primarily by changes in transport, due to the variation in the sea level gradient and consequently in the pressure gradient between the two ocean basins. Interestingly we see a relationship of years of wider Mindanao Current and El Niño events (Figure 5.12) suggesting extreme events may have influence in Mindanao current width. This suggests that inter-annual variability plays on the current dynamics, alternating between non-linear and frictional patterns.

Comparing the 18-year timeseries of current width in Mindanao, measured by the streamline method, and the El Niño/Southern Oscillation index for the same years (Figure 5.12), we see that periods with larger current width correspond to stronger climate events like El Niño and La Niña. Increases in current width follow a period of large El Niño Index, but occur during La Niña periods. These are the cases in 1997/1998 and 2009/2010 as we see current width increase after a prolonged El Niño period. Then throughout the La Niña event, current width decreases, as seen during 1998/1999 and then again in the La Niña event in 2011.

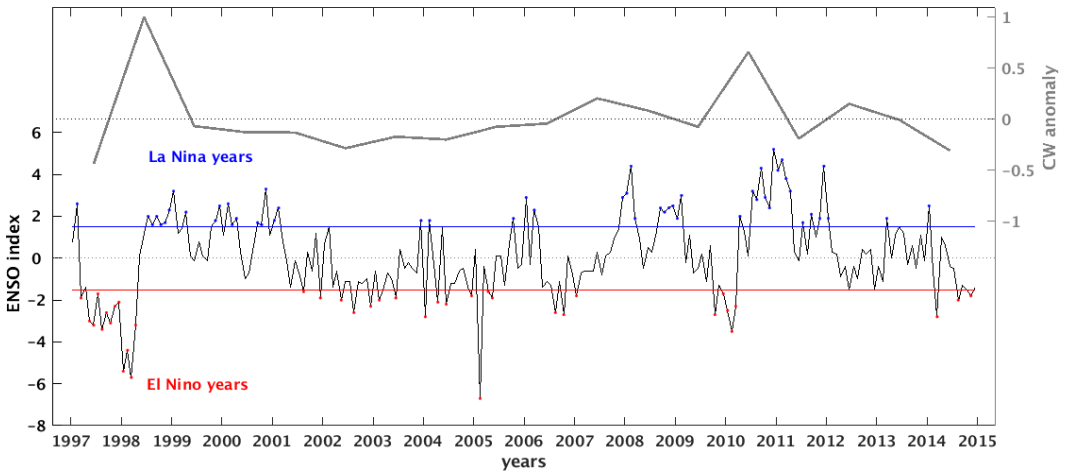

Figure 5.12: Current width anomaly in Mindanao (thick grey line) and relation to El Niño/La Niña events indicated as red/blue dots under/above the limit of ENSO index -1.5/1.5.

Although, the relationship we find between current width and the El Niño index show a clear influence of climate modes in current width, it is important to mention that the method we use to measure current width in the model OFAM3 needs to be carefully considered. The final question remains, what causes changes in western boundary current width. Theories for the steady wind-driven ocean circulation predict the existence of western boundary currents (Section 4.2 in Chapter 4). On inter-annual timescales, the WBC system in the Pacific moves northwards or southwards (Hu et al., 2015; Yuan et al., 2018). This latitudinal shift of the system can have implications for current width. We know during El Niño/La Niña periods the WBC system is shifted northwards and southwards, respectively. We see that El Niño years precede large current width calculated here from OFAM3 outputs annual averages (Figure 5.12), but large current width occurs during the onset of La Niña periods. Therefore, when the bifurcation that originates the Mindanao boundary current is at northernmost position is when current width gets wider, and Mindanao Current is also stronger (Hu et al., 2015). From WBC traditional theories, as discussed in Chapter 4, we know friction and non-linearity are the components of current dynamics and have effects on current width. Other processes such as change in the position of the WBC can also contribute to ITF variability on the same scales, as proposed by Yuan et al. (2018).

5.6 Conclusion

We confirm the relation we found in Chapter 4, that current width in Makassar controls partitioning in Lombok Strait, even when the ITF is subject to inter-annual variability. However, Makassar Strait current width is saturated and this results in partitioning in Lombok Strait not exhibiting inter-annual variability but held approximately constant at 20%. Partitioning in Makassar Strait, however, changes by 40%.

Inter-annual changes in current width at the entry of the ITF are important to the eastern pathway. The saturation in current width at Makassar Strait combined with years when Mindanao current width is wider produces increased flow to Banda Sea, via Maluku Strait. This is because a wider Mindanao Current cannot entirely fit in Makassar Strait. The water that cannot fit in Makassar Strait flows out of Celebes Sea and a portion of it into Banda Sea. This is a contribution of North Pacific water to the eastern pathway that was has not been previously reported and ultimately contributes to Timor Passage but via eastern pathway.

The ITF responds to inter-annual variability and we show these responses are an effect of variations on the inflow ITF from Mindanao Current width, which are linked to eastern pathway activation and Timor Passage outflow transport. Those areas are important when studying variability in the ITF dynamics.

Chapter 6

Conclusion

The main objective of this Thesis was to investigate the mechanism for the partitioning of the ITF. Given that each ITF outflow strait has different water properties in terms of heat and freshwater content, which depend on the route of the source ITF, it is crucial to understand how and why the flow partitions. We wondered what the control at the outflow straits that sets the ITF partitioning is and why the westernmost passage, Lombok Strait, has the lowest transport. We consider the ITF as a boundary current that does not behave as the theories predict. We simplify the complexity of the ITF system using an idealised high-resolution regional model that simulates a steady ITF. Using perturbation experiments, we explore the dynamics governing the ITF and identify and test the mechanism for the ITF partitioning. In this Chapter, we outline the main contributions of our results to the ITF knowledge. We discuss the implications of our findings to the ITF understanding and possibly to the global oceans and climate change. In the last section, we suggest the next steps for this study and potential future work.

6.1 Contributions

The ITF flow is both divided by route (inflow western and eastern pathways) and is a layered system (shallow - 0-300 m, intermediate - 300-600 m, and deep - below 600 m) where all layers behave differently and exchange little mass. Because of this complexity, we reconsider the ITF partitioning concept. This study considers only the western pathway for partitioning, which is the ratio between Lombok and Makassar Straits transport. The partitioning that considers the portion between the three outflows does not take into account the ITF complexity in terms of routes and dynamics.

The partitioning of the steady ITF in the western pathway (upper 300 m), considered as the fraction of water from Makassar Strait that exits at Lombok Strait, is controlled by the current width in Makassar Strait. Non-linearity, or advection of relative vorticity, balances changes in planetary vorticity as the ITF flows southward in Makassar Strait. Therefore, non-linearity is the leading order term in the vorticity balance and is what sets the current width in our high-resolution regional ITF model. A wider current does not fit in a narrow passage, and this is what determines the portion of the water flowing through Lombok Strait. We show that this geometrical relation between the channel and the flow structure is essential for partitioning, like in our reduced gravity 1.5 layer model, where a limited gap splits the upstream flow. The remaining water that does not fit in the gap flows eastward to find other gaps. This extension of the WBC theory to flow through a gap near the western boundary explains the behaviour of the ITF as it exits through Lombok Strait.

When the ITF has inter-annual variability, we observe that the controlling relation between Makassar current width and Lombok partitioning for the upper layer of the ITF is still appropriate. However, transport in Makassar Strait shows inter-annual variability as the flow accelerates/decelerates but keeps the current width. Therefore, the ITF can be understood as a sequence of chocking points where the current width of the upstream flow is what controls

how much water can fit in the chocking points.

We find that at inter-annual time scales the Makassar Strait current width and partitioning in Lombok Strait is nearly constant (approximately 20%). However, upstream of the Makassar Strait, there is considerable inter-annual variability in the Mindanao Current width. These results suggest that Makassar Strait is saturated in terms of current width. The water that cannot fit in Makassar Strait, in the years when Mindanao Current is wide, affects the contribution of North Pacific water to the eastern pathway, ranging from 0 to -4 Sv. This contribution is concentrated in intermediate to upper levels and is identified by the increase in transport of water from Celebes Sea to the Banda Sea via Maluku Strait. An increase in transport is also observed in Timor Passage transport. The choice of the pathway, western or eastern, consequently affecting the choice of the outflow strait and therefore the properties characteristics in each exit flow, is essential for heat contribution to the Indian Ocean. This is because the modification of ITF waters as they transit the Indonesian Seas is different depending on the western or eastern pathway or time that they spend in the Indonesian Seas.

6.2 Implications

Partitioning as the ratio of the western pathway (0 - 300 m) that flows through Lombok Strait can be a useful concept for the ITF dynamics study. This quantity can be used to check if models adequately simulate the ITF. We find that the portion of the Makassar Strait transport that flows through Lombok Strait is approximately constant. Therefore, the Lombok partitioning determines what to expect for the simulated transport in Lombok Strait. In terms of observations, the Makassar saturation in current width suggests there is no need to measure Lombok Strait transport. The partitioning in our control run for the steady ITF in Chapter 4 (26.9%) and the approximately constant partitioning we find in

Chapter 5 (20%) when the ITF has inter-annual variability, suggest that partitioning can be a proxy for the transport in Lombok Strait. That way, Makassar Strait transport can be used to predict Lombok Strait transport, that likely does not need to be measured. However, Ombai Strait and Timor Passage are important to be measured, given that their transports are a combination of waters from both eastern and western pathways.

The heat content to the Indian Ocean is influenced by which route the ITF takes. The longer duration the water is in transit, which is the case for the eastern pathway compared to the more direct western pathway, the more mixing the water is subject to, and more properties modification might happen. We know the outflows carry different heat and freshwater content. Therefore, understanding the dynamics involved in the pathway choice, for example, the saturation in Makassar Strait and the increases in Mindanao current width activating the North Pacific contribution to the eastern pathway, is essential to understand the ITF heat contribution to the Indian Ocean. How this heat contribution relates to the ITF mechanisms considering future changes in ITF is critical for climate change studies.

The future ITF is expected to be weaker (Gupta et al., 2016), and weaker flows are expected to have characteristics of a frictional system. This change could affect the ITF vorticity budget and likely have the friction term as the leading order term in the balance of change in planetary vorticity. Consequently, friction would become the main controller of current width and therefore partitioning. Furthermore, a current with less non-linearity (or more friction) has weaker overshoots advection of momentum) past the boundaries, and the flow concentrates to the boundary. In some areas, the overshoot seems to provide adequate conditions for upwelling, as it creates space between the boundary and the current. For example, between Java and Lombok Strait jet exiting to the Indian Ocean, an important upwelling spot. The lack of current overshoot could enable the current to occupy this space, reducing upwelling and affecting productivity in the area, consequently affecting fisheries.

6.3 Future work

Our high-resolution regional model of the steady-state ITF can be improved to include tides, given its importance for mixing, and further studies that consider the influence of mixing need to be conducted. We explored the inter-annual variability in a global model. It would be interesting to consider the same timescale variability in the high-resolution regional model, particularly given the resolution dependency of ITF outflow transport (Kiss et al., 2019) and compare to our findings for the 10-km global model. For example, check the Makassar Strait saturation in terms of current width and the contribution of North Pacific water to the eastern pathway.

More investigation is needed regarding this contribution of North Pacific water that comes from the Mindanao Current and Celebes Sea to the eastern pathway. The influence of this contribution in the modification of waters and the effect on the outflows heat content is not evident. Previous studies have shown that the property modification is dependent on the pathway of the ITF through the Indonesian Seas (Koch-Larrouy et al., 2007). Here we show that the water that flows via the western or eastern pathway is influenced by the current width control upstream of these pathways, at the entrance of the ITF in an inter-annual timescale. But the details of these process need to be further studied.

It is essential to explore how future changes in the ITF will affect the system dynamics. In terms of the partitioning control by current width and the dominance of non-linearity on setting up current width, the next question is how a strong or a weak ITF behaves. We suspect a weak ITF may become a system dominated by friction, instead of by advection of relative vorticity, as we find in our vorticity budget for the present ITF. Could a strong ITF be so non-linear that the current width would be narrow enough to fit all in Lombok Strait? To do that we can develop a model to evaluate the effect of velocity on non-linearity so we could explore the relationship between current width and flow strength suggested by the WBC theory. A non-linear experiment with different current velocity with the same

boundary condition configuration, either slip or non-slip would be the appropriate setup for that study. Another example would be to use a boundary condition from global models that predict weaker ITF in the future. Then evaluate if the ITF dynamics would still have non-linearity as the main control for current width. Lastly, the relation between current width and partitioning should be tested in other models with different parameterisation, grid configuration, higher resolution, variable forcing, so we can check if non-linearity is still the main control for current width.

A last consideration is why the current width changes, outside of the Indonesian Seas, in Mindanao Current. We found increases in current width follow a period of large El Niño Index, but occur during La Niña periods. Does the ITF become more or less linear/non-linear and in which event? If the system is more frictional, which could be the case for El Niño and for the future ITF (both weaker ITF) and current width gets very wide, the contribution to the eastern pathway could be more significant, changing the heat contribution at the outflows considerably.

The more we learn about the ITF and understand its complexity, the more questions we raise. Based on our findings, we summarise the open questions that remain unanswered:

- How the heat content in the ITF jets is affected, and properties are modified depending on which pathway the water takes?
- Our analysis did not consider mixing, could it be the reason why there is little or no communication in the intermediate layer, between the upper and deep layer?
- How is the partitioning in the high-resolution regional model with variability, and its control by current width? As we conclude, the straits resolution is important to resolve the outflows, to obtain the correct distribution between the straits.
- How does variability affect the vorticity balance? A weaker ITF would make the friction term to be the dominant on balancing the change in planetary vorticity?

BIBLIOGRAPHY

Ayers, J. M., Strutton, P. G., Coles, V. J., Hood, R. R., and Matear, R. J. (2014). Indonesian throughflow nutrient fluxes and their potential impact on Indian Ocean productivity. *Geophysical Research Letters*, 41(14):5060–5067.

Carrier, G. F. and Robinson, A. R. (1962). On the theory of the wind-driven ocean circulation. *Journal of Fluid Mechanics*, 12(1):49–80.

Castruccio, F. S., Curchitser, E. N., and Kleypas, J. A. (2013). A model for quantifying oceanic transport and mesoscale variability in the Coral Triangle of the Indonesian/Philippines Archipelago. *J. Geophys. Res. Oceans*, 118(11):6123–6144.

Charney, J. G. (1955). The Gulf Stream as an inertial boundary layer. *Proc Natl Acad Sci U S A*, 41(10):731–740.

Chen, X., Qiu, B., Chen, S., Cheng, X., and Qi, Y. (2018). Interannual Modulations of the 50-Day Oscillations in the Celebes Sea: Dynamics and Impact. *J. Geophys. Res.-Oceans*, 123(7):4666–4679. WOS:000441888200014.

Clement, A. C., Seager, R., and Murtugudde, R. (2005). Why Are There Tropical Warm Pools? *Journal of Climate - J CLIMATE*, 18:5294–5311.

Cresswell, G. R. and Luick, J. L. (2001). Current measurements in the Halmahera Sea. *Journal of Geophysical Research: Oceans*, 106(C7):13945–13951.

Dee, D. P. and Uppala, S. (2009). Variational bias correction of satellite radiance data in the ERA-Interim reanalysis. *Quarterly Journal of the Royal Meteorological Society*, 135(644):1830–1841.

Domingues, C. M., Maltrud, M. E., Wijffels, S. E., Church, J. A., and Tomczak, M. (2007). Simulated Lagrangian pathways between the Leeuwin Current System and the upper-ocean circulation of the southeast Indian Ocean. *Deep Sea Research Part II: Topical Studies in Oceanography*, 54(8-10):797–817.

Edinger, E. N., Kolasa, J., and Risk, M. J. (2000). Biogeographic variation in coral species diversity on coral reefs in three regions of Indonesia. *Diversity and Distributions*, 6(3):113–127.

England, M. H. and Huang, F. (2005). On the Interannual Variability of the Indonesian Throughflow and Its Linkage with ENSO. *Journal of Climate*, 18(9):1435–1444.

Ffield, A. and Gordon, A. L. (1992). Vertical Mixing in the Indonesian Thermocline. *J. Phys. Oceanogr.*, 22(2):184–195.

Ffield, A. and Gordon, A. L. (1996). Tidal Mixing Signatures in the Indonesian Seas. *J. Phys. Oceanogr.*, 26(9):1924–1937.

Fieux, M., Andrié, C., Delecluse, P., Ilahude, A. G., Kartavtseff, A., Mantisi, F., Molcard, R., and Swallow, J. C. (1994). Measurements within the Pacific-Indian oceans throughflow region. *Deep Sea Research Part I: Oceanographic Research Papers*, 41(7):1091–1130.

Fofonoff, N. (1954). Steady Flow in a Frictionless Homogeneous Ocean. *J. Mar. Res.*, 13(3):254–262. WOS:A1954XR65600003.

Godfrey, J. S. (1989). A sverdrup model of the depth-integrated flow for the world ocean allowing for island circulations. *Geophysical & Astrophysical Fluid Dynamics*, 45(1-2):89–112.

Godfrey, J. S. (1996). The effect of the Indonesian throughflow on ocean circulation and heat exchange with the atmosphere: A review. *J. Geophys. Res.*, 101(C5):12217–12237.

Godfrey, J. S., Hirst, A. C., and Wilkin, J. (1993). Why Does the Indonesian Throughflow Appear to Originate from the North Pacific? *Journal of Physical Oceanography*, 23:1087–1098.

Gordon, A. (2005). Oceanography of the Indonesian Seas and Their Throughflow. *Oceanography*, 18(4):14–27.

Gordon, A., Sprintall, J., Wijffels, S., Susanto, D., Molcard, R., Van Aken, H. M., Ffield, A. L., de Ruijter, W., Lutjeharms, J., Speich, S., and others (2010a). Interocean Exchange of Thermocline Water: Indonesian Throughflow;" Tassie" Leakage; Agulhas Leakage. *Proceedings of OceanObs*, 9.

Gordon, A. L. and Fine, R. A. (1996). Pathways of water between the Pacific and Indian oceans in the Indonesian seas. *Nature*, 379(6561):146–149.

Gordon, A. L., Giulivi, C. F., and Ilahude, A. G. (2003). Deep topographic barriers within the Indonesian seas. *Deep Sea Research Part II: Topical Studies in Oceanography*, 50(12):2205–2228.

Gordon, A. L., Huber, B. A., Metzger, E. J., Susanto, R. D., Hurlburt, H. E., and Adi, T. R. (2012). South China Sea throughflow impact on the Indonesian throughflow. *Geophysical Research Letters*, 39(11).

Gordon, A. L., Sprintall, J., Van Aken, H. M., Susanto, D., Wijffels, S., Molcard, R., Ffield, A., Pranowo, W., and Wirasantosa, S. (2010b). The Indonesian throughflow during 2004–2006 as observed by the INSTANT program. *Dynamics of Atmospheres and Oceans*, 50(2):115–128.

Gordon, A. L., Susanto, R. D., Ffield, A., Huber, B. A., Pranowo, W., and Wirasantosa, S. (2008). Makassar Strait throughflow, 2004 to 2006. *Geophys. Res. Lett.*, 35(24):L24605.

Griffies, S. M. and Hallberg, R. W. (2000). Biharmonic Friction with a Smagorinsky-Like Viscosity for Use in Large-Scale Eddy-Permitting Ocean Models. *Mon. Wea. Rev.*, 128(8):2935–2946.

Gupta, A. S., McGregor, S., Sebille, E. v., Ganachaud, A., Brown, J. N., and Santoso, A. (2016). Future changes to the Indonesian Throughflow and Pacific circulation: The differing role of wind and deep circulation changes. *Geophysical Research Letters*, 43(4):1669–1678.

Haney, R. L. (1971). Surface Thermal Boundary Condition for Ocean Circulation Models. *J. Phys. Oceanogr.*, 1(4):241–248.

Hirst, A. C. and Godfrey, J. S. (1993). The Role of Indonesian Throughflow in a Global Ocean GCM. *J. Phys. Oceanogr.*, 23(6):1057–1086.

Hu, D., Wu, L., Cai, W., Gupta, A. S., Ganachaud, A., Qiu, B., Gordon, A. L., Lin, X., Chen, Z., Hu, S., Wang, G., Wang, Q., Sprintall, J., Qu, T., Kashino, Y., Wang, F., and Kessler, W. S. (2015). Pacific western boundary currents and their roles in climate. *Nature*, 522(7556):299–308.

Kashino, Y., Atmadipoera, A., Kuroda, Y., and Lukijanto (2013). Observed features of the Halmahera and Mindanao Eddies. *J. Geophys. Res.-Oceans*, 118(12):6543–6560. WOS:000329926200015.

Kashino, Y., Firing, E., Hacker, P., Sulaiman, A., and Lukiyanto (2001). Currents in the Celebes and Maluku Seas, February 1999. *Geophysical Research Letters*, 28(7):1263–1266.

Kashino, Y., Watanabe, H., Herunadi, B., Aoyama, M., and Hartoyo, D. (1999). Current variability at the Pacific entrance of the Indonesian Throughflow. *Journal of Geophysical Research: Oceans*, 104(C5):11021–11035.

Kida, S. and Wijffels, S. (2012). The impact of the Indonesian Throughflow and tidal mixing on the summertime sea surface temperature in the western Indonesian Seas. *J. Geophys. Res.*, 117(C9):C09007.

Kiss, A. E., Hogg, A. M., Hannah, N., Boeira Dias, F., Brassington, G. B., Chamberlain, M. A., Chapman, C., Dobrohotoff, P., Domingues, C. M., Duran, E. R., England, M. H., Fiedler, R., Griffies, S. M., Heerdegen, A., Heil, P., Holmes, R. M., Klocker, A., Marsland, S. J., Morrison, A. K., Munroe, J., Oke, P. R., Nikurashin, M., Pilo, G. S., Richet, O., Savita, A., Spence, P., Stewart, K. D., Ward, M. L., Wu, F., and Zhang, X. (2019). ACCESS-OM2: A Global Ocean-Sea Ice Model at Three Resolutions. *Geoscientific Model Development Discussions*, pages 1–58.

Koch-Larrouy, A., Atmadipoera, A., van Beek, P., Madec, G., Aucan, J., Lyard, F., Grelet, J., and Souhaut, M. (2015). Estimates of tidal mixing in the Indonesian archipelago from multidisciplinary INDOMIX in-situ data. *Deep Sea Research Part I: Oceanographic Research Papers*, 106:136–153.

Koch-Larrouy, A., Lengaigne, M., Terray, P., Madec, G., and Masson, S. (2009). Tidal mixing in the Indonesian Seas and its effect on the tropical climate system. *Clim Dyn*, 34(6):891–904.

Koch-Larrouy, A., Madec, G., Blanke, B., and Molcard, R. (2008). Water mass transformation along the Indonesian throughflow in an OGCM. *Ocean Dynamics*, 58(3-4):289–309.

Koch-Larrouy, A., Madec, G., Bouruet-Aubertot, P., Gerkema, T., Bessières, L., and Molcard, R. (2007). On the transformation of Pacific Water into Indonesian Throughflow Water by internal tidal mixing. *Geophys. Res. Lett.*, 34(4):L04604.

Large, W. G., McWilliams, J. C., and Doney, S. C. (1994). Oceanic vertical mixing: A review and a model with a nonlocal boundary layer parameterization. *Reviews of Geophysics*, 32(4):363–403.

Lee, S.-K., Park, W., Baringer, M. O., Gordon, A. L., Huber, B., and Liu, Y. (2015). Pacific origin of the abrupt increase in Indian Ocean heat content during the warming hiatus. *Nature Geosci*, 8(6):445–449.

Liu, Q.-Y., Feng, M., Wang, D., and Wijffels, S. (2015). Interannual variability of the Indonesian

Throughflow transport: A revisit based on 30 year expendable bathythermograph data. *Journal of Geophysical Research: Oceans*, 120(12):8270–8282.

Luick, J. L. and Cresswell, G. R. (2001). Current measurements in the Maluku Sea. *J. Geophys. Res.*, 106(C7):13953–13958.

Marshall, J., Adcroft, A., Hill, C., Perelman, L., and Heisey, C. (1997a). A finite-volume, incompressible Navier Stokes model for studies of the ocean on parallel computers. *Journal of Geophysical Research: Oceans*, 102(C3):5753–5766.

Marshall, J., Hill, C., Perelman, L., and Adcroft, A. (1997b). Hydrostatic, quasi-hydrostatic, and nonhydrostatic ocean modeling. *Journal of Geophysical Research: Oceans*, 102(C3):5733–5752.

Masumoto, Y., Kagimoto, T., Yoshida, M., Fukuda, M., Hirose, N., and Yamagata, T. (2001). Intraseasonal eddies in the Sulawesi Sea simulated in an ocean general circulation model. *Geophysical Research Letters*, 28(8):1631–1634.

Mayer, B., Damm, P. E., Pohlmann, T., and Rizal, S. (2010). What is driving the ITF? An illumination of the Indonesian throughflow with a numerical nested model system. *Dynamics of Atmospheres and Oceans*, 50(2):301–312.

Metzger, E. J., Hurlburt, H. E., Xu, X., Shriver, J. F., Gordon, A. L., Sprintall, J., Susanto, R. D., and van Aken, H. M. (2010). Simulated and observed circulation in the Indonesian Seas: 1/12°global HYCOM and the INSTANT observations. *Dynamics of Atmospheres and Oceans*, 50(2):275–300.

Meyers, G., Bailey, R. J., and Worby, A. P. (1995). Geostrophic transport of Indonesian throughflow. *Deep Sea Research Part I: Oceanographic Research Papers*, 42(7):1163–1174.

Molcard, R., Fieux, M., and Ilahude, A. G. (1996). The Indo-Pacific throughflow in the Timor Passage. *J. Geophys. Res.*, 101(C5):12411–12420.

Molcard, R., Fieux, M., and Syamsudin, F. (2001). The throughflow within Ombai Strait. *Deep Sea Research Part I: Oceanographic Research Papers*, 48(5):1237–1253.

Morey, S. L., Shriver, J. F., and O'Brien, J. J. (1999). The effects of Halmahera on the Indonesian throughflow. *Journal of Geophysical Research: Oceans*, 104(C10):23281–23296.

Munk, W. H. (1950). On the wind-driven ocean circulation. *J. Meteor.*, 7(2):80–93.

Nagai, T. and Hibiya, T. (2015). Internal tides and associated vertical mixing in the Indonesian Archipelago. *J. Geophys. Res. Oceans*, pages n/a–n/a.

National Geophysical Data Center (2006). 2-minute Gridded Global Relief Data (ETOPO2) v2. National Geophysical Data Center, NOAA. doi:10.7289/v5j1012q, Accessed 30 july 2015.

Nof, D. (1995). Choked Flows from the Pacific to the Indian Ocean. *J. Phys. Oceanogr.*, 25(6):1369–1383.

Oke, P. R., Griffin, D. A., Schiller, A., Matear, R. J., Fiedler, R., Mansbridge, J., Lenton, A., Cahill, M., Chamberlain, M. A., and Ridgway, K. (2013). Evaluation of a near-global eddy-resolving ocean model. *Geoscientific Model Development*, 6:591–615.

Potemra, J. T., Hautala, S. L., and Sprintall, J. (2003). Vertical structure of Indonesian throughflow in a large-scale model. *Deep Sea Research Part II: Topical Studies in Oceanography*, 50(12–13):2143–2161.

Schiller, A., Wijffels, S. E., Sprintall, J., Molcard, R., and Oke, P. R. (2010). Pathways of intraseasonal variability in the Indonesian Throughflow region. *Dynamics of Atmospheres and Oceans*, 50(2):174–200.

Schneider, N. (1998). The Indonesian Throughflow and the Global Climate System. *J. Climate*, 11(4):676–689.

Schott, F. A. and McCreary, J. P. (2001). The monsoon circulation of the Indian Ocean. *Progress in Oceanography*, 51:1–123.

Shriver, J. F. and Hurlburt, H. E. (1997). The contribution of the global thermohaline circulation to the Pacific to Indian Ocean throughflow via Indonesia. *Journal of Geophysical Research: Oceans*, 102(C3):5491–5511.

Smagorinsky, J. (1963). General circulation experiments with the primitive equations. *Mon. Wea. Rev.*, 91(3):99–164.

Song, Q. W., Gordon, A. L., and Visbeck, M. (2002). Spreading of the Indonesian Throughflow in the Indian Ocean.

Sprintall, J., Gordon, A. L., Koch-Larrouy, A., Lee, T., Potemra, J. T., Pujiana, K., and Wijffels, S. E. (2014). The Indonesian seas and their role in the coupled ocean-climate system. *Nature Geosci*, 7(7):487–492.

Sprintall, J., Gordon, A. L., Wijffels, S. E., Feng, M., Hu, S., Koch-Larrouy, A., Phillips, H., Nugroho, D., Napitu, A., Pujiana, K., Susanto, R. D., Sloyan, B., Yuan, D., Riama, N. F., Siswanto, S., Kuswardani, A., Arifin, Z., Wahyudi, A. J., Zhou, H., Nagai, T., Ansong, J. K., Bourdalle-Badié, R., Chanut, J., Lyard, F., Arbic, B. K., Ramdhani, A., and Setiawan, A. (2019). Detecting Change in the Indonesian Seas. *Front. Mar. Sci.*, 6.

Sprintall, J., Potemra, J. T., Hautala, S. L., Bray, N. A., and Pandoe, W. W. (2003). Temperature and salinity variability in the exit passages of the Indonesian Throughflow. *Deep Sea Research Part II: Topical Studies in Oceanography*, 50(12–13):2183–2204.

Sprintall, J. and Revelard, A. (2014). The Indonesian Throughflow response to Indo-Pacific climate variability. *J. Geophys. Res. Oceans*, 119(2):1161–1175.

Sprintall, J., Wijffels, S. E., Molcard, R., and Jaya, I. (2009). Direct estimates of the Indonesian Throughflow entering the Indian Ocean: 2004–2006. *J. Geophys. Res.*, 114(C7):C07001.

Stommel, H. (1948). The westward intensification of wind-driven ocean currents. *Eos, Transactions American Geophysical Union*, 29(2):202–206.

Susanto, R. D., Gordon, A. L., and Zheng, Q. (2001). Upwelling along the coasts of Java and Sumatra and its relation to ENSO. *Geophys. Res. Lett.*, 28(8):1599–1602.

Sverdrup, H. U. (1947). Wind-Driven Currents in a Baroclinic Ocean; with Application to the Equatorial Currents of the Eastern Pacific. *Proc Natl Acad Sci U S A*, 33(11):318–326.

Talley, L. D. (2005). Deep expression of the Indonesian Throughflow: Indonesian Intermediate Water in the South Equatorial Current. *Journal of Geophysical Research*, 110(C10).

Tillinger, D. and Gordon, A. L. (2010). Transport weighted temperature and internal energy transport of the Indonesian throughflow. *Dynamics of Atmospheres and Oceans*, 50(2):224–232.

van Aken, H. M., Brodjonegoro, I. S., and Jaya, I. (2009). The deep-water motion through the Lifamatola Passage and its contribution to the Indonesian throughflow. *Deep Sea Research Part I: Oceanographic Research Papers*, 56(8):1203–1216.

van Sebille, E., Sprintall, J., Schwarzkopf, F. U., Sen Gupta, A., Santoso, A., England, M. H., Biastoch, A., and Böning, C. W. (2014). Pacific-to-Indian Ocean connectivity: Tasman leakage, Indonesian Throughflow, and the role of ENSO. *J. Geophys. Res. Oceans*, 119(2):1365–1382.

Veron, J., Devantier, L. M., Turak, E., Green, A. L., Kininmonth, S., Stafford-Smith, M., and Peterson, N. (2009). Delineating the Coral Triangle. *Galaxea, Journal of Coral Reef Studies*, 11(2):91–100.

Vranes, K., Gordon, A. L., and Ffield, A. (2002). The heat transport of the Indonesian Throughflow and implications for the Indian Ocean heat budget. *Deep Sea Research Part II: Topical Studies in Oceanography*, 49(7):1391–1410.

Wajsowicz, R. C. (1996). Flow of a western boundary current through multiple straits: An electrical circuit analogy for the Indonesian throughflow and archipelago. *Journal of Geophysical Research: Oceans*, 101(C5):12295–12300.

Wang, C., Zhang, L., Lee, S.-K., Wu, L., and Mechoso, C. R. (2014). A global perspective on CMIP5 climate model biases. *Nature Climate Change*, 4(3):201–205.

Wang, Z. and Yuan, D. (2012). Nonlinear Dynamics of Two Western Boundary Currents Colliding at a Gap. *J. Phys. Oceanogr.*, 42(11):2030–2040.

Wang, Z. and Yuan, D. (2014). Multiple Equilibria and Hysteresis of Two Unequal-Transport Western Boundary Currents Colliding at a Gap. *J. Phys. Oceanogr.*, 44(7):1873–1885.

Wattimena, M. C., Atmadipoera, A. S., Purba, M., Nurjaya, I. W., and Syamsudin, F. (2018). Indonesian Throughflow (ITF) variability in Halmahera Sea and its coherency with New Guinea Coastal Current. *IOP Conference Series: Earth and Environmental Science*, 176:012011.

Wentz, F. J., Scott, J., Hoffman, R., Leidner, M., Atlas, R., and Ardizzone, J. (2015). Remote Sensing Systems Cross-Calibrated Multi-Platform (CCMP) 6-hourly ocean vector wind analysis product on 0.25 deg grid, Version 2.0, subset from years 2004 to 2006. *Remote Sensing Systems, Santa Rosa, CA.*, Available online at www.remss.com/measurements/ccmp. Accessed 15 Jan 2016.

Wiggert, J. D., Murtugudde, R. G., and Christian, J. R. (2006). Annual ecosystem variability in the tropical Indian Ocean: Results of a coupled bio-physical ocean general circulation model. *Deep Sea Research Part II: Topical Studies in Oceanography*, 53(5):644–676.

Wijffels, S. and Meyers, G. (2004). An Intersection of Oceanic Waveguides: Variability in the Indonesian Throughflow Region. *Journal of Physical Oceanography*, 34(5):1232–1253.

Wijffels, S. E., Meyers, G., and Godfrey, J. S. (2008). A 20-yr average of the Indonesian Throughflow: Regional currents and the interbasin exchange. *Journal of Physical Oceanography*, 38(9):1965–1978.

Wijffels, S. E., Schmitt, R. W., Bryden, H. L., and Stigebrandt, A. (1992). Transport of Freshwater by the Oceans. *J. Phys. Oceanogr.*, 22(2):155–162.

Wyrtki, K. (1987). Indonesian through flow and the associated pressure gradient. *J. Geophys. Res.*, 92(C12):12941–12946.

Yuan, D., Li, X., Wang, Z., Li, Y., Wang, J., Yang, Y., Hu, X., Tan, S., Zhou, H., Wardana, A. K., Surinati, D., Purwandana, A., Azis Ismail, M. F., Avianto, P., Dirhamsyah, D., Arifin, Z., and Storch, J.-S. v. (2018). Observed Transport Variations in the Maluku Channel of the Indonesian Seas Associated with Western Boundary Current Changes. *J. Phys. Oceanogr.*, 48(8):1803–1813.